

**Delineation, Characterization and Modeling of
Basement Shear Zones Hosting Uranium
Mineralisation Using Magnetic and IP/Resistivity
Survey in Devri area, Surguja District, Chhattisgarh,
India**

*Dissertation submitted in accordance with the requirements
of the University of Hyderabad for the degree of*

**Master of Technology
in
Mineral Exploration**

by

Rajeeva Ranjan

(09ESDE02)



**Centre for Earth and Space Sciences
University of Hyderabad
Hyderabad 500 046
2011**

C E R T I F I C A T E

This is to certify that, Shri Rajeeva Ranjan, sponsored candidate of Atomic Minerals Directorate for Exploration and Research (AMD), Department of Atomic Energy (DAE), has carried out the project work titled "*Delineation, Characterization and Modeling of basement shear zones hosting Uranium mineralisation using Magnetic and IP/Resistivity survey in Devri area, Surguja District, Chhattisgarh, India*" at Centre for Earth and Space Sciences (CESS), University of Hyderabad towards partial fulfillment of M. Tech degree in Mineral Exploration under our joint supervision. It is further certified that the contribution is original in nature and had not been submitted either in part or whole elsewhere.

(Dr. M.N.Chary)
Project Mentor
Scientific Officer - E
Atomic Minerals Directorate for
Exploration and Research, Central
Region, Naghpur-440 001

(Prof. V. Chakravarthi)
Project Mentor
Faculty, CESS
Center for Earth & Space Science
University of Hyderabad
Hyderabad – 500 046

(Prof. A. C. Narayana)
Director
Center for Earth & Space Science (CESS)
University of Hyderabad
Hyderabad – 500 046

CONTENTS

	Page No.
ACKNOWLEDGEMENT	i
SUMMARY	ii

CHAPTER- I

INTRODUCTION

1.1. General	1
1.2. Location and Accessibility	3
1.3. Physiography	3
1.4. Previous Work	3
1.5. Radioactivity	4
1.6 Regional Geology	5
1.7 Local Geology	6
1.8 Structure	7

CHAPTER-II

GEOPHYSICAL SURVEY

2.1 General	14
2.2. Magnetic Survey	17
2.2.1. Origin of Magnetic Field	17
2.2.2. Principle of magnetic prospecting	18
2.2.3. Instruments	19
2.2.4. Data Acquisition	20
2.2.5. Corrections	21
2.2.6. Interpretation	21
2.3. Electrical Survey	22
2.3.1a. Principles of Resistivity Survey	23
2.3.1b. Principles of Induced Polarization	24
2.3.2. Instruments	27

2.3.3. Data Acquisition	28
2.3.4. Corrections	28
2.3.5. Interpretation	29

CHAPTER - III

PLANNING OF GEOPHYSICAL SURVEY

3.1. General	30
3.2. Planning of Magnetic Survey	30
3.2.1 Data Collection	30
3.3 Planning of IP (TD)/ Resistivity Survey	31
3.3.1. Data Collection	32
3.4. Measurement of Magnetic Susceptibility	33
3.4.1. Principle	33
3.4.2. Instrument	34
3.4.3. Data Collection and Interpretation	35

CHAPTER - IV

INTERPRETATION

4.1. General	40
4.2. Magnetic Anomaly Map	41
4.2.1. Upward Continuation	42
4.2.2. Reduced to Pole (RTP)	42
4.2.3. Horizontal and vertical Derivatives	45
4.2.4. Analytical Signal	46
4.2.5. Tilt Derivative Map	47
4.2.6. Euler Deconvolution	48
4.2.7. 2D Profile Modeling	49
4.2.8. Depth Estimation by 3 D inversion	51
4.3. Resistivity/ Induced Polarization	51

4.3.1. Resistivity Map	52
4.3.2. Chargeability Map	53
4.4. Miscellaneous	54
4.4.1. Radiometric Measurement	54
4.4.2 Data Acquisition and Interpretation	55

CHAPTER – V

CONCLUSION	98
REFERENCES	100

LIST OF FIGURES AND TABLES

Fig No.	Description	Page No.
1.1	Geological and Structural Map of Central Surguja Shear Zone	10
1.2	Geological Map of Dumhat-Devri Area, Surguja District, Chhattisgarh.	11
1.3	Location and Approach Map of Study Area.	12
1.4	Plunging syncline and anticline developed in calc-silicate rock, representing 3 rd generation of fold, Gharhari Nala section	13
1.5	Hook shape fold developed in calc-silicate rock due to superimposition of 2 nd and 3 rd phase of folding, Barahaul, 64M/2	13
1.6	Development of garnet crystals in metabasic rock due to high grade metamorphism, borehole DEV-4/136.25m	13
1.7	Development of garnet crystals in metabasic rock due to high grade metamorphism, borehole DEV-3/278.00m.	13
1.8	Partial melting (insitu) of psammitic rocks gave rise to granitic composition rock, Jhoj nala.	13
2.1	Principle of Proton Precession Magnetometer	19
2.2	Transient response to square wave current pulse (time domain).	24
2.3	Dipole-Dipole Array configuration	26
2.4	Plotting point for dipole-dipole array is mid point of total spread	27
2.5	TSQ -3 IP Transmitter	28
2.6	Scintrex, IPR-10A (TD) IP receiver connected with porous pots	28
3.1	Geophysical Traverse Line	30
3.2	Magnetic Layout Map of Devri Area	31
3.3	IP/Resistivity Layout Map of Devri Area	32
3.4	KT-10 Kappameter Instrument	34
3.5	Correlation Log of Mag. Susceptibility and Gamma Ray Log, DEV-3	36
3.6	Correlation Log of Mag. Susceptibility and Gamma Ray Log, DEV-4	37
3.7	Correlation Log of Mag. Susceptibility and Gamma Ray Log, DEV-5	38
3.8	Correlation Log of Mag. Susceptibility and Gamma Ray Log, DEV-6	39
4.1	Magnetic Profile Along W-26 Traverse Line	41

4.2	Magnetic Contour Map of Devri Area	83
4.3	Upward Continuation Map of Devri Area	84
4.4	RTP Map of Devri Area	85
4.5	Vertical (Z) derivative Magnetic Anomaly Image	86
4.6	Horizontal (X) derivative Magnetic Anomaly Image	86
4.7	Analytical Signal Map of Devri	87
4.8	Tilt Deravative (RTP) Map of Devri Area.	87
4.9a,b	Standered Euler Depth Map of Devri Are	88
4.10	2D Profile Modeling along AB Profile.	89
4.11	2D Profile Modeling along L1 Profile.	90
4.12	2D Profile Modeling along L2Profile.	91
4.13	3D Depth Inversion	92
4.14	Resistivity/ IP Profile along W-46 Traverse Line	52
4.15	Resistivity Map of Devri Area	93
4.16	Pyrite Crystals in Core	53
4.17	Chargeability Map of Devri Area	94
4.18	Low Resistivity and High Chargeability Contours Superimposed on Magnetic Map	95
4.19	PGRS Instrument	54
4.20	Total Radioelement Concentration Map of Devri Area	96
4.21	Thorium Contour Map of Map of Devri Area	96
4.22	Uranium Contour Map of Map of Devri Area	96
4.23	Potassium Contour Map of Map of Devri Area	97
4.24	U/Th Contour Map of Devri area	97

List of Tables

Table No	Description	Page No
1.1	Generalised Lithostratigraphic Succession of Dumhat-Devri area	6
3.1	Magnetic Susceptibility of Rocks on Outcrop	35
4.1	Magnetic Anomaly (nT) Data Sheet	57
4.2	Resistivity (Ohm m) and Chargeability (mV/V) Data Sheet	72

ACKNOWLEDGEMENT

I express my deep sense of gratitude to Shri P.B. Maithani, Director, Atomic Minerals Directorate for Exploration and Research (AMD), Hyderabad for providing me the opportunity to learn new dimension of earth science during M. Tech. course in Mineral Exploration at University of Hyderabad and providing all the facilities to complete my thesis work.

I am extremely grateful to, Prof. A. C. Narayana, Director, CESS, University of Hyderabad, for his support, encouragement and valuable suggestions for the dissertation work. I am also thankful to Prof. V. Chakravarthi, mentor of this project, for his constant encouragement, guidance and all kind of support in formulating this report.

I feel pleasure to extend my sincere gratitude and thanks to Shri P. S. Parihar, Shri K. Umamaheshwar, and Dr. M.K. Roy, Additional Directors, AMD, Hyderabad for their constant support and encouragement.

I am extremely grateful to Prof. K. V. Subba Rao, and S. Srilaksmi, faculty, CESS, University of Hyderabad for their guidance and support during the entire M.Tech course.

I express my pleasure and deep sense of gratitude to Shri Amit Majumdar, Regional Director, AMD, Central Region, Nagpur, for their encouragement, guidance and providing me all facilities to complete my thesis work.

I am sincerely thankful to Shri P.K.Sinha, Incharge, Vindhyan-Sarguja-Gondwana investigation, Nagpur, Shri R.L Narsimha Rao and Shri J.K Das Incharge EGPG, Hyderabad and Nagpur for his guidance, encouragement and support.

I am extremely indebted to my mentors cum field partner Dr. M.N. Chary, AMD, C.R, Nagpur for his consistent support in field as well as in preparation of this report.

I am grateful to Resident Geologists, Shri R. Gurjar and U.P. Sharma for their fruitful discussion in the field and senior colleagues Shri Subhash Ram, V.K Shrivastava and A.K. Verma for their suggestions and discussion on the topic.

I acknowledge the help and support of friends like Sarang, Chandrashekar, Mahendra, Nagalaxmi, Vani, Sravanthi and all CESS staff members. It is special for me to acknowledge the vital role of my classmates during entire course.

Last but not the least; I am indebted to my parents, family members, above all my Master who have provided me the much needed support in all facets of my life.

Rajeeva Ranjan

SUMMURY

Central Surguja Shear Zone traversing Surguja Crystalline Complex (SCC), is prominent shear zone trending ENE-WSW is believed to be an extension of Chhotanagpur Gniessic Complex in the environ of Central India Tectonic Zone. Rocks of Surguja Crystallines viz, metasediments, granite-gneiss, granites, metabasics and pegmatites are shatters due to shearing and fracturing. Uranium mineralization within Surguja Shear dates back to late sixties and two small uranium deposits were established at Dumhat and Jajawal area. The present geophysical studies encompassing magnetic, IP/Resistivity, Radiometric and Magnetic Susceptibility measurement were taken to characterize the shear zone present under soil covered portion at Devri area, therefore title of the project **"Delineation, characterization and modeling of basement shear zones hosting uranium mineralisation using magnetic and IP / Resistivity surveys at Devri area, Surguja district, Chhattisgarh, India."**

Magnetic survey infers that the Central Surguja Shear zone is continuing under the soil cover portion with the established trend of ENE-WSW. Low magnetic in the central part could be attributed to this shear. A very conspicuous ENE-WSW trending magnetic body has been picked up in southern part of the area. Similar kind of basic body has given very good uranium mineralized bands in Dumhat area. It seems that this basic body is emplaced along the axial plane of 3rd phase of folding. This indicates reactivation of the area in time and again which falls under the structural grain of Satpura Orogeny.

Induced Polarization/Resistivity survey revealed presence of two low resistivity and corresponding two high chargeability zone in the north and south of the area. Northern zone follow the trend of shear zone (ENE-WSW) whereas the southern zone trend NE-SW. Concentration of disseminated sulphides are indicated by high chargeability in the survey and a peak value of 72mV/V was recorded in the western most traverse line. Therefore a new

target location for subsurface exploration has been established by this study.

Magnetic susceptibility and gamma ray correlation logs of four boreholes suggest positive association of radioactivity and sulphides and/or ferromagnesian minerals. The chief minerals responsible for high magnetic susceptibility are pyrite, pyrrhotite, ilmenite, magnetite, biotite and associated chief uranium minerals are pitchblende, uraninite, coffinite and uranophane.

Radioelemental mapping of the area signifies that uranium minerals present in the rocks of shear zone have been leached out and must have migrated with meteoric water below the water table where it can precipitate under reducing conditions. High potassium content in fresh rock exposure indicates evolved nature of granite which is a good indication for uranium mineralisation point of view.

Chapter 1

Introduction

1.1 General

Minerals and powers are backbone for industrial development of any country. Development of any country is gauged by consumption of per capita power. Uranium is among the sources of power generation along with coal, gas, hydel, wind and solar energy. Power production in India by coal accounts for 65%, hydel 22%, renewable 10% and nuclear 3%. Coal and gas fired power plant are chief sources power generation in India but they also substantially produce green house gases which are major concerned for our environment, therefore we have to look for alternative source of power production and nuclear energy is one of them. Uranium comes under the strategic mineral resource which is used for power generation, medicine, agriculture, and defense.

Exploration of concealed type uranium mineralisation is a challenge to exploration geologists. Direct methods are useful where geological signatures are exposed on the surface. For concealed type, indirect methods like geophysical techniques (gravity, magnetic, electromagnetic, electrical, seismic etc) are utilized as a successful tool to locate the subsurface geological signatures or probable locale associated with mineralisation. Some time they are directly related to geophysical signature specially in the case of iron ore and sulphide mineralisations in favorable geological conditions. Geophysical methods involve mapping the distribution of subsurface physical properties to know the subsurface geology. These geophysical attributes are correlated with the probable subsurface geological signatures. Finally,

combination of two or more geophysical methods is applied to strengthen the inferences in the desired area.

This dissertation deals with the geophysical work carried out in parts of Sarguja Crystalline Complex (SCC). A prominent shear zone (Fig-1.1) called Central Sarguja Shear Zone (CSSZ) trending ENE-WSW traversing in the area with ~100 km length and variable width. Major lithounits present in the Sarguja Crystallines are quartzites, quartz-mica schist, chlorite-biotite schist, graphite schist, calc-silicates, amphibolites and their migmatized equivalents, and granites. Lithounits falling within the shear zone are brecciated, cataclastized and mylonitized, irrespective of their composition. Due to pervasive nature of lithounits present within the shear zone, uranium mobilization and its fixation along these fractures/ shears has taken place. Hydrothermal solutions have played a major role in mobilizing the uranium bearing fluids and its fixation with presence of sulphides, chlorites, iron oxides etc which act as reductants.

The objective of this survey was to study the basement configuration, fault, fractures, shears, basic bodies etc because these structural grains are sometime related to mineralization in some or other way. In present case, major part of surveyed area are occupied by soil covers/cultivated land with sporadic exposures of younger granites, pegmatites, gneisses and quartzites. Geophysical techniques used here are, ground magnetic survey, Induced Polarization (time domain), Resistivity, and Gamma ray spectrometry. Measurement of magnetic susceptibility of grab as well as borehole core samples were also carried out for the modeling of magnetic data and correlation between magnetic susceptibility and gamma ray values of boreholes were also established.

1.2 Location and Accessibility

The study area (Fig-1.2) forms parts of Toposheet No. 64M/2 of survey of India and bounded by 23.5040° to 23.531° & 23.5090° to 23.5364° latitude and 83.132° to 83.142° & 83.1454° to 83.1573° longitude. It falls in the Surguja district of Chhattisgarh state whose district headquarter is located at Ambikapur. Ambikapur is connected to all weather roads from Bilaspur and Raipur and by South Eastern Railway from Raipur. Devri area is located ~70km north of Ambikapur town by all weather metalled road on Ambikapur- Varanasi road highway (Fig-1.3).

1.3 Physiography

The area of investigation (Devri) is represented by pene planed topography with major part covered by cultivated land. Sporadic exposures of quartzites, granite gneiss and pegmatites are making small mounds in the area with linearity in exposures of quartzite hillocks in ENE-WSW to NE-SW directions. Average R.L of the area is 560m from MSL. Drainage pattern in the area are following structural grains and some of the important nala /nadi are Jhoj Nala, Dudhania nala, Godkatwa nala, Pakni nala etc and all of them draining into Mahan River which is a tributary to Rihand River which ultimately meets to Son River. The temperature ranges in area from 43°C in summer to 1°C in winter with annual rain fall of ~1000mm. Forest covers in the area comprises of Sal, Mahua, Mango, Babul, Char, Tendu, Anwala, teak, bamboo, shrubs, creepers and bushes. Chief crop in the area are rice, kodo, kutki, wheat and pulses.

1.4 Previous Work

Exploration for uranium in Sarguja Crystalline Complex (SCC) dates back to 1969 when first breakthrough was made in the form of uranium anomaly associated

with Syenite at Dhabhi (Seshadri 1970). Subsequent ground radiometric and airborne surveys brought out significant radioactivity anomalies at Dumhat (Saxena, 1975), Jajawal (Joshi, 1976), Jhirat (Chaki, 1976) and at several other places viz, Jhor, Pakni, Haraipahar, Kansisot, Garia etc (Saxena et al., 1998 and references therein). The airborne survey carried out during F.S. 1971-73 has played a major role in identifying extend of Sarguja Shear Zone (SSZ), and later on the ground radiometric survey led to identifying Dumhat anomaly within the SSZ. Dumhat area is located (23°28'N to 23°34'N and 83°08'E to 83°13'E, T.S. No- 64M/2) around 70k north of Ambikapur town (Seth 1989, Saxena et al., 1990). The subsequent exploration in the Dumhat area by drilling resulted in establishing a structurally controlled vein type small uranium deposit of about 450te of uranium oxide. Radiometric survey continued in the area during F.S. 1975-76, and significant uranium anomalies were located in the same shear zone at Jajawal (Joshi 1976). Detailed exploration including drilling and underground mining have established a low grade and small “vein type” uranium deposit at Jajawal. This uranium deposit is located south of Jajawal village (23°31'40": 83°03'12") in Survey of India toposheet no. 64 M/2 in Surguja district, Chhattisgarh. All kind of exploration activity have been abandoned in these area in late nineties and the Dumhat block has been reconsidered for further exploration to prove its strike and dip continuity in F.S. 2007-08. Due to logistic problems in Dumhat area, Devri area has been taken for subsurface exploration in F.S. 2009-10, which fall in strike of Dumhat area with a spatial separation of about 1500m in westward direction.

1.5 Radioactivity

Radioactivity reported from various places in the area viz, Dumhat, Jajawal are mainly confined to the shear zone and the rock hosting the mineralization are

quartzo feldspathic cataclasites, mylonite, sheared granites & gneisses and metabasics. Uranium minerals occur as disseminations and fracture fillings as well as closely associated with biotite flakes and they are pitchblende, uraninite, coffinite and uranophane. Other accessory minerals are magnetite, hematite, pyrite, chalcopyrite, sphalerite, galena, covellite, ilmenite, rutile, calcite and fluorites (Saxena et al., 1998). Recent studies of radioactive core from Devri area reveal presence of coffinite and uraninite as major uranium minerals along with rutile, monazite, ilmenite, xenotime, magnetite, pyrite, spessartite etc as accessory minerals (AMD report no- AMD/NMT/8/2011, 30.05.2011)

1.6 Regional Geology

Sarguja Crystalline Complex (SCC) is part of Proterozoic Mobile Belt confined to Son-Narmada-Tapti lineament trending ENE-WSW comprises Palaeo- to Mesoproterozoic metasediments and unclassified crystallines exposed as inliers in major Gondwana terrain. Crystallines are mostly represented by granites, gneisses and migmatites (Seth, 1989, Saxena et al., 1990, Saxena et al., 1992, Saxena et al., 1998). It covers an area of about 3000 sq.km in the state of Chhattisgarh and Jharkhand extending from Binda Nagnaha of Palamau district of Jharkhand, with its possible extension further east into Chhotanagpur Gneissic Complex (Ramakrishnan, M and Vaidyanadhan, R., 2010) and its westward extension in Chhattisgarh upto Mahan River with mostly covered by Gondwana sediments and Deccan Trap, leaving only isolated patches as inliers. The generalized lithostratigraphic succession of the area is given in the table-1.1.

Table –1.1: Generalised Lithostratigraphic Succession of Dumhat-Devri area (modified after AMD)

Age	Formation / Rock type
Cretaceous	Deccan Trap (Basic flow and dykes)
Triassic	Mahadeva Fm. (sandstones and shales)
Permo-carboniferous	Barakar Fm. (sandstone, shale and coal seams) Talchir Fm. (boulder beds, sandstones, needle shales)
	~~~~~Unconformity/ Faulted contact ~~~~~
Upper to Middle Proterozoic	Tourmaline granites (640 Ma) Pegmatite and Q-vein 886-934 Ma Pink foliated granite (1030 Ma)
Middle to Lower(?) Proterozoic	Grey foliated granite (1392 Ma), Gneissic complex- biotite gneiss, biotite-microcline porphyritic gneiss, migmatites
Archaean	Amphibolite, quartzites, biotite-muscovite-chlorite schist, biotite-muscovite schist and calc-silicates

### 1.7 Local Geology

Geophysical surveys have been carried out in the Devri area, which falls in-between the Dumhat and Jajawal uranium deposits. The area covered is bounded by (23.504°,23.5090°,23.531°,23.5364°N and 83.142°, 83.1573°,83.132°, 83.1454°E, T.S. No- 64M/2). Major part of the surveyed area is covered by soil/cultivated land with sporadic exposures of quartzites, schists, granites and pegmatites. Quartzites and pegmatite exposures are making small mounds in the area.

**Quartzites:** Observed in the central and southern part of the surveyed area and they are hard, compact, medium grained and highly ferruginised in nature. Shear foliation developed in the quartzite show Mostly N70°E trend with vertical to high dip towards north, where as quartzite exposures present in Godkatwa nala in the southern side show swing in the strike with strike of N45°E. Low order radioactivity is also observed at these locations.

**Schists:** Schistose rocks are observed in the central part of the surveyed area with very limited exposures in Godkatwa nala sections due to its soft and prone to weathering nature. They are occurring in the low lying nala sections or few road cutting sections, and represented by quartz-biotite-muscovite schists. Schists also follow the foliation trend of N70°E.

**Granites:** Grey granites are well exposed in the northern and central part of the surveyed area. Few exposures are also noticed in newly excavated ponds in southern side of the area. They are medium to coarse grained and at times porphyritic in nature and represented by biotite-muscovite granite to grey granite with foliation trend of N70°E. Geochemical study of the granites indicates that they are S-type, and were generated by partial melting of metapelites. S-type granites are fertile and good for uranium mineralization point of view because of being source for labile uranium.

### **1.8 Structures**

The main structural grain of the area is parallel to ENE–WSW to E–W, sympathetic to Satpura lineament. The satellite imagery studies have indicated that Sarguja Crystallines are highly disturbed and constitute a tectonic block characterized by dominance of ENE-WSW trending lineament. The northern and southern part of this block show less tectonic disturbance along with change in lineament pattern (Nair et al., 1988). Within the Sarguja Crystalline two sub-parallel shears, separated by about 1 to 10 km. have been identified (Kak et al., 1983). Folding and deformation of SCC (Sarguja Crystalline Complex) has taken place in several stages. Tight isoclinal folds (F1) due to north-south compressional forces lead to first phase of folding with ENE-WSW trending axial planes. Increased compression and shear stress lead to rupture along axial regions with development

of shears, essentially parallel to axial trace of the folds. The open to tight upright folds (F2) with their axes aligned perpendicular to F1, were superimposed during the second phase of deformation. F2 fold depicts variable angle plunge towards east or west or both. This phase of deformation marked by emplacement of pink granite. The last phase of folding F3 is shown by the closure of the outcrop along the strike, with their axes running parallel to F1 axes (Fig-1.4). Due to superimposition of 2nd and 3rd phase of folding hook shape folds are developed (Fig-1.5). Intrusion of pegmatites, aplites and basic dykes marked the culmination of this phase.

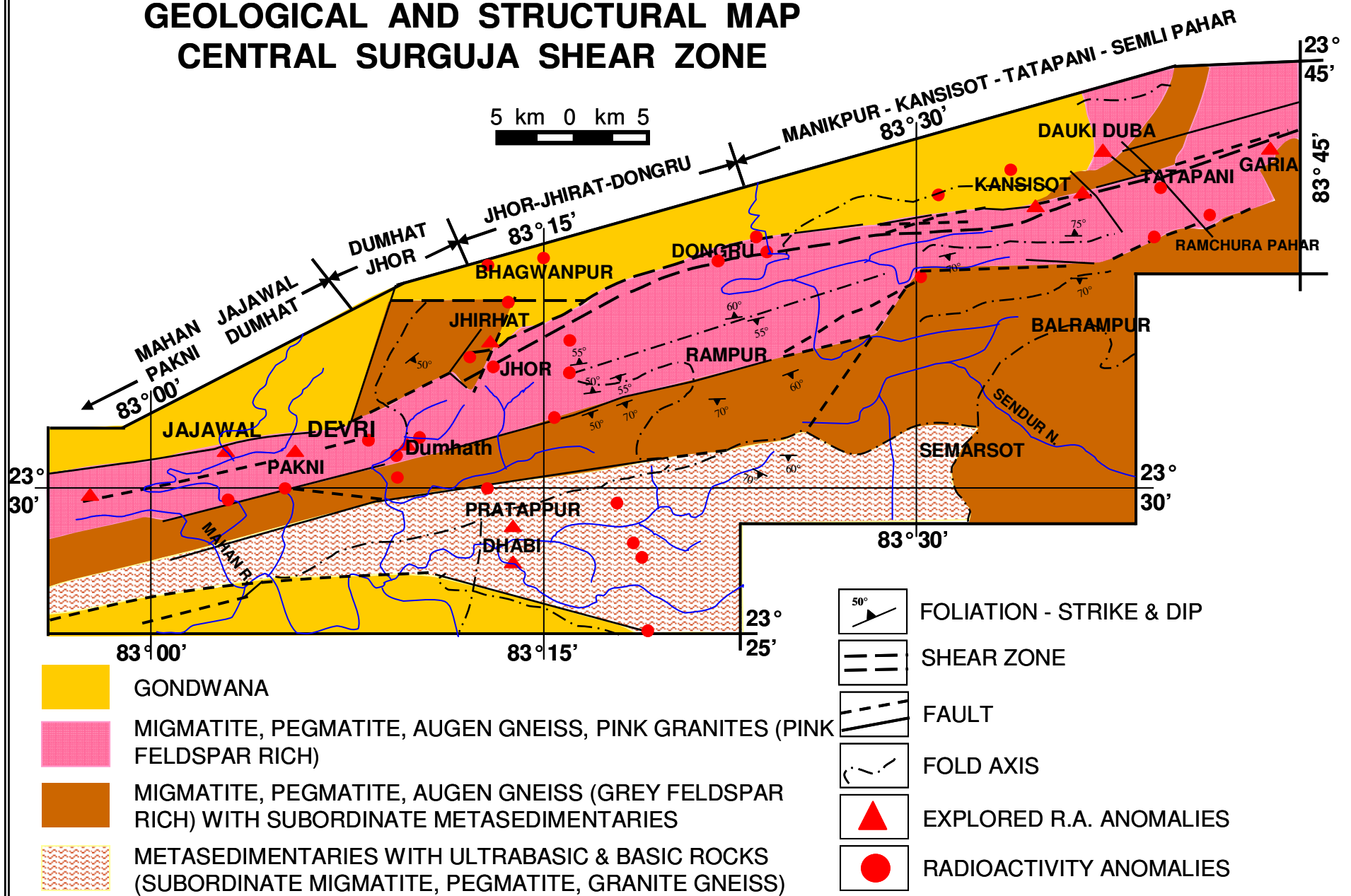
The meta-sedimentary suite of rocks present in the area were subjected to regional/ contact metamorphism upto amphibolite facies and a series of tight, doubly plunging antiform and synforms were generated with pro-grade metamorphism and partial melting and migmatization of precursor rocks.

Pro-grade metamorphism of pre-existing rock due to emplacement of granitic bodies reached upto amphibolite facies, which are evident in the form of development of garnet crystals in mafic and acidic rocks (Fig- 1.6 and 1.7). Similar kind of phenomenon has been observed in Jhoj nala section (Fig-1.8) where pre-existing rocks (metapellites and psammites) converting into granitic composition due to anatexis. They generally occur in the highest grade of regional metamorphic terranes as well as close to igneous intrusions (Vernon and Clarke 2008). This kind of evidence in the field has been observed, where rocks in the northern side in Jhoj nala section are migmatites whereas further south to this are granitic rocks exposed, therefore, Jhoj nala section could be inferred as contact zone of the two (Fig-1.8). The entire phenomenon viz, tectonism and metamorphism has mobilized and redistributed the uranium at several times, and were finally concentrated along the

shear zone/ cataclasite zone in substantial amount to make them a sizeable uranium occurrences.

With this analogy, systematic ground magnetic, IP (Time Domain)/Resistivity, susceptibility measurement and Gamma Ray Spectrometry (PGRS) surveys were carried out as part of M. Tech dissertation project work on “**Delineation, characterization and modeling of basement shear zones hosting uranium mineralisation using Magnetic and IP / Resistivity surveys at Devri area, Surguja district, Chhattisgarh, India.**” during the academic year 2010-11.

Fig- 1.1, Geological and Structural Map of Central Surguja Shear Zone  
**GEOLOGICAL AND STRUCTURAL MAP**  
**CENTRAL SURGUJA SHEAR ZONE**



# Geological Map of Dumhat-Devri Area, Sarguja District, Chhattisgarh, India Toposheet No.- 64M / 2 and 3

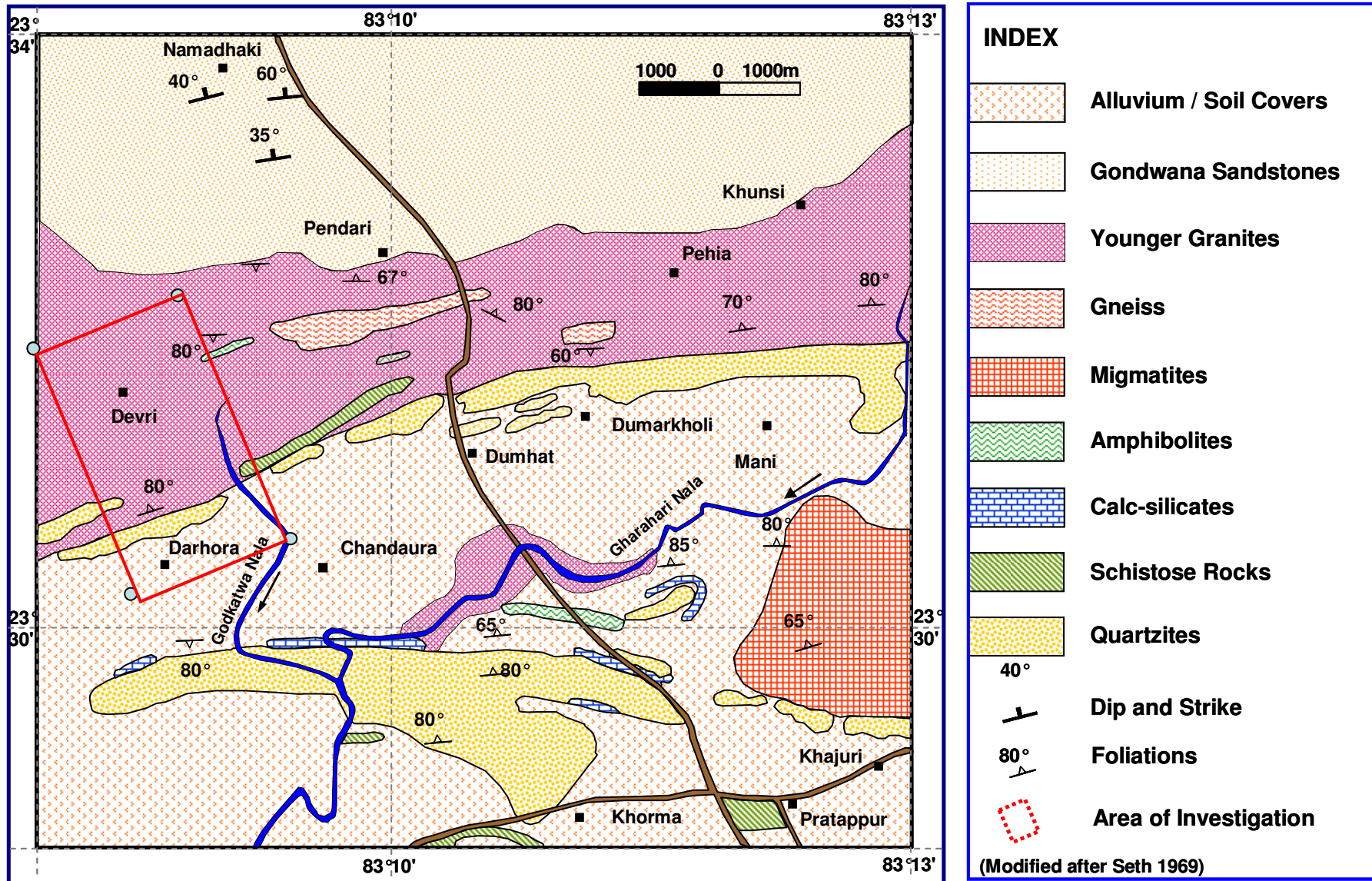


Fig- 1.2, Geological Map of Dumhat-Devri Area

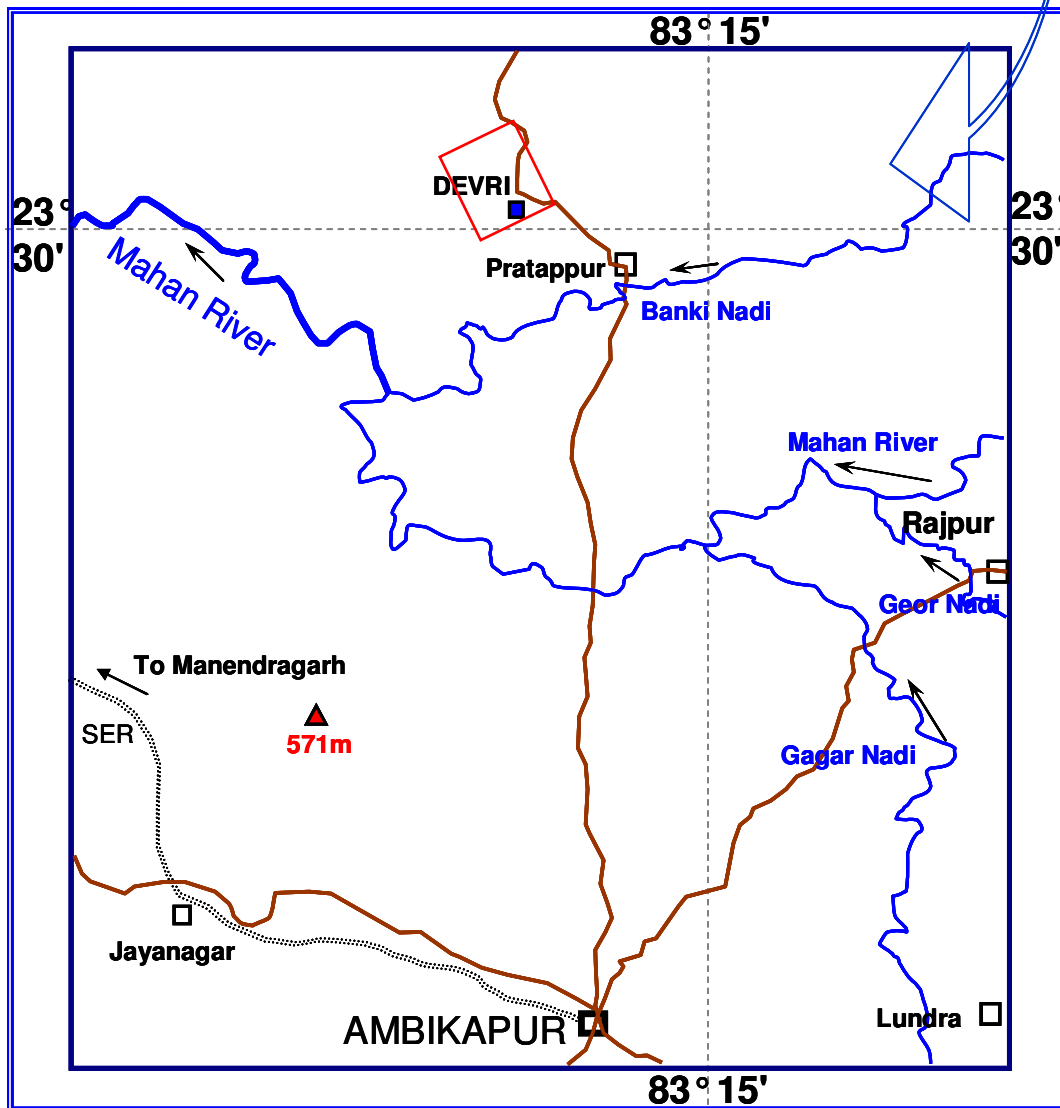
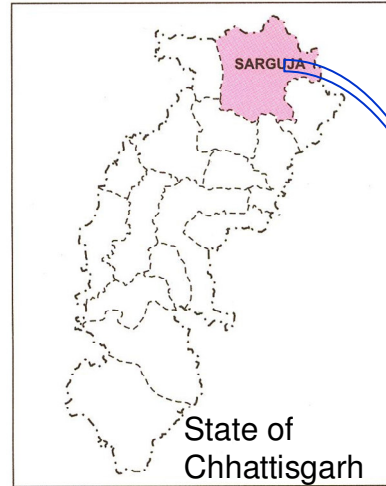
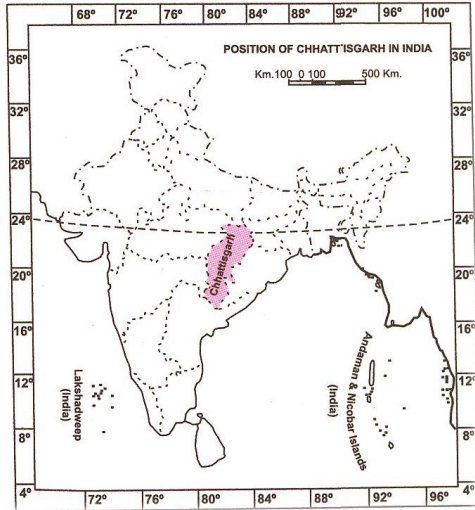


Fig-1.3 Location Map of Area



Fig-1.4 Plunging syncline and anticline developed in calc-silicate rock, representing 3rd generation of fold, Gharhari Nala section, 64M/3

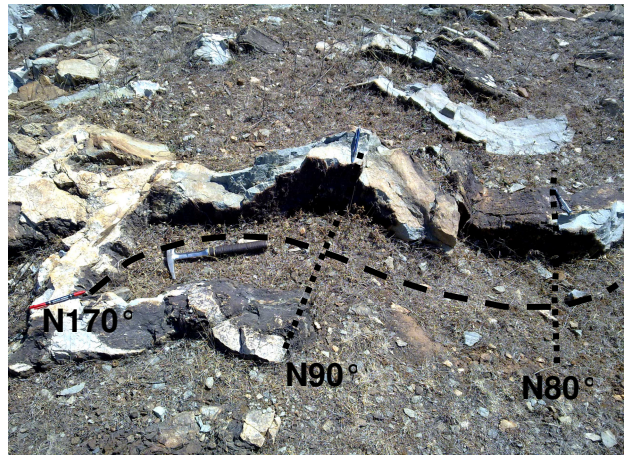


Fig-1.5 Hook shape fold developed in calc-silicate rock due to superimposition of 2nd and 3rd phase of folding, Barahaul, 64M/2

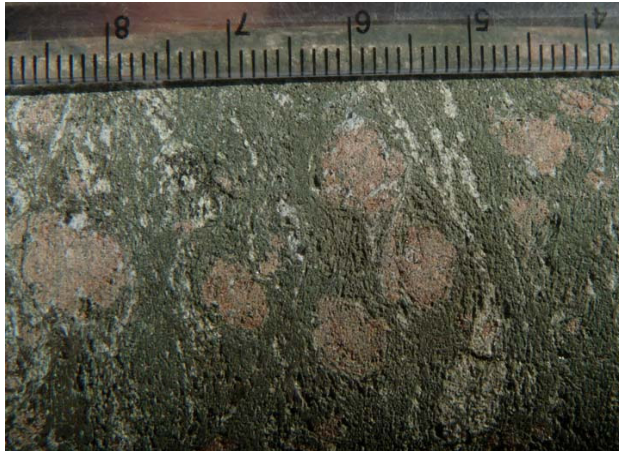


Fig-1.6 Development of garnet crystals in metabasic rock due to high grade metamorphism, borehole DEV-4/136.25m



Fig-1.7 Development of garnet crystals in metabasic rock due to high grade metamorphism, borehole DEV-3/278.00m



Fig-1.8 Partial melting (insitu) of psammitic rocks gave rise to granitic composition rock, Jhoh nala, 64M/2

## Field Photographs

# Magnetic Contour Map of Devri Area Sarguja district, Chhattisgarh, India Toposheet No.- 64M/2

Scale 1:10000  
100 0 100 200 300  
(m)

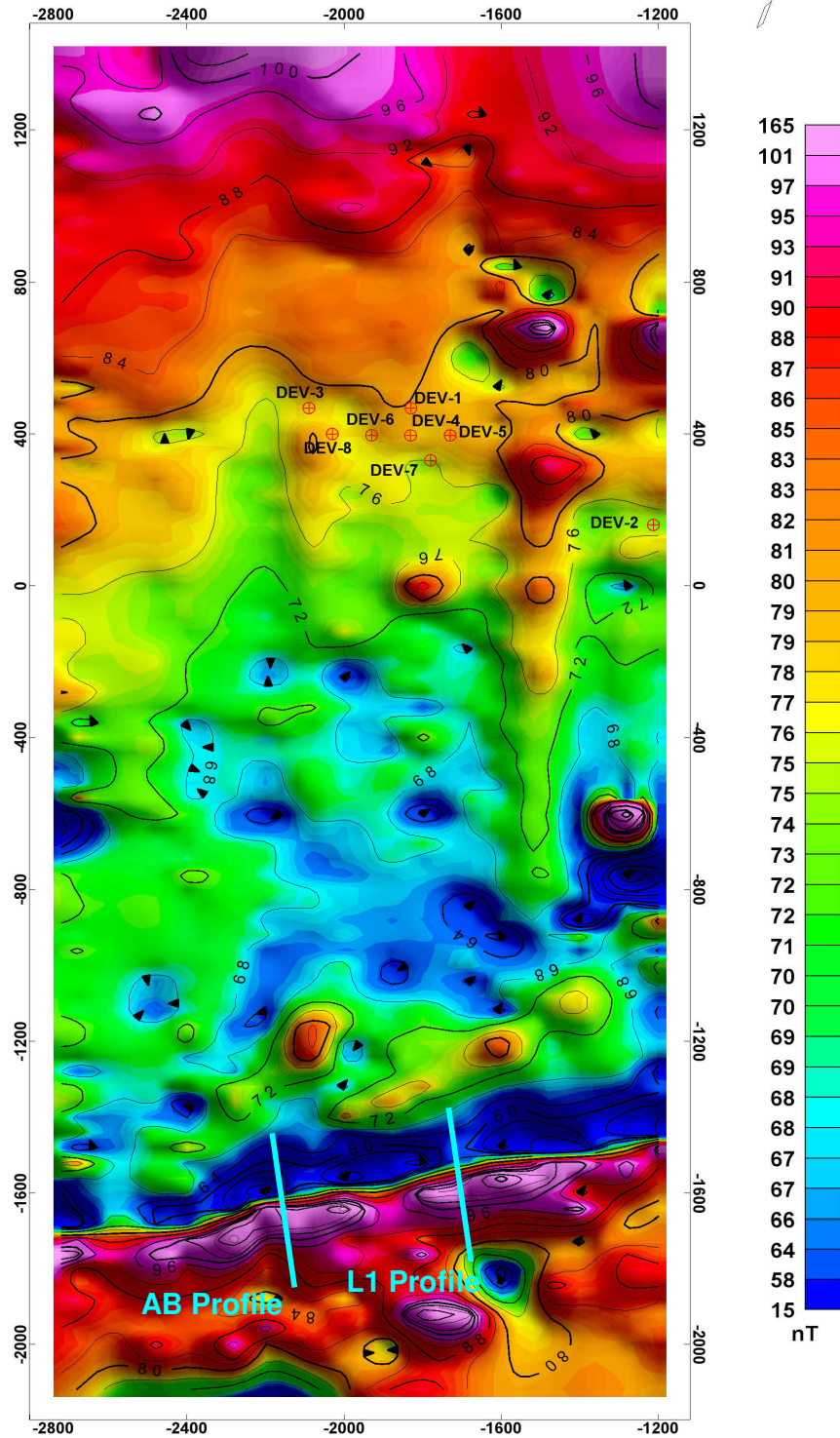


Fig-4.2

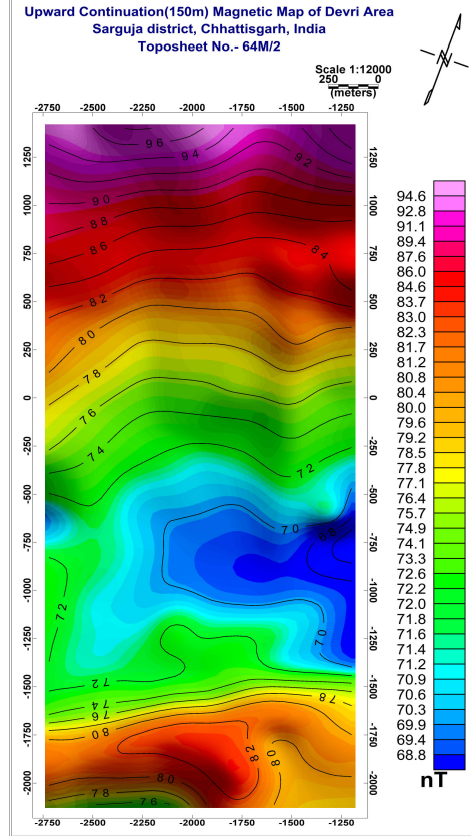
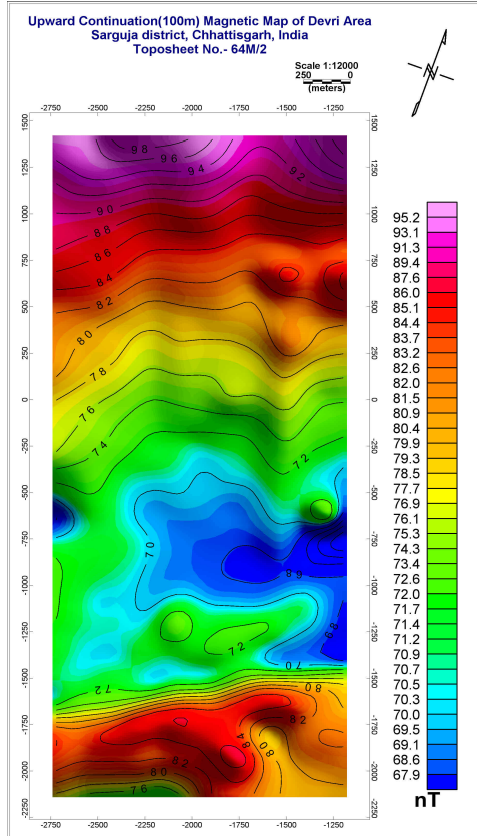
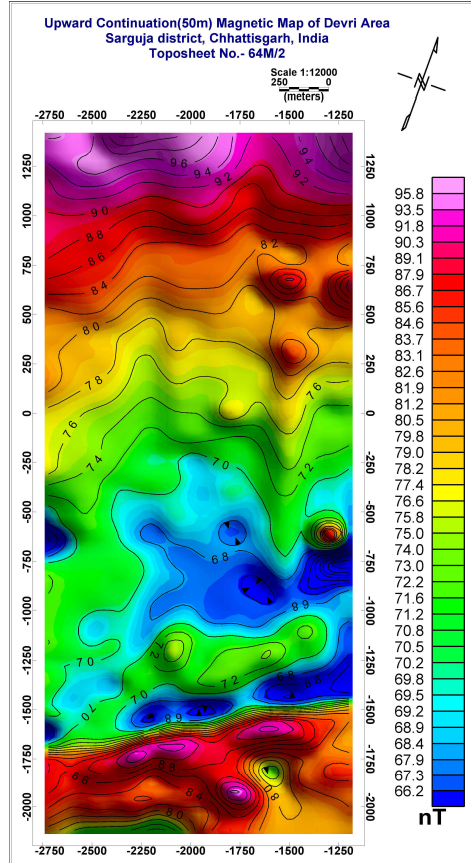
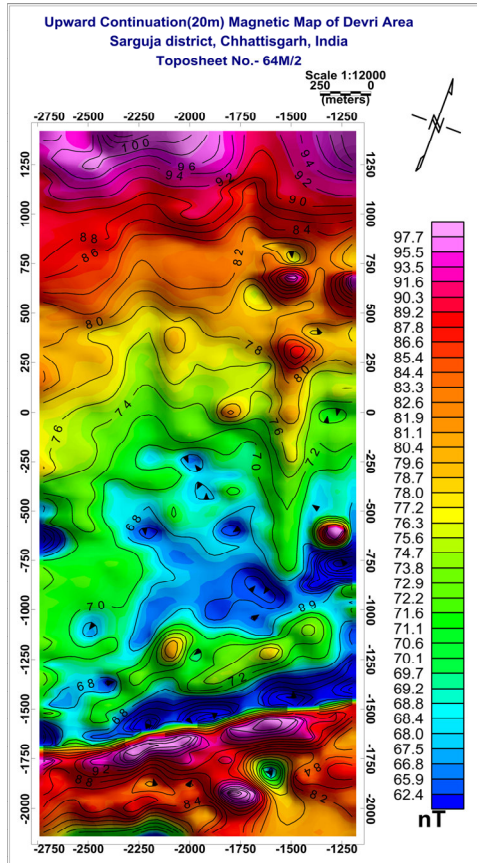


Fig-4.3

Reduced to Pole (RTP) Image of Devri Area  
 Sarguja district, Chhattisgarh, India  
 Toposheet No.- 64M/2

Scale 1:12000  
 250 0  
 (meters)

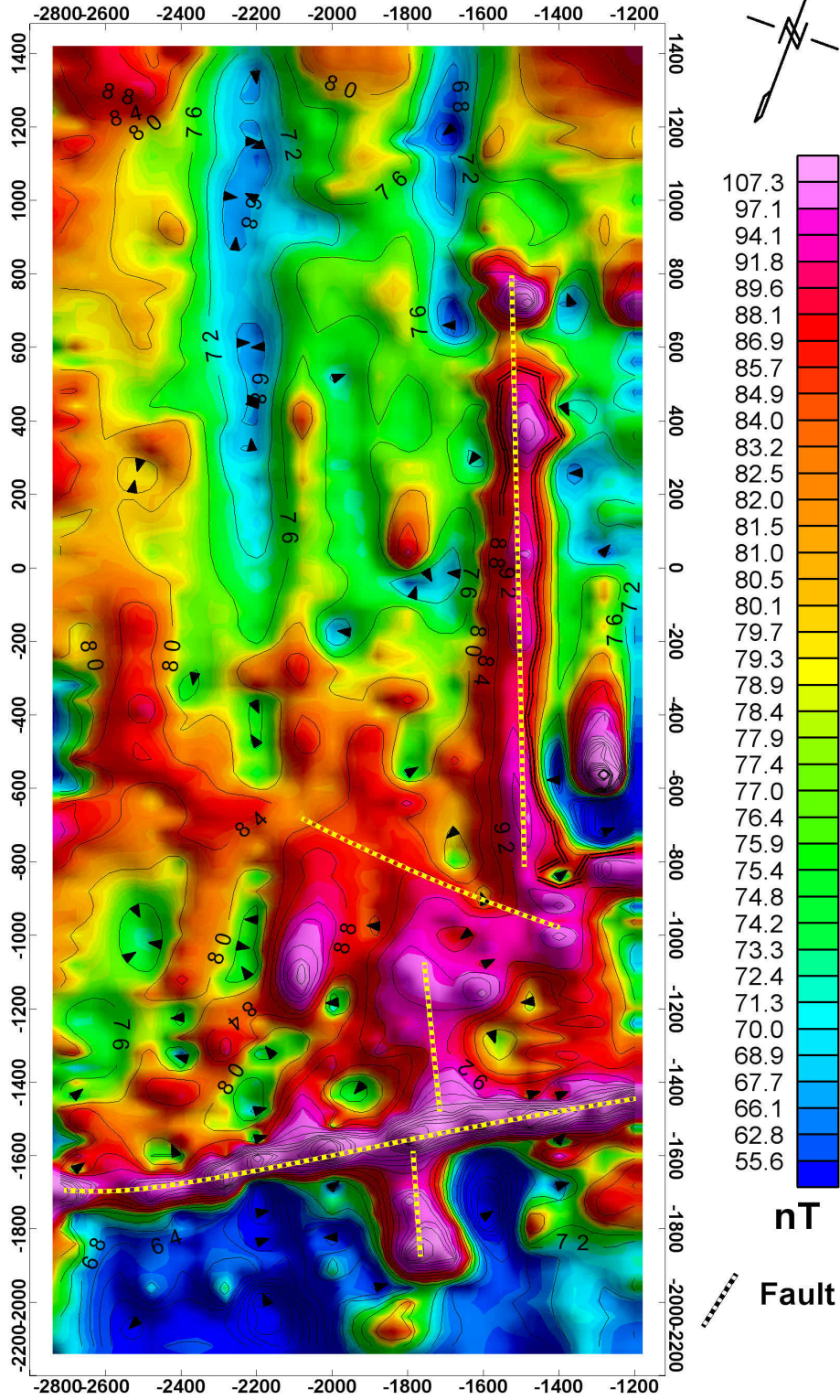


Fig-4.4

Horizontal (X) derivative Magnetic Anomaly Image

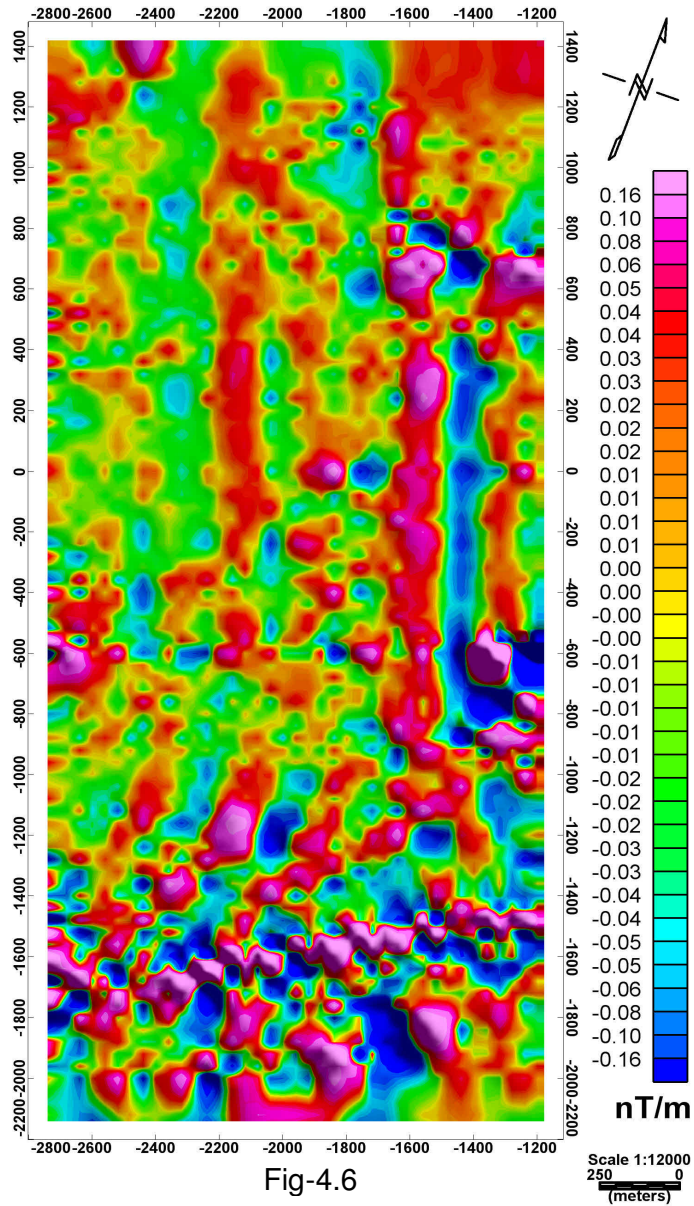


Fig-4.6

Vertical (Z) derivative Magnetic Anomaly Image

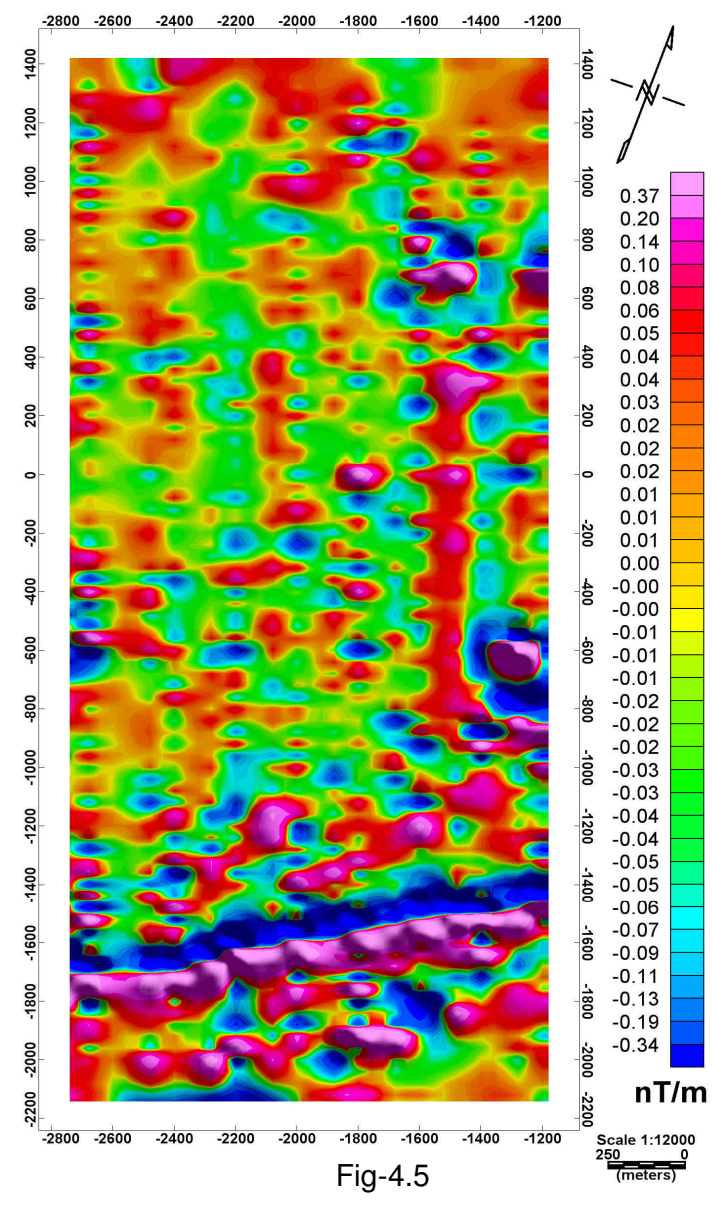


Fig-4.5

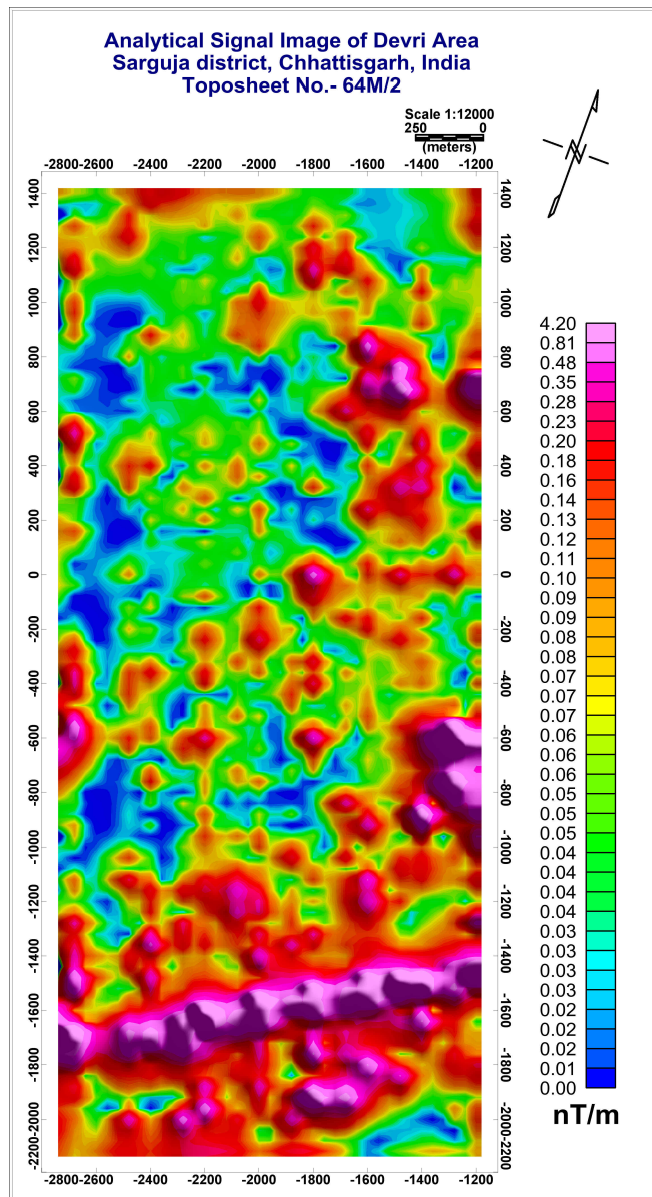


Fig-4.7

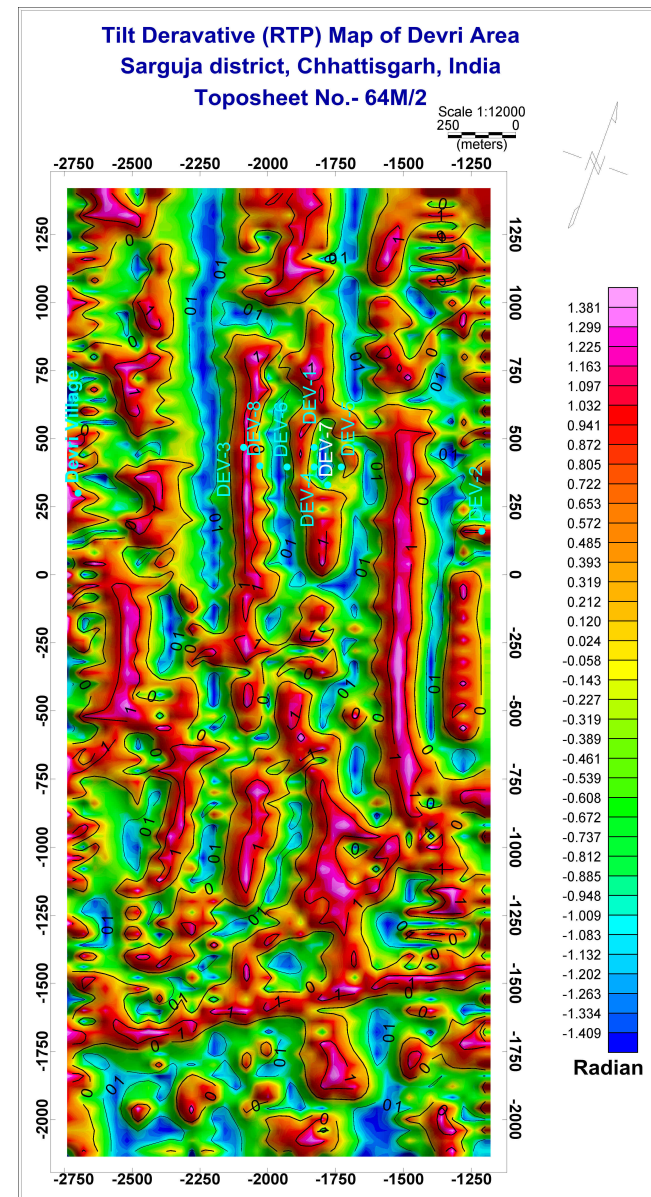


Fig-4.8

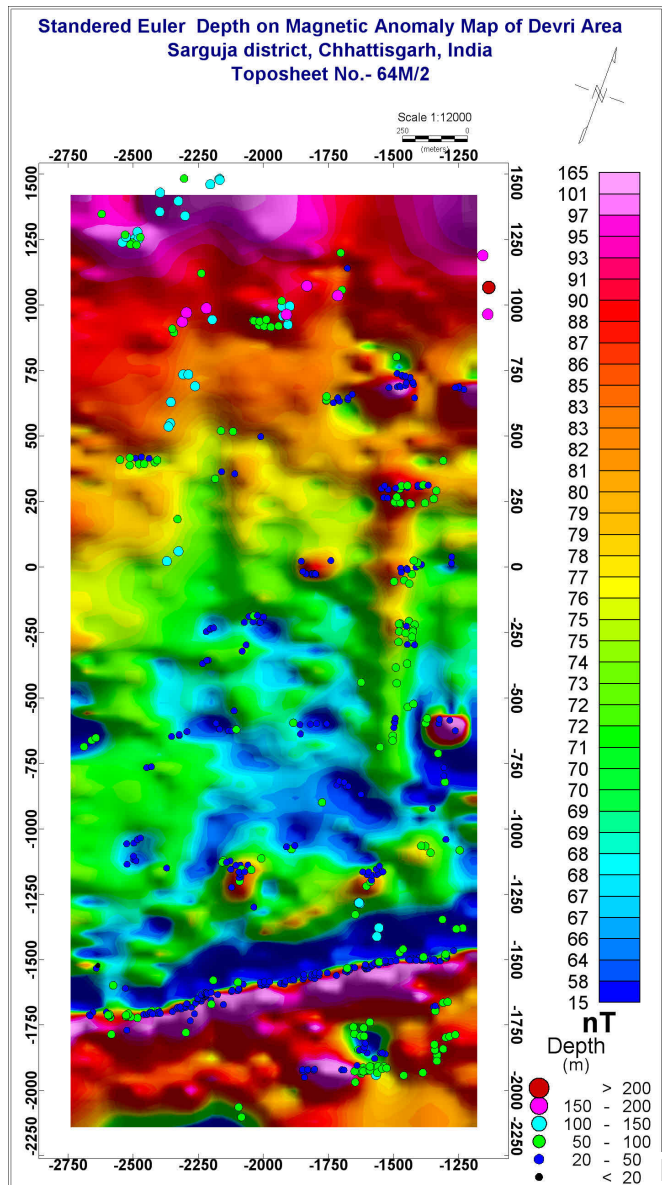


Fig-4.9a

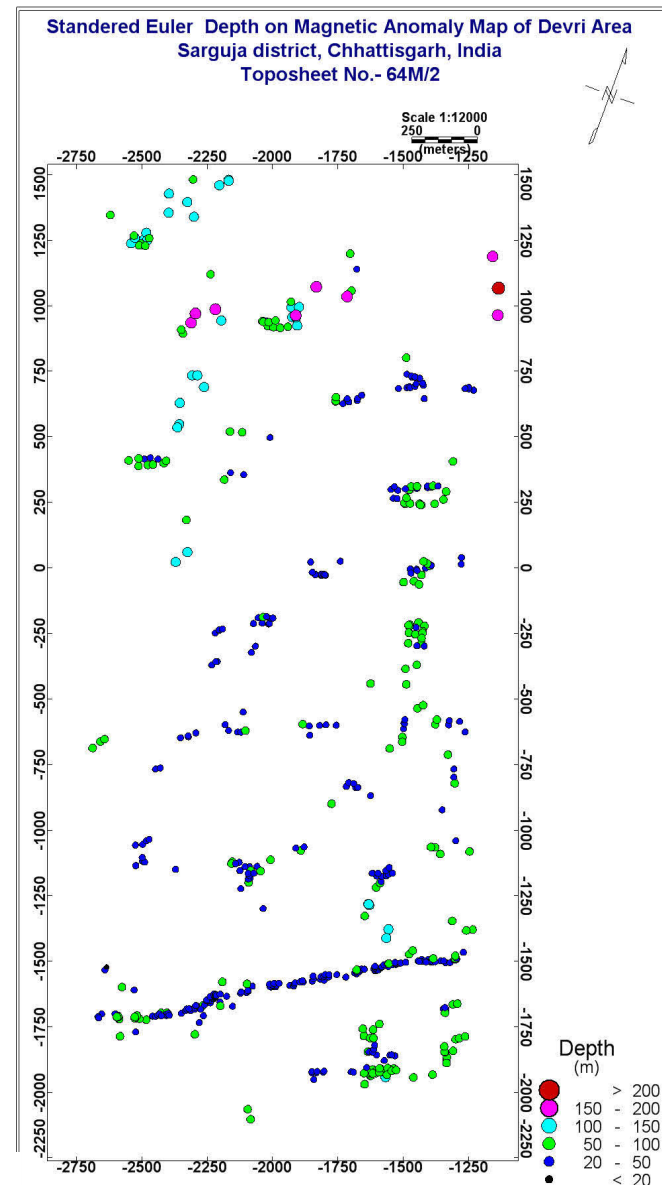
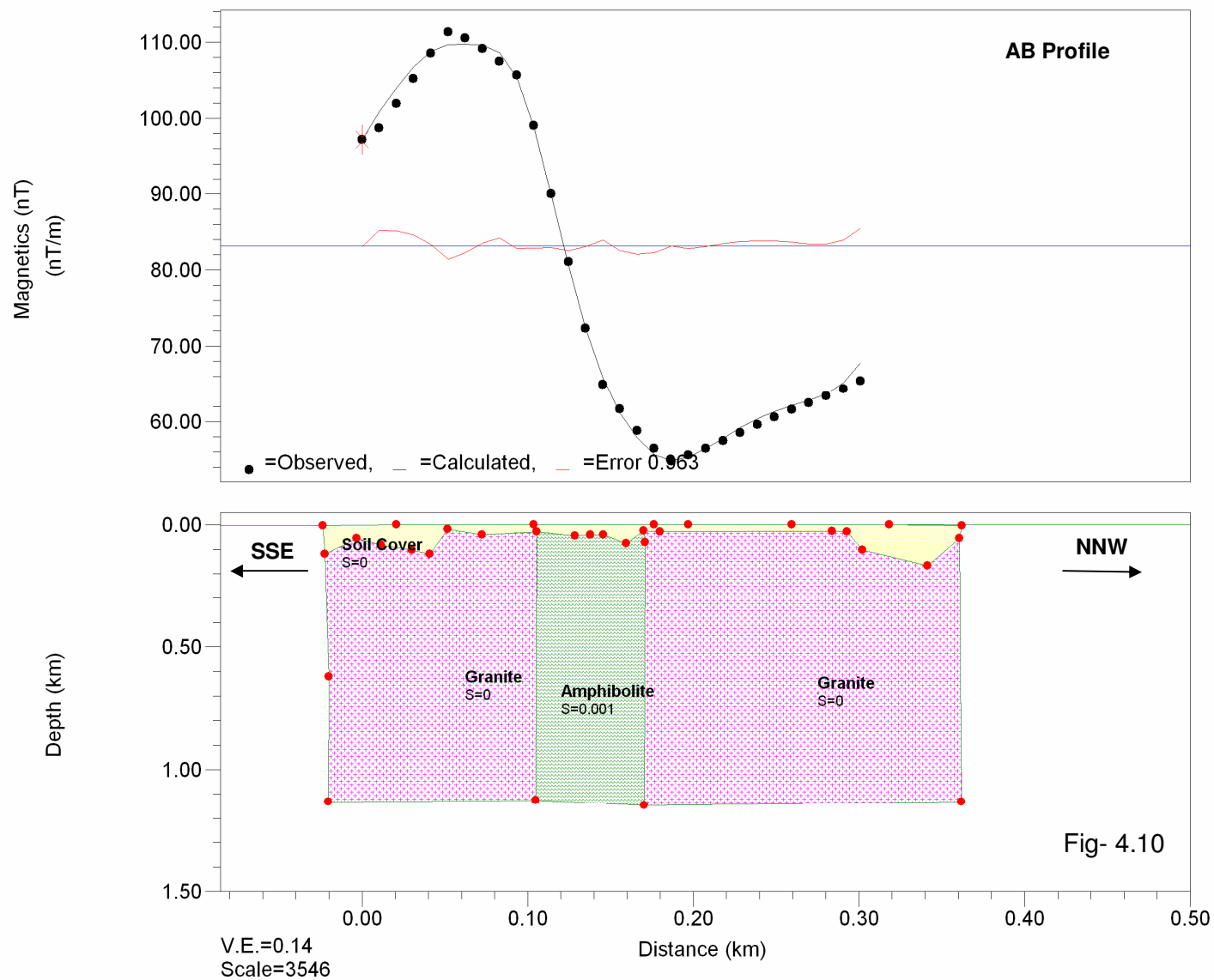


Fig-4.9b

### 2D Profile Modeling along AB Profile.



### 2D Profile Modeling along L1 Profile.

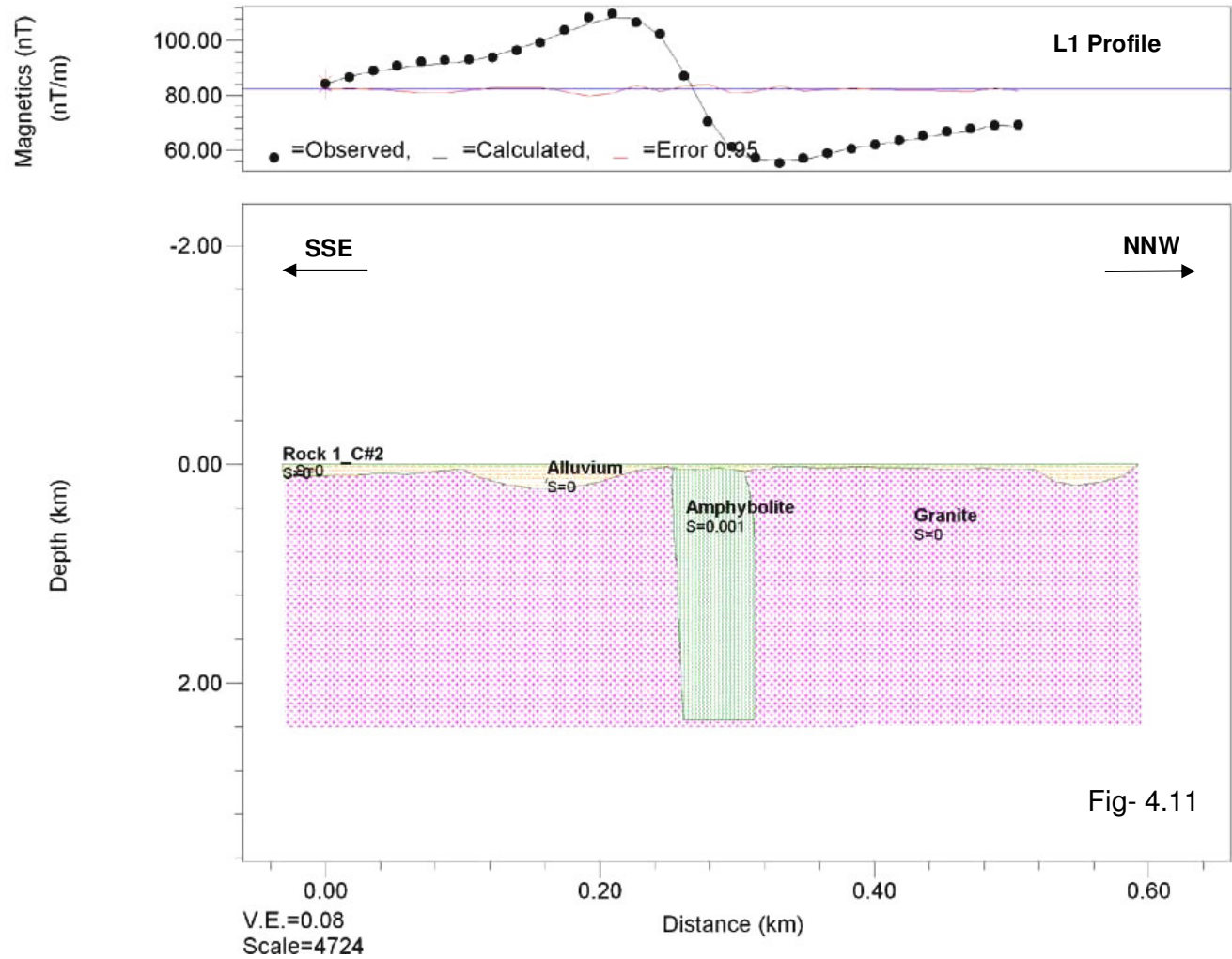


Fig- 4.11

### 2D Profile Modeling along L2 Profile.

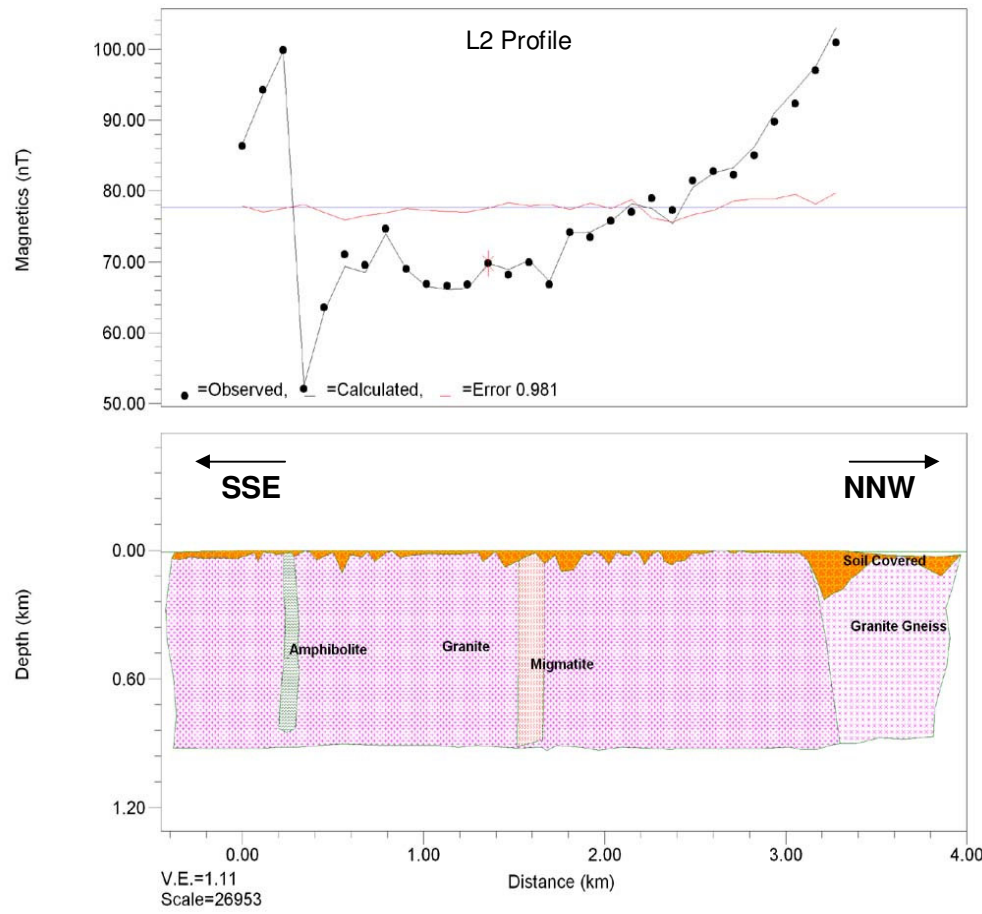
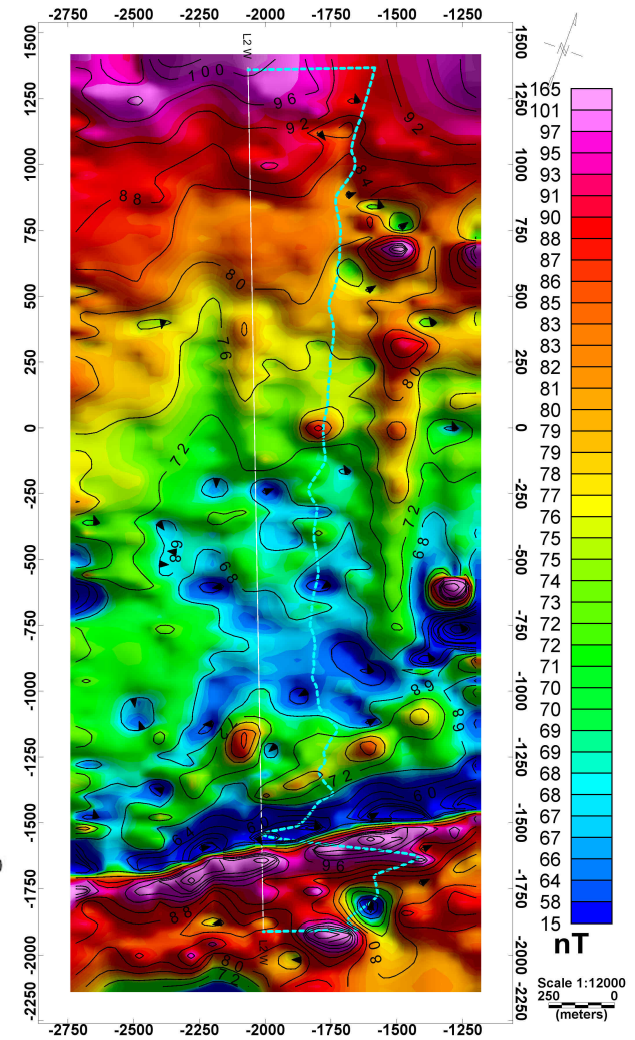
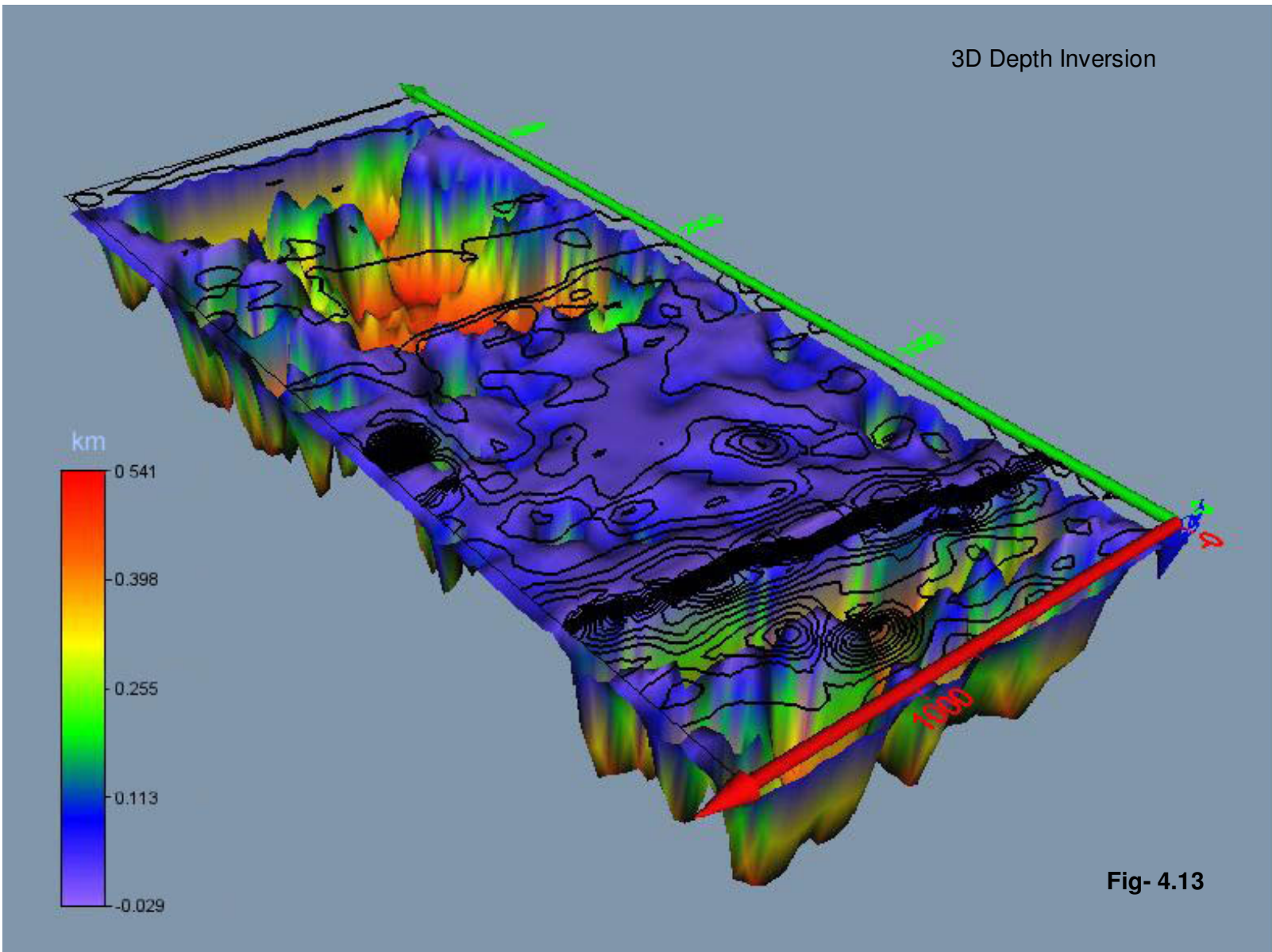


Fig- 4.12





# Resistivity Map of Devri Area District Sarguja, Chhattisgarh, India Toposheet No.- 64M/2

Scale 1:5000  
50 0 50 100 200 300  
(meters)

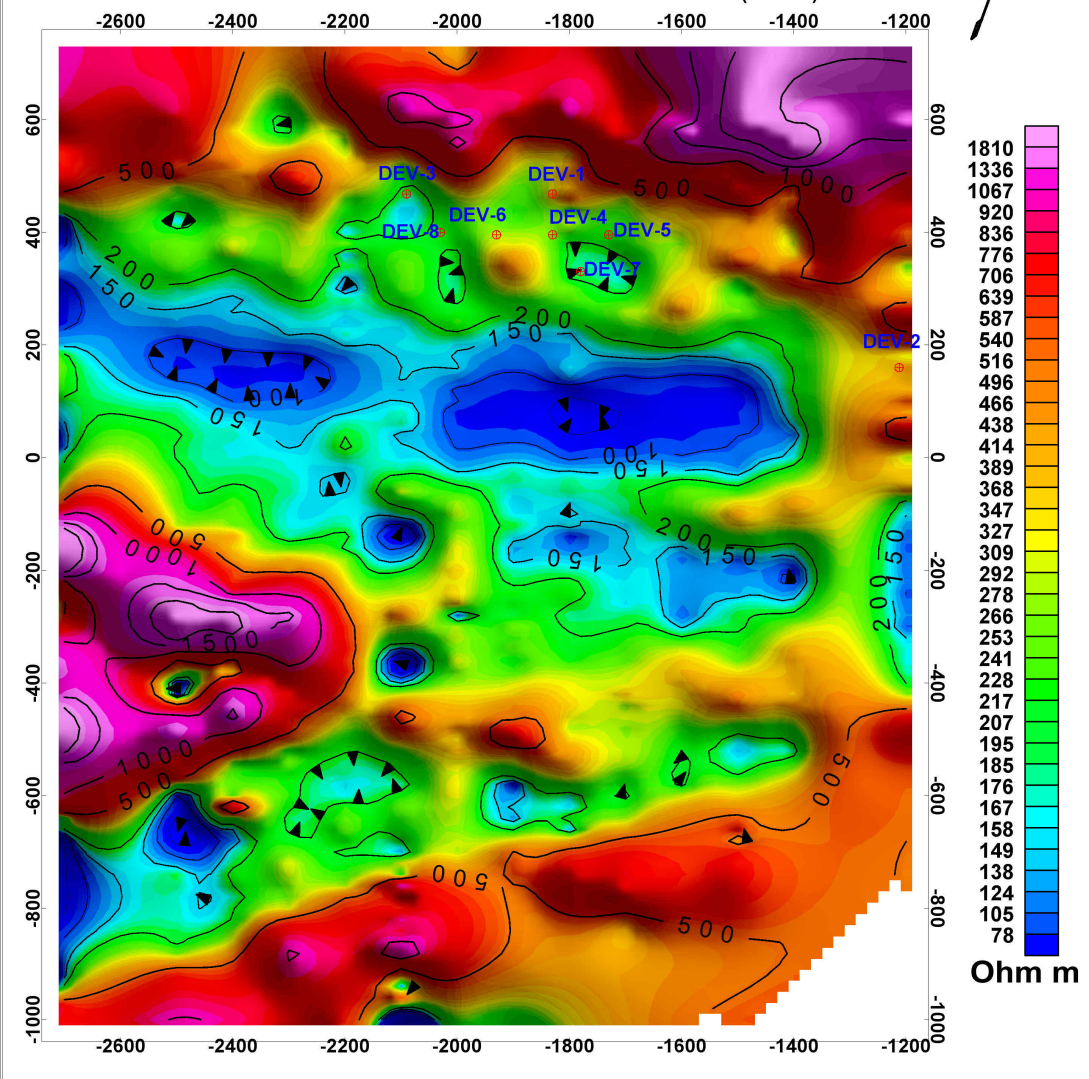


Fig- 4.15

Chargeability Map of Devri Area  
Sarguja district, Chhattisgarh, India  
Toposheet No.- 64M/2

Scale 1:5000  
50 0 50 100 200 300  
(m)

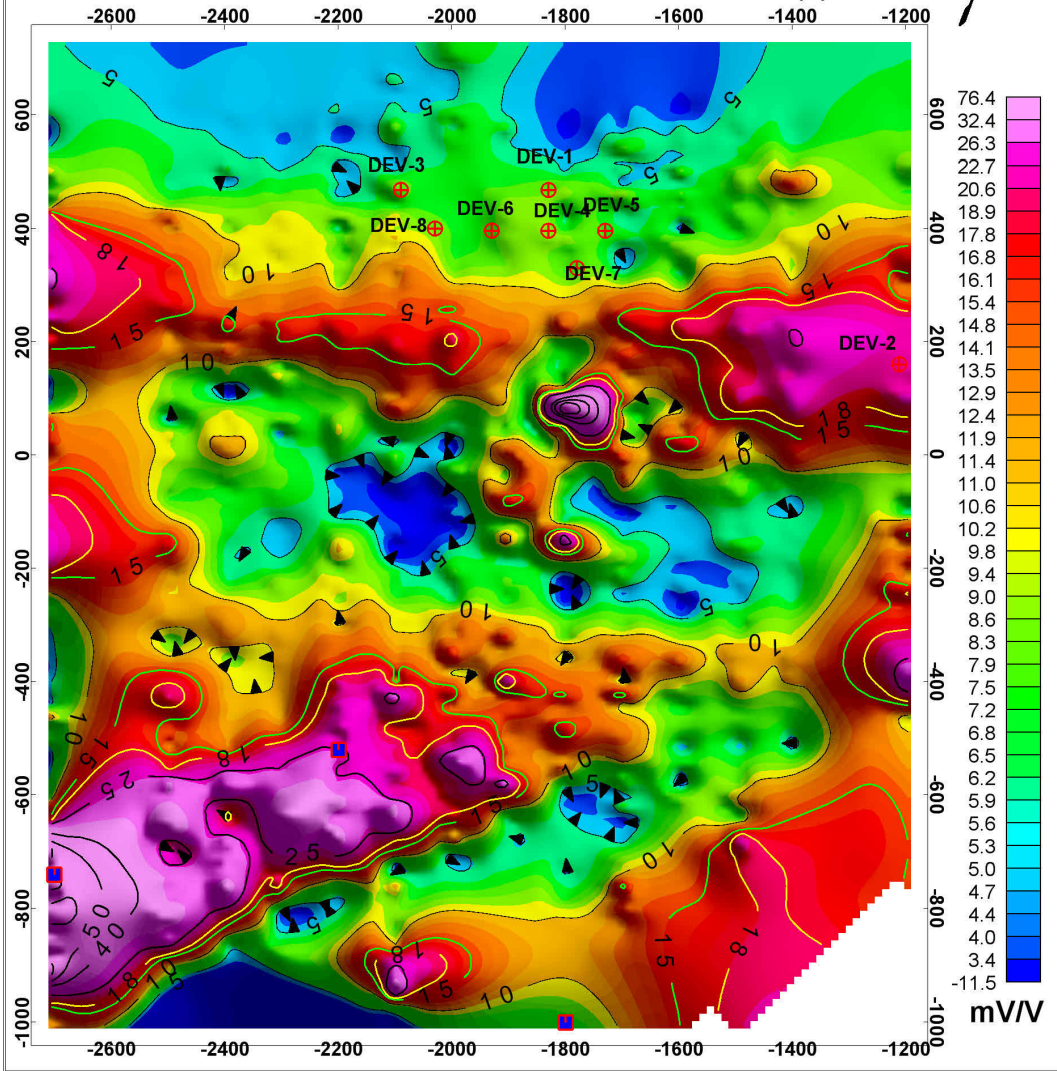


Fig- 4.17

**Low Resistivity And High Chargeability Contours Superimposed Over  
Magnetic Image of Devri Area**

**Sarguja district, Chhattisgarh, India**

**Toposheet No.- 64M/2**

Scale 1:12000  
250 0  
(m)

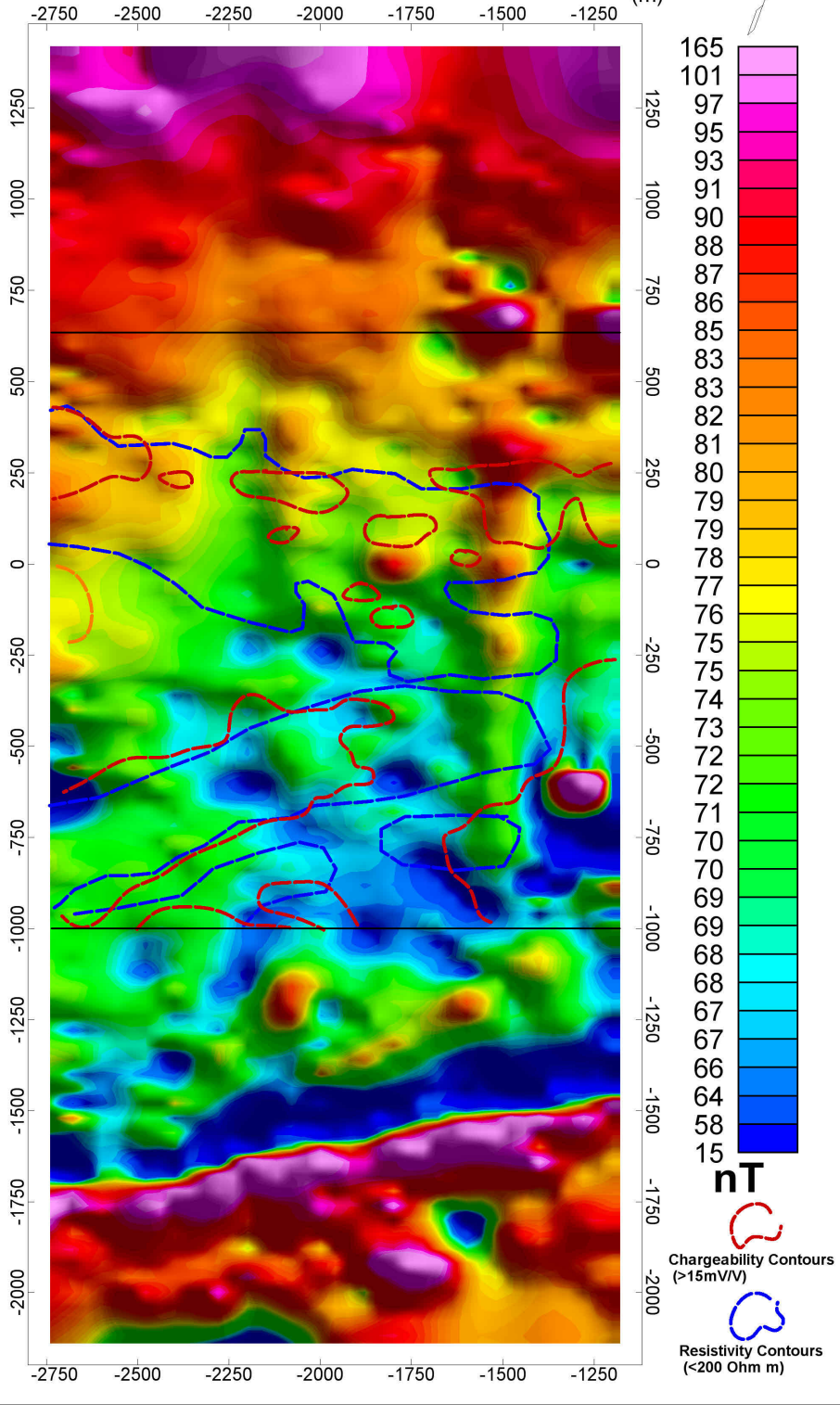


**Fig- 4.18**

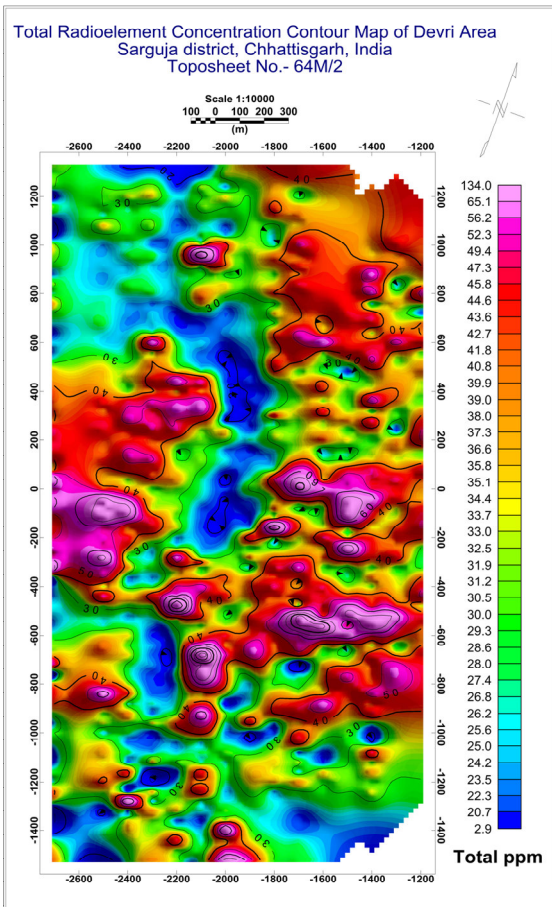


Fig-4.20

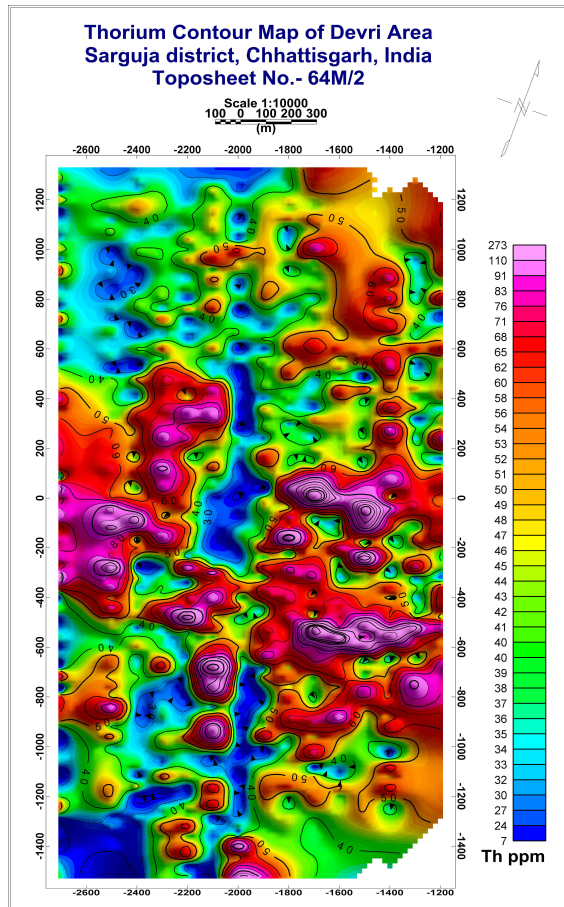


Fig-4.21

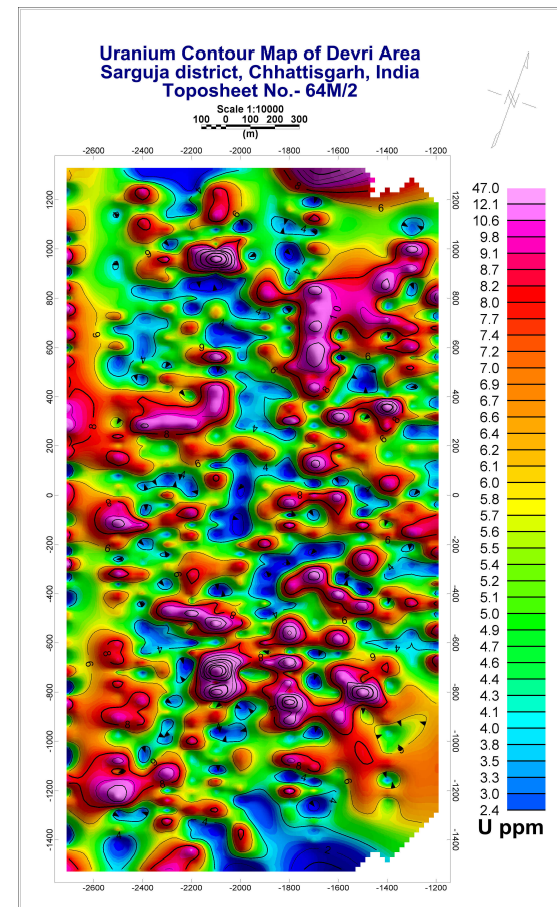
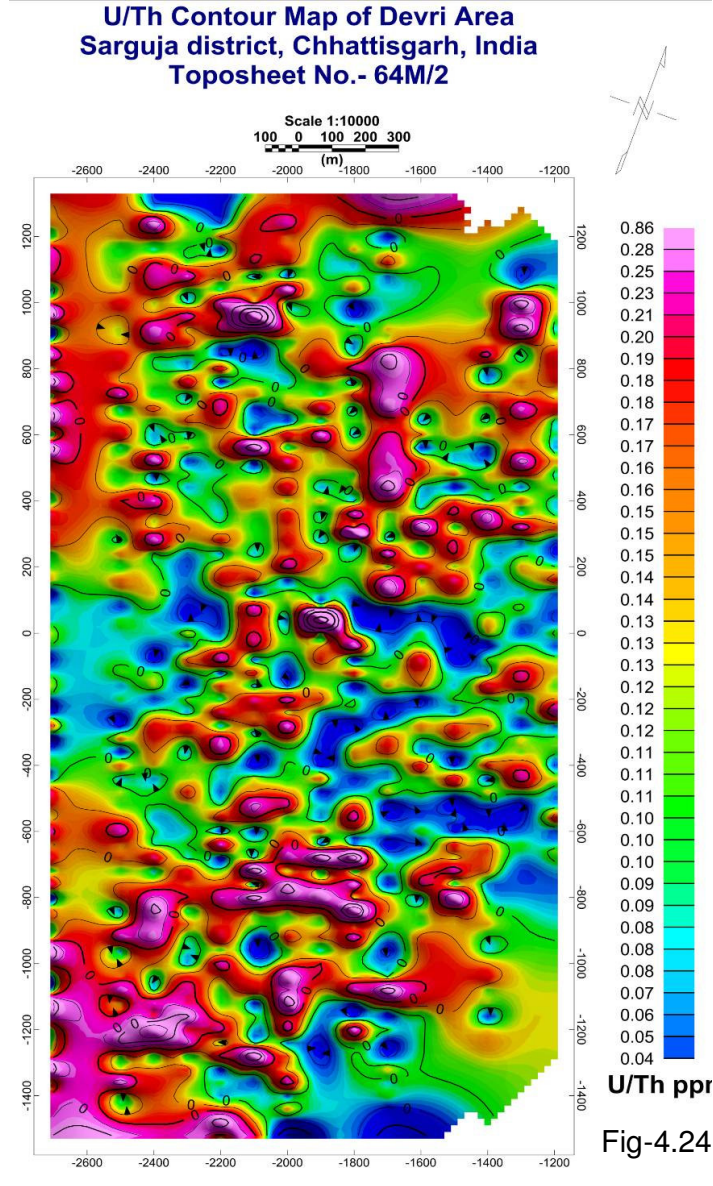
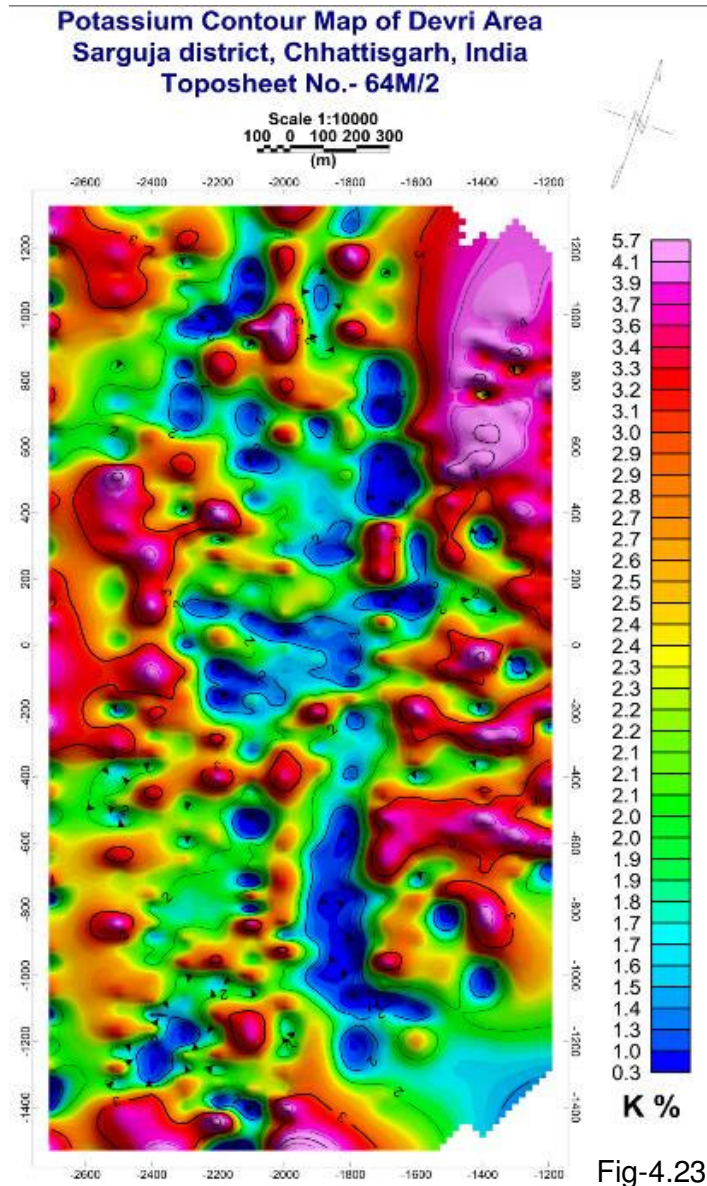


Fig-4.22



# ***Chapter 2***

## **Geophysical Surveys**

### **2.1 General**

The enhanced expansion in the demand for natural resources of all kinds led to the development of many geophysical techniques of ever increasing sensitivity for the detection and mapping of unseen deposits and structures. In this direction, some of the geophysical methods like gravity, magnetic, electrical, electromagnetic, seismic etc. play an important and indispensable role in comprehending the various intricacies of the subsurface of the earth. Further, the advent and advancement of computer hard and softwares besides a sea change in geophysical instrumentation, the task of data acquisition, processing and interpretation become elegant and efficient besides being effective.

Deducing some aspects of the earth's subsurface structure on the basis of measurements taken at the surface is invariably an inverse problem. Generally, such inverse problems suffer from an inherent ambiguity or non-uniqueness either at interpretation stage or in the conclusions. The degree of uncertainty in geophysical interpretation can often be reduced to an acceptable level by the general expedient of taking additional field measurements. However, the problem of inherent ambiguity cannot be circumvented. It is true that significant differences from an actual subsurface geological situation may give rise to insignificant or immeasurably small differences in the quantities actually measured during a geophysical survey. Thus, ambiguity arises because many different geological configurations could reproduce the observed measurements. This basic limitation

results from the inevitable fact that geophysics attempts to solve a cumbersome inverse problems.

It is to be realized that experimentally derived quantities are never exactly determined and experimental error adds a further degree of indeterminacy to that caused by the incompleteness of the field data and the ambiguity associated with the inverse problem. Generally, a unique solution can't be found from a set of field measurements, geophysical interpretation is concerned either to determine properties of the subsurface that all possible solutions share or to introduce assumptions to restrict the number of admissible solutions. In spite of the inherent problems, however, geophysical methods are inevitable tools for the investigation of subsurface geology and occupy a key role in exploration programs for geological resources.

Identification of concealed geological structures holding mineralization is indeed a critical exercise in exploration programs. Many geophysical methods, which work on different physical properties, are in vogue to provide solutions to such geological problems. These methods are based on different physical property principles and therefore have different operational techniques. The success of any geophysical method to solve a geological problem depends on the physical property contrast of the source of interest with the surrounding rock formations. The target of interest, in general, responds quite differently to different fields of input. Therefore, results that are more acceptable can be expected by studying these responses in an integrated manner.

Geophysical exploration methodology comprises measurement and interpretation of geophysical signals from natural and induced physical

phenomena generated as a result of spatial changes in one or more physical properties of a subterranean formation. These signals measured at several points of space and times are appropriately interpreted, considering the available geological information, in terms of sub surface structures or features of geological interest.

The inhomogeneities in physical properties of the subsurface rocks, in general, produce micro level deviations in the measured physical fields or parameters. These deviations of the measured quantities from the normal distribution, expected due to homogeneous subsurface conditions, are referred to as geophysical anomalies and they form diagnostic measures to the inhomogeneities in the subsurface. Detailed study of the intensity, character and distribution of these geophysical anomalies, amenable to locate the inhomogeneities, giving rise the observed departures in the physical fields or properties.

Unequivocally, the spatial location of concealed targets and geologic translation of geophysical measurements/interpretation still poses a formidable challenge to practicing geophysicists and at times continues to be cumbersome. In this direction, deducing some aspects of the earth's subsurface structure on the basis of measurements taken at the surface is invariably an inverse problem. Generally, such inverse problems suffer from an inherent ambiguity or nonuniqueness either during interpretation or toward conclusions. The degree of uncertainty in any geophysical interpretation often can be reduced to an acceptable level by integrating other geophysical field measurements to solve such problems, thereby minimizing or eliminating inherent ambiguity.

Based on the above criteria an integrated geophysical methodology comprising of magnetic, resistivity and IP is adopted for geophysical fieldwork in the study area to identify potential target zones for Uranium exploration. Electrical and magnetic methods measure different rock properties, and each one is more effective when the contrast is significant, although these contrasts may occur at different depths for each method. For example, resistivity data are more sensitive to vertical resistivity changes; in contrast, magnetic data are more sensitive to lateral changes in the magnetization of the rock formations.

A brief description of each method including its operation principles, data acquisition and subsequent processing and modeling are discussed hereunder.

## **2.2 Magnetic surveys**

Magnetic surveys play vital and significant roles in mineral exploration, regional geological mapping and mining exploration. When the surveys are aimed to trace basement configuration the alluvium cover is generally presumed to be nonmagnetic acts as magnetically transparent medium, whereas underlying basement consisting of magnetic minerals produces the magnetic anomalies. These magnetic anomalies can be analyzed quantitatively for the basement configuration after properly accounting for regional magnetic field.

### **2.2.1 Origin of magnetic field**

Before carrying out magnetic survey, it is necessary to understand the origin and factors influencing the Earth's magnetic field. The cause of geomagnetic field is attributed to a dynamo action produced by the circulation of charged particles in coupled convective cells within the outer, fluid part of the Earth's core. The exchange of dominance between such cells is believed to produce the periodic changes in the polarity of the geomagnetic field revealed by palaeomagnetic studies. The circulation patterns within the core are not fixed and change slowly with time. This is reflected in a slow, progressive, temporal

change in all the geomagnetic elements known as secular variation. Magnetic effects of external origin cause the geomagnetic field to vary on a daily basis to produce diurnal variations. Occasionally the earth's magnetic field is affected by strong solar flux caused by sunspots, which creates a magnetic storm. The interaction of the earth's field with rocks induces a magnetic field proportional to the magnetic susceptibility. Time variations in the magnetic field must be removed to map the spatial distribution of the field, which is useful for mapping the subsurface geology.

### **2.2.2 Principle of magnetic prospecting**

Magnetic method works on measuring the properties of the magnetic field of the earth. The induced magnetic field in crustal rocks has a magnitude approximately proportional to the earth's magnetic field, and lies close to the direction of the earth's field. The crustal rocks also possess a permanent magnetization, namely the remnant magnetization acquired during the process of their origin and the magnitude and direction of this magnetization are unrelated to the present earth's field. The crustal rocks are thus magnetized with a magnitude and in the direction, of the resultant of the induced and remnant magnetizations. By virtue of this resultant magnetism, all the crustal rocks produce their own magnetic fields superimposed over the normal field. The earth's normal field can be calculated or determined based on its uniform variation over large areas, and removed from the observed, for the magnetic field anomalies. The magnetic anomalies can be measured in three components viz., the vertical, horizontal and the total field. Except the case of vertical field anomalies, the total and horizontal field anomalies are calculated making an indispensable assumption that the earth's normal field is undisturbed by the anomalous field. But the magnetic anomalies are often large and can deflect the

earth's field from its normal position appreciably. Therefore, the quantity measured with a total field magnetometer is the magnitude of

$$F+F_1 = (F^2+F_1^2+2FF_1\cos\theta)^{1/2}$$

Where  $F$  is the earth's normal field and  $F_1$  is the anomalous field and  $\theta$  is the angle between  $F$  and  $F_1$ . The quantity finally calculated is equal to

$$(F^2+F_1^2+2FF_1\cos\theta)^{1/2} - F$$

and will be equal to  $\Delta F=F_1\cos\theta$ , only if  $F_1 \ll F$ .

Assuming that the magnetization is caused purely by induction, a body striking at an angle  $\alpha$  due west at the equator will be magnetized by the component  $H \sin\alpha$  in a horizontal direction perpendicular to the strike. Here,  $H$  is the horizontal component of total magnetic field vector along the magnetic north. Since the vertical component is zero, the effective magnetization is horizontal for all values of  $\alpha$  and hence the magnetic anomalies for different values of  $\alpha$  differ only in size. Further, there is no distinction between the total field and its horizontal component at the equator and hence total field anomalies will be identical to horizontal magnetic field anomalies.

### 2.2.3 Instruments

In present study proton precession magnetometer (model **GSM 19T**) was used for field data collection whereas **Geomatrix G-856** system was used for base station data collection. PPM works on the principle of spin of protons in a magnetic field, which is given by modified Larmor equation. (Kearey and Brooks, 2002).

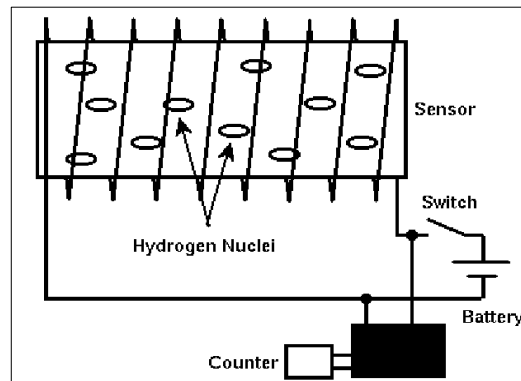


Figure 2.1 Principle of Proton Precession Magnetometer

$$f = \gamma B / 2\pi$$

f - Angular frequency;

$\gamma$  - Gyromagnetic ratio and B-Magnetic field strength.

The sensor of the proton precision magnetometer is a cylindrical container filled with liquid rich in hydrogen atoms such as kerosene or decane, or distilled water or alcohol and is surrounded by a coil (Figure-2.1). The sensor is connected to the precession unit (power supply, amplifier, frequency counter and display units) by a cable. The hydrogen atoms act as small dipoles and normally align parallel to the ambient geomagnetic field. When switch is on, a DC current is directed through the coil, producing a relatively strong magnetic field (50-100 times higher the geomagnetic field) in the fluid filled cylinder in different direction. This causes the protons to realign in this new direction. The current to the coil is then switched off so that the polarizing field is rapidly removed. The protons return to their original alignment by spiraling or precessing, in phase around this direction with a period of about 0.5 milliseconds, taking 1-3 seconds to attain their original orientation. This precession produces time varying magnetic field that induces a small alternating current in the coil. The frequency of the AC current is equal to the frequency of the precession of the nuclei and is proportional to the strength of the total magnetic field.

#### **2.2.4 Data Acquisition**

Magnetic surveys are planned based on the targets being looked for, areas to be investigated in addition to the nature of anomalies sought. In the present case the surveys are carried out with an aim to investigate the characteristics of shear and fracture zones hosting uranium mineralization, which

mostly occur in lenses of small dimensions. Keeping the dimensions of the objectives in view data were collected at 20m interval along a series of profiles. The trend of the shear zone is N70°E-S70°W; therefore the traverse lines were laid perpendicular to it in N20°W-S20°E direction.

### **2.2.5 Corrections**

The magnetometer readings recorded in the field not only relate to the earth's magnetic field but also include various extraneous disturbances in addition to the anomalies due to local geology. Aim of the magnetic survey is to get appropriate response from target. Hence, it is necessary to remove the former two components. The diurnal correction is applied to correct for temporal variations in the measured magnetic field. For applying this correction a base station is established in such a manner that it should be away from extraneous disturbances such as high power lines, metalled roads and it should be far removed from underground anomalous sources. Keeping all these factors in mind, primary magnetic base station was established near to camp (Dhabi). The diurnal correction is achieved by subtracting the field magnetometer reading at the base at the start of the survey from all the field readings and the residues are corrected for the variation as recorded by the base magnetometer. The application of diurnal correction yields absolute difference in the main magnetic field between the field and base station and the anomaly due to the magnetized target.

### **2.2.6 Interpretation**

Magnetic anomalies are mainly due to the variation in susceptibility and/or the remnant magnetism of rocks and minerals. The interpretation of magnetic

anomalies is generally complex because of the fact that the anomalies are of bipolar in nature; the shape of the anomaly is dependent on both the magnetic latitude and strike of the anomalous body. In addition, the presence of remnant magnetism, which is unknown many a time, would further complicate the interpretation.

Magnetic data can be interpreted in two distinct ways viz: qualitative and quantitative. The qualitative process is largely map-based and dominates the early stages of a study. The resultant preliminary structural element map is the cornerstone of the interpretation. Qualitative interpretation involves recognition of the nature of discrete anomalous bodies including intrusions, faults and lenticular intrasedimentary bodies with relative ages of intersecting faults and structural styles. In this stage, various maps and images are generated to highlight or suppress specific patterns, features and trends in the data.

Quantitative interpretation can be done either in profile mode or in grid pattern to quantify the anomalous sources.

### **2.3 Electrical Survey**

Electrical prospecting involves the detection of surface effect produced by electrical current flow in the ground and resulting potential differences are measured at the surface. Deviation in pattern of potential differences as expected from homogeneous ground, provide information on the form and electrical property of subsurface inhomogeneities. Using this method one can measure the potential, current and electromagnetic field that occur naturally. The measurement can be made in variety of ways to determine different results. This method includes self potential, resistivity, induced polarization, magnetotellurics

etc. In present case resistivity and induced polarization methods of electrical method were used to find out the apparent resistivity and chargeability of the ground which in turn reflect the geology and structures present underneath.

### **2.3.1a Principles of Resistivity Survey**

Resistivity techniques are based on the response of the earth to the flow of electrical current. In this method, direct or low frequency alternating current is introduced into the ground by means of two metal electrodes and the resulting potential differences are measured at the surface between another two suitably arranged electrodes. Deviation from the pattern of the potential differences expected from homogeneous ground, provide the information on the form and electrical properties of subsurface material.

Most rock forming minerals are insulators, and electric current is carried through rock mainly by the passage of ions in pore waters. Thus, most rocks conduct the electricity by electrolytic rather than electronic processes therefore porosity play major role in resistivity of rocks.

The resistance  $R$  is directly proportional to the length and inversely proportional to the cross sectional area, i.e.  $R \propto L/A$  or  $R = \rho L/A$  where  $\rho$  is electrical specific resistance. As per the ohm's law, the resistance is  $R=V/I$  and the equation become  $\rho =A/L \times V/I$ . As we know resistivity is a physical property of material and ground materials under investigation are heterogeneous, therefore resistivity will vary with the relative positions of the electrodes and surface locations. Therefore the value computed in the survey is apparent resistivity ( $\rho_a$ ) which is expressed as  $\rho_a = k (V/I)$ , where  $V$  is measured voltage,  $I$  is the current and  $K$  is the geometry of the electrode array.

### 2.3.1b Principles of Induced Polarization

The passage of current through a rock is accomplished mainly by electrolytic flow in the pore fluid. Most of the rock forming minerals have a net negative charge on their outer surfaces in contact with the pore fluid and attract the positive ions onto this surface. The concentration of positive ions extends about 100 micrometer into the pore fluid, and if this distance is of the same order as the diameter of the pore space, the ion in the fluid will move when voltage is given. Negative and positive ions thus built up on either side of the blockage and, on removal of the applied voltage, return to their original location over a finite period of time causing a gradually decaying voltage. This effect is known as **membrane or electrolytic polarization**. It is mostly observed in clay minerals (Kearey and Brooks, 2002).

When metallic minerals are present in a rock, an alternate, electronic path is available for current flow. When a voltage is applied, positive and negative charges are imposed on opposite side of the metal grain. Negative and positive ions then accumulate on either side of the grain, which are attempting

either to release the electrons to accept the electron conducted through the grain. When the

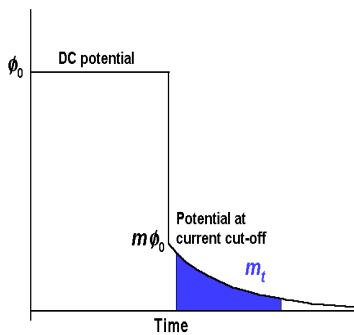


**Figure 2.2:** Transient response to square wave current pulse (time domain). Most IP receivers measure the integral of the decay voltage signal over a fixed interval, ( $mt$ ) as a measure of the IP effect.

voltage is removed, the ions slowly diffuse back to their original locations and results in decaying voltage. This effect is known as **electrode polarization or over voltage**. *Metallic sulphides, pyrite, pyrrhotite, copper and lead sulphides and molybdenite show*

*high I.P. effect. Amongst the oxides, magnetite, pyrolusite and cassiterite produce I.P. effect (Telford, Geldart and Sheriff, 1990).*

Field measurements of the IP effect divided into two main groups, the time-domain and frequency domain methods (Kearey and Brooks, 2002) In the present course of investigation, time domain IP measurements were carried out. The study of the decaying potential difference (Figure 2.2) as a function of time is known as the study of induced polarization (IP) in the time domain.

In the time domain, the IP effect is measured by the residual decay voltage after the current is switched off (Figure 2.2). Chargeability (M) is measured by sending a square wave pulsating current through the ground and is usually expressed in millivolt per volt (mV/V) or in milliseconds (m-sec). This creates an exchange of ions between the mineral grains and surrounding pore fluids. The exchange actually creates a voltage which acts as a barrier to current flow. Extra voltage, called "over voltage" is necessary to drive the current through the barrier. When the current supply is suddenly stopped, the voltage drops immediately to an intermediate value, and then gradually dissipates. The behavior is called "induced polarization" or "I.P.". Chargeability is related to the ratio of the over voltage value to the intermediate voltage value, and the lapse time it takes the ground to "depolarise" after the electrical charge is cut off at the transmitter. The IP effect due to sulfide mineralization (the electrode polarization effect) is much larger than that due to clay minerals (membrane polarization) in sandstone and siltstones. High chargeability is usually caused by the presence of metallic or conductive minerals. A chargeability reading is defined by the following formula (Kearey and Brooks, 2002)

$$M = \frac{1}{V_p} \int_{t_1}^{t_2} V(t) dt$$

Where,  $V_p$ - Voltage applied  
 $V_t$ - Residual Voltage  
 $t_1, t_2$ - time gates

Various configurations for electrode arrangement have been advocated in the literature as per the requirement. In present study dipole-dipole electrodes arrangement (Figure-2.3) has been used because of low EM coupling effect and better ground penetration. The current electrodes are generally metallic rods (iron) whereas the potential electrodes are made up of copper rod dipped in copper sulphate solution kept in porous pots. The spacing between the current electrodes pair, C1-C2, and potential electrodes P1-P2 is given as “a” (here 80m). The distance between the C2 and P1 electrodes are represented in the terms of “nth” time of “a”. Here the “a” spacing is fixed at 80m and “n” is kept 3, therefore the distance between C2 and P1 is 240m (3×80 =240m). In this way the total spread of electrodes become 400m. The plotting point of data is midway of total array spread (Figure 2.4). As a rule of thumb for dipole-dipole array the depth of investigation is one third times of the total spread, hence with the present arrangement we can investigate the I.P. response up to 130 m depth.

### Dipole - Dipole

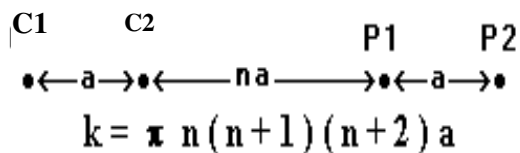


Fig-2.3 Dipole-Dipole Array configuration

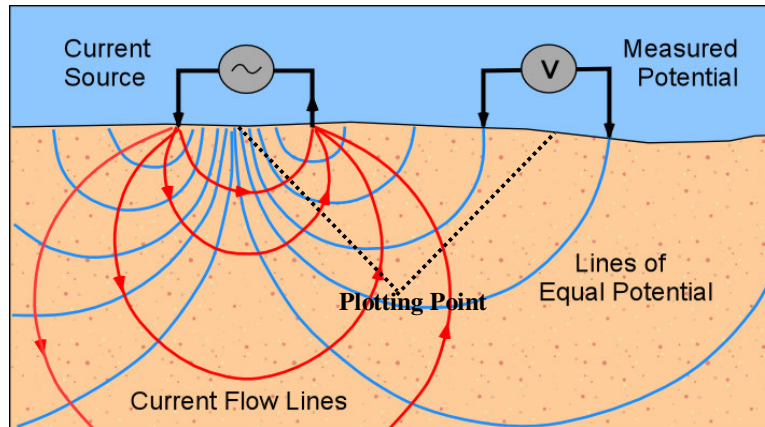


Figure 2.4: Plotting point for dipole-dipole array is mid point of total spread

### 2.3.2 Instruments

In the present work, *TSQ-3 Time and Frequency Domain IP Transmitter* of Scintrex Ltd. (Figure- 2.5) and *Scintrex, IPR-10A IP Receiver* (Figure-2.6) is used for IP and resistivity measurements. Chargeability (M) is measured by sending a square wave pulsating current through the ground and is usually expressed in millivolt per volt (mV/V) or in milliseconds (m-sec). This creates an exchange of ions between the mineral grains and surrounding pore fluids. The receiver used here constitutes the two non-polarizable potential electrodes consists a copper rod in contact with saturated solution of copper sulphate. With this TD-IP equipment, it is possible to measure current applied, received primary voltage and chargeability of the ground (i.e. how well materials tend to retain electrical charges) after the current cut-off, in addition to self potential (SP) gradient. The primary voltage ( $V_p$ ) measured (at 2 seconds) with receiver and current (I) passed with transmitter (at 2 seconds) and geometric factor (k) are used in apparent resistivity calculation ( $\rho_a = K \cdot \Delta V/I$ ). The variation in resistivity provides valuable clues on the presence of subsurface geological

features. These features play an important role in uranium exploration especially when the mineralisation is structurally controlled.



Fig- 2.5 TSQ -3 IP Transmitter



Fig- 2.6 Scintrex, IPR-10A Time Domain IP receiver connected with porous pot.

### 2.3.3 Data Acquisition

Resistivity measurement needs ground contacts of electrodes therefore two current electrodes and two potential electrodes are used. Current electrodes are connected to transmitter and potentials to receivers. Separation of the electrodes is maintained depending on ground conditions and depth penetration required for investigation. After collection of data at a point whole array moves forward to next station. In present survey traverse line trending N20°W-S20°E were followed across the trend of shear zone. Profile separation was maintained at 100m with 20 m sampling interval.

### 2.3.4 Corrections

In resistivity and IP data as such no correction is applied other than manually recognizing the noise due to coupling effect or improper electrode

fixing. The chargeability data (n=1070) acquired during the survey were subjected to statistical analysis to find out the mean and threshold values so that the genuine anomaly of chargeability can be fixed. Data are positively skewed in nature, therefore outliers were removed and data were normalized. After normalization, mean and SD (standard deviation) are noticed to be 9.1mV/V and 4.212 respectively. Hence threshold is fixed at 17.5mV/V (mean + 2SD). This way a total of 175 anomalous values above threshold were obtained

### **2.3.5 Interpretation**

Electrical survey is among the most difficult of the geophysical method to interpret quantitatively, because of the complex theoretical basis of the technique (Kearey and Brooks, 2002). It is an efficient method for delineation of shallow layered sequence or vertical discontinuities. Quantitative analysis of resistivity data is carried out by curve matching techniques and computer based algorithms. The interpretations will yield the information on the number of layers present beneath the ground surface with their thickness and true resistivity.

Results obtained in IP (Time Domain) give chargeability of ground which reflects presence of disseminated sulphides present in the rocks.

# Chapter 3

## Planning of Geophysical Surveys

### 3.1 General

Geophysical exploration methodology comprises measurement and interpretation of geophysical signals from natural and induced physical phenomena generated as a result of spatial changes in one or more physical properties of a sub terranean formation. These signals measured at several points of space and time is appropriately interpreted, considering the available geological information, in terms of sub surface structures or features of geological interest.

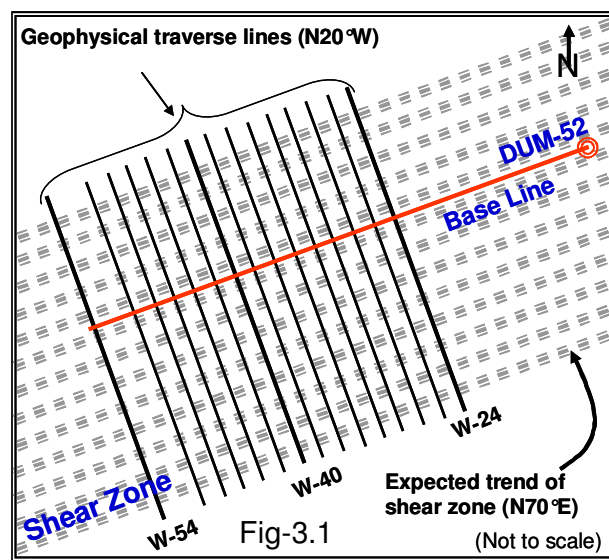
### 3.2 Planning of Magnetic Survey

Orientation surveys in the study area reveal that geological lithounits present in the area show  $N70^{\circ}E-S70^{\circ}W$  strike with vertical to sub-vertical dip towards the north. Using Theodolite, all profile lines trending  $N20^{\circ}W-S20^{\circ}E$  with 100m spacing are laid perpendicular to the general strike of the formations. Magnetic surveys were carried out along each of these profiles at an interval of 20 m (Figure-3.1).

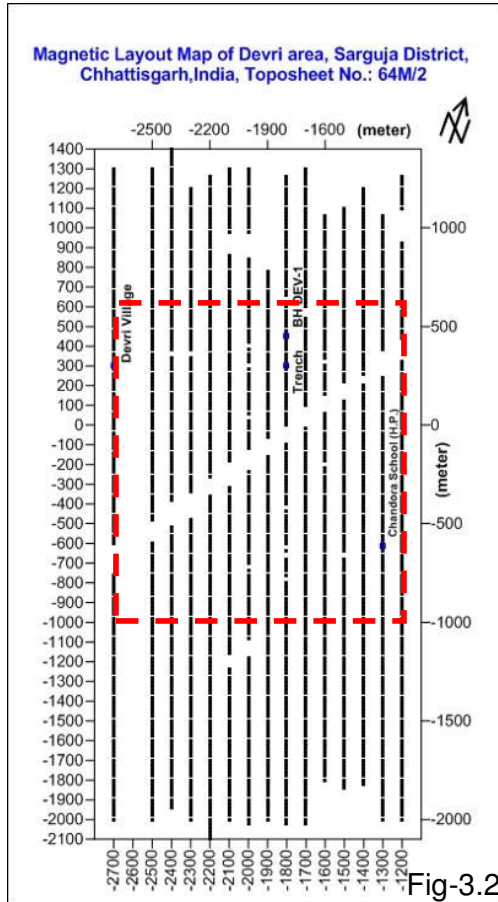
#### 3.2.1 Data Collection

Data was collected from W-24 profile to W-54 profile. W-24 line is

located 1200m west of the base station (borehole DUM-52) whereas W-54 at



2700m respectively. DUM-52 has been chosen as the base location for geophysical survey, because the same reference grid is also followed in the Devri area for sub surface exploration. On an average in northern side data were



collected upto N-65 station (20mx65=1300m) and towards the south up to S-100 (20mx100=2000m), thereby making an average length of 3.3km with 165 data points for each traverse line. This way a total of 15 traverse lines were covered (Figure-3.2). Proton precision magnetometer "GEMS SYSTEM" (GSM 19T) used for magnetic survey is having an accuracy, resolution and sensitivity of  $\pm 0.01\text{nT}$ ,  $0.01\text{nT}$  and  $0.015\text{nT}$  respectively, The magnetic inclination of the area is  $35.34^\circ$  and declination is -

Fig-3.2

$0.48^\circ$  whereas total magnetic field is  $45,000\text{nT}$ . Hence, both magnetometers were tuned to the existing field. A total of **46.00** line km data was collected on the above mentioned grid pattern. Diurnal correction has been applied to the data and profile and contour/images were prepared.

### 3.3 Planning of IP (TD)/ Resistivity Survey

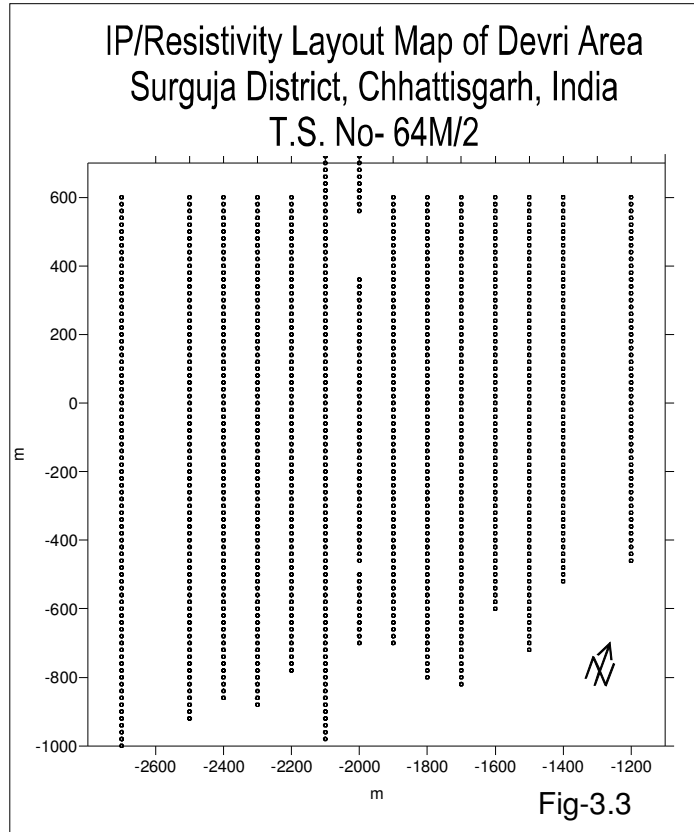
IP/ Resistivity survey was planned to get the response form subsurface in the form of apparent resistivity and chargeability. Same layout has been followed as of magnetic so that data can be correlatable. Apart from chargeability value, the magnitude of current applied and the resulting potential difference are

measured and using the geometric array of electrode, apparent resistivity was calculated.

### 3.3.1 Data Collection

Induced polarization/ resistivity survey was carried out from 700m in north to 1000m south of the base line. The area covered by this survey is indicated in

the IP/Resistivity plan (Figure 3.3). The length of the area chosen on the basis of master profile taken along the central part of the survey revealed that there are two distinct chargeability zones present in the area. High chargeability zones are indicative of the presence of disseminated sulphides in the host rock which in



turn is having positive correlation with the occurrence of uranium mineralization in the area.

A total of 2.1 sq.km area with 1070 data points were covered by this method. Data collected in the field were tabulated in excel work sheet with calculation of apparent resistivity for every point and chargeability value.

### 3.4 Measurement of Magnetic Susceptibility

Magnetic susceptibility of rocks is in principle controlled by the type and amount of magnetic minerals contained in a rock. Sometimes, it is dominantly controlled by paramagnetic minerals (mafic silicates such as olivine, pyroxenes, amphiboles, micas, tourmaline, garnets), often by ferromagnetic minerals (iron oxides or sulphides, represented by magnetite and/or pyrrhotite, respectively) and much less frequently by diamagnetic minerals (calcite, quartz) (Frantisek Hrouda et al., 2009). As the ferromagnetic minerals mostly belong to accessory minerals that are often sensitive indicators of geological processes, the magnetic susceptibility can be used as an additional parameter to solve some petrological problems.

#### 3.4.1 Principle

Magnetic susceptibility characterizes the ability of a substance to be magnetized when it is subjected to external magnetic field. In magnetically isotropic substances, it is defined as follows

$$M = k H,$$

where  $M$  represents the vector of the induced magnetization (in SI unit, -- A/m),  $H$  is the vector of the intensity of magnetic field (also in A/m) and  $k$  is the magnetic susceptibility (dimensionless scalar entity).

According to magnetic structure, materials can be divided into three basic groups; for their magnetization to field intensity relationship and their variation with field. The first group is represented by **diamagnetic** materials whose magnetic susceptibility is negative; in general low in absolute value and independent of the magnetizing field ( $k$  is negative constant). The second group is represented by **paramagnetic** materials whose susceptibility is positive, in

general higher than in diamagnetic materials but still relatively low in absolute value and also independent of the magnetizing magnetic field ( $k$  is positive constant). The third, and most important group, is represented by the materials with ordered magnetic structure, called the **ferromagnetic materials**. These materials are characterized by the existence of spontaneously magnetized sublattices (magnetic domains) even in the absence of external magnetic field. They are extremely important in palaeomagnetism because they can carry remanent magnetism. Their magnetic susceptibility is positive, often very high in absolute value and dependent in a complex way on the magnetizing field

### 3.4.2 Instrument

Various instruments for measurement of magnetic susceptibility in the field on rock outcrops are available in the market. Among these, the Kappameters of the KT series are most recent and advanced instrument, because they are light weight and of pocket size, very sensitive ( $1 \times 10^{-6}$  [SI] in the KT-10 model). It measure the susceptibility very rapidly (one measurement takes a few seconds), and data can be stored in the



memory (up to 500 measurements) and USB connectivity is available for transferring the measured data into computer. Measurement can be made in normal mode (outcrop/lab samples), core mode (depends on size of cores) and scanner mode.

### 3.4.3 Data Collection and Interpretation

In present study data has been collected by using KT-10 series kappameter (Figure-3.4), both on the outcrop and core samples. The relevant mode according to outcrop sample or size of the core has been selected for measurement. Data collected on the outcrop is summarized in table 3.1.

**Table-3.1 Magnetic Susceptibility of Rocks on Outcrop**

Rock Type	Granite Gneiss	Granite	Pegmatite	Schist	Quartzite	Syenite
Magnetic Susceptibility ( $\times 10^{-3}$ S.I. Unit)	0.0507 (n=40)	0.0099 (n=34)	0.019 (n=11)	0.140 (n=8)	0.0048 (n=29)	0.0215 (n=25)

Apart from measurement of susceptibility on the out crop, borehole cores samples were also used. The boreholes in the studied area are drilled by *Atomic Minerals Directorate for Exploration and Research* for exploration of uranium. A total of four borehole (DEV-3, DEV-4, DEV-5 and DEV-6) core samples were studied using kappameter and readings were taken at every 1.0m interval (at places at 10cm interval where radioactivity occurs). Litho units with presence of high ferromagnesian minerals viz. metabasic, amphibolites, granite gneiss, migmatites (melanosome) and schists are in general show high magnetic susceptibility in comparison to younger granite, pegmatite and quartzite bands. Magnetic susceptibility and radioactivity (gamma ray) vs depth correlation logs were prepared for the above mentioned boreholes (Fig-3.5,6,7&8) which show good positive correlation between the presence of radioactive bands and high magnetic susceptibility rock present in the core. It has been observed that

minerals which are responsible for the high magnetic susceptibility near radioactive bands are pyrite, pyrrhotite, biotite chunks, chlorites etc.

Fig

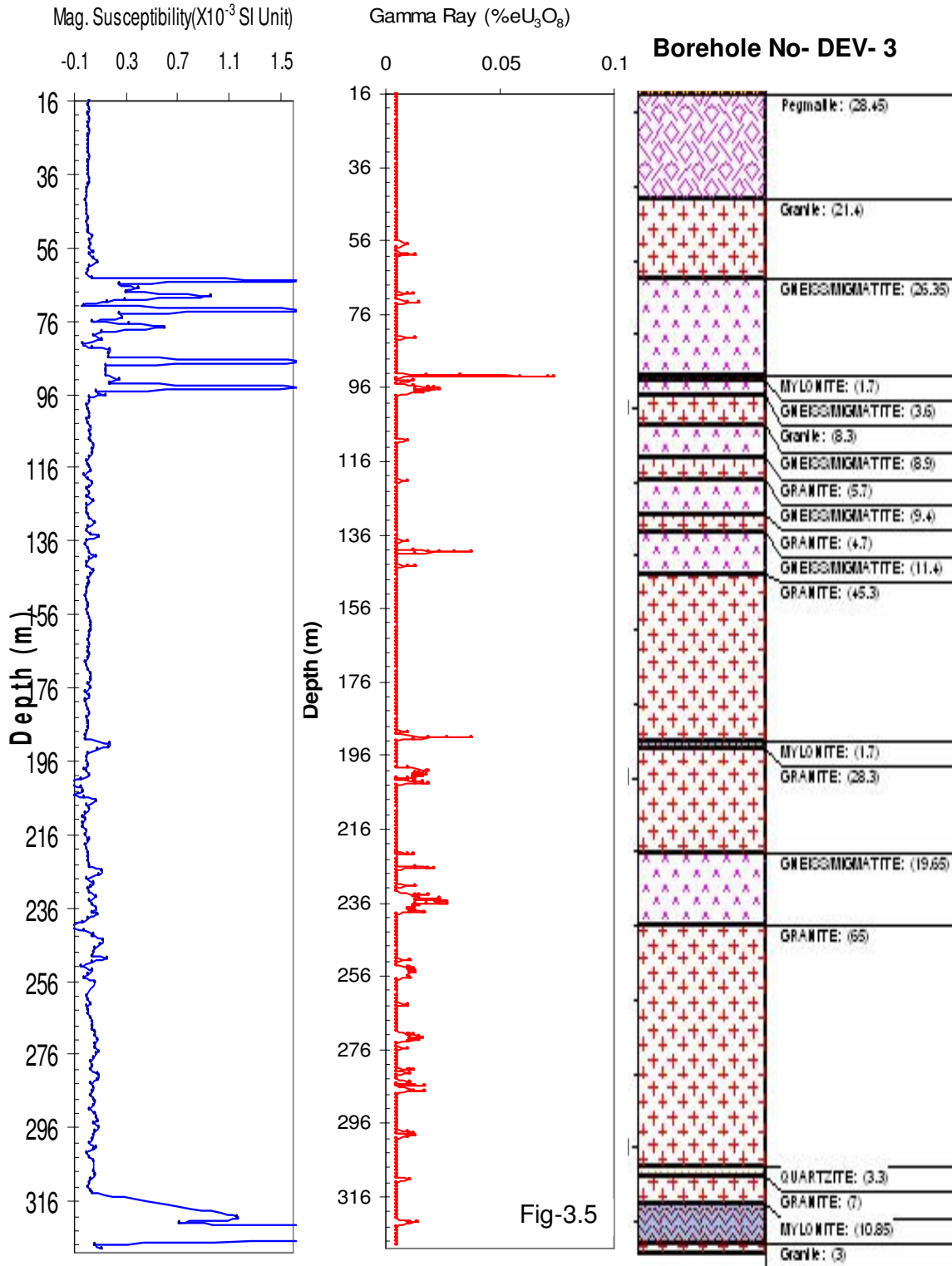


Fig-3.5

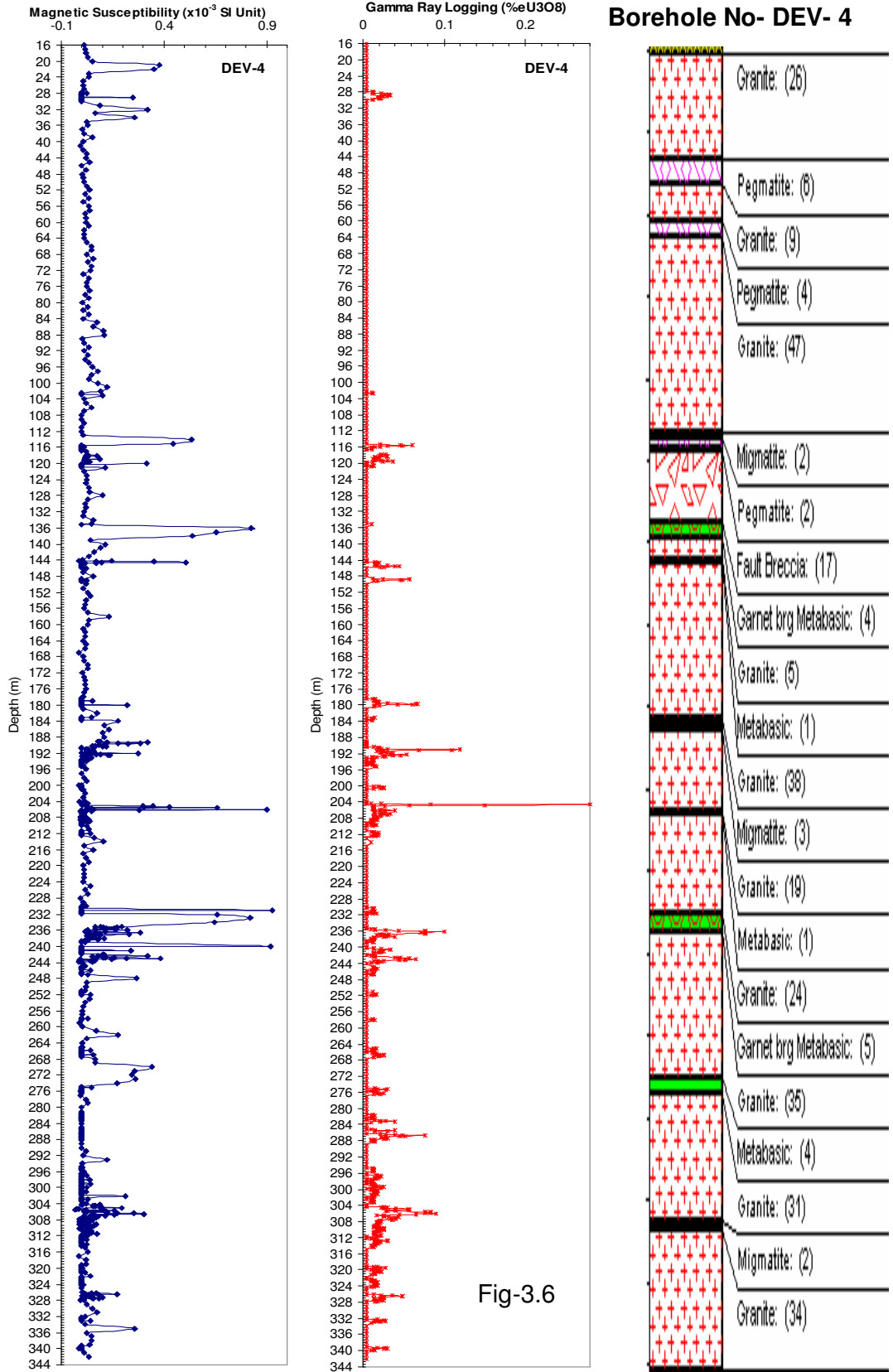
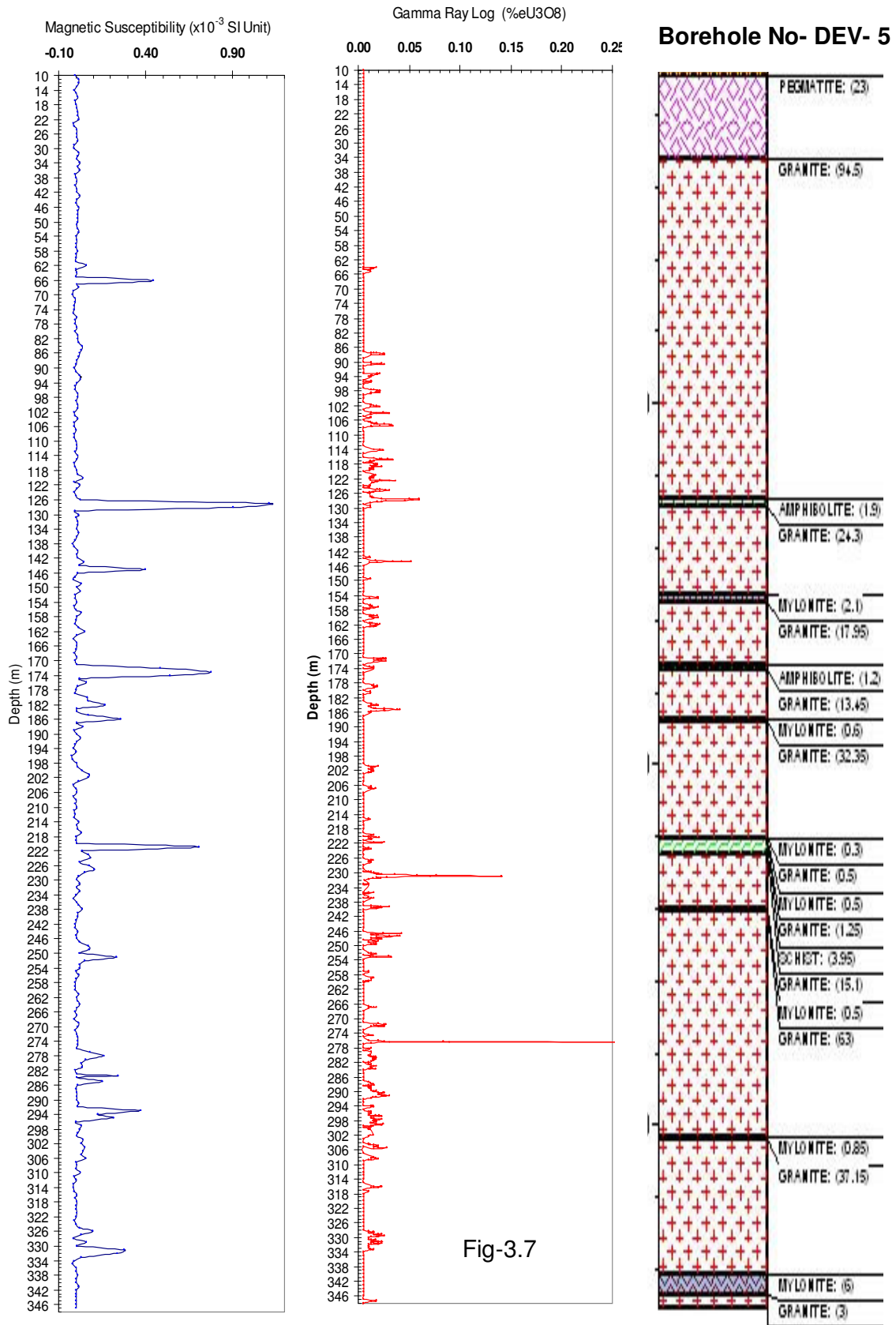


Fig-3.6



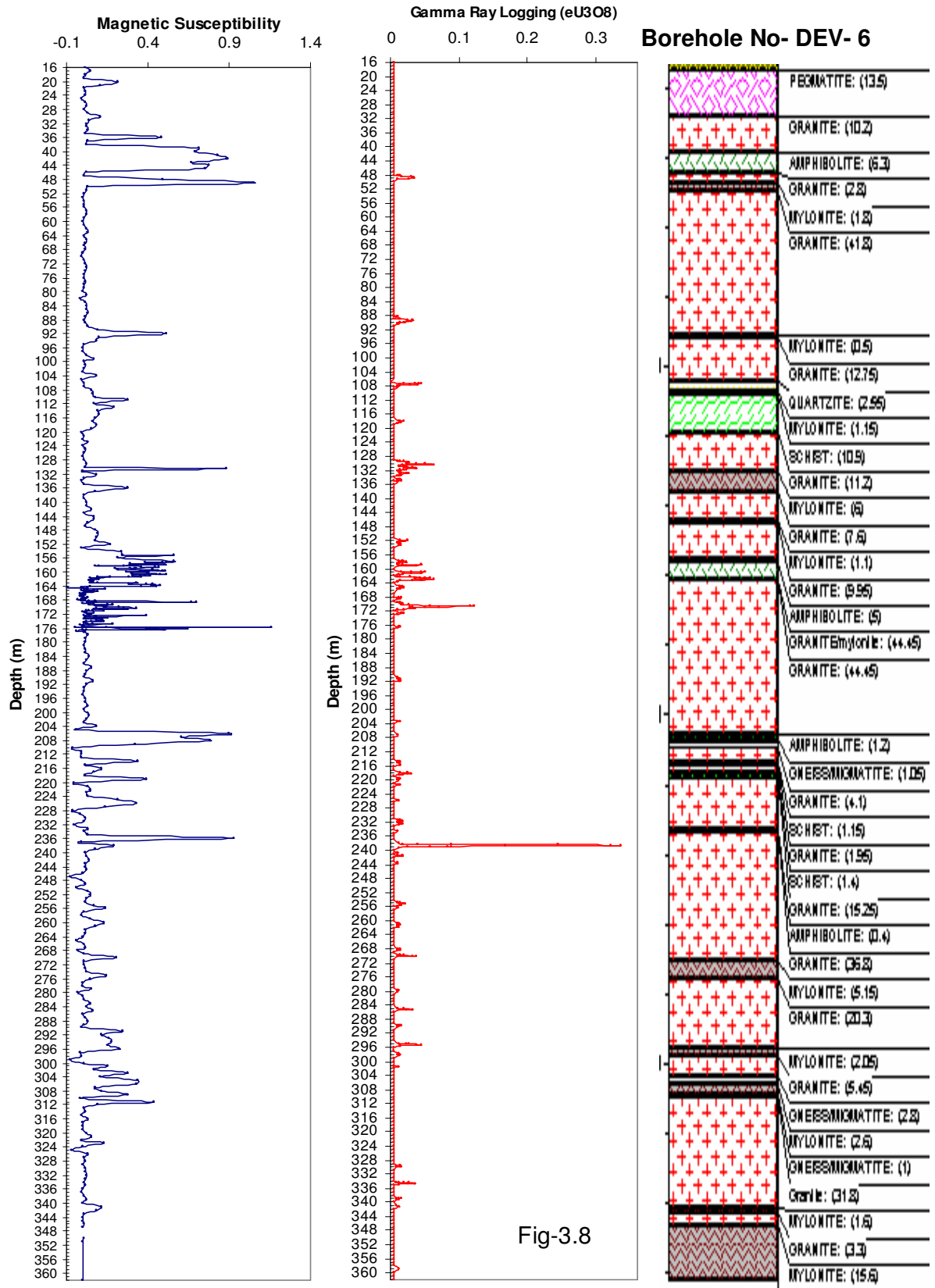


Fig-3.8

# ***Chapter 4***

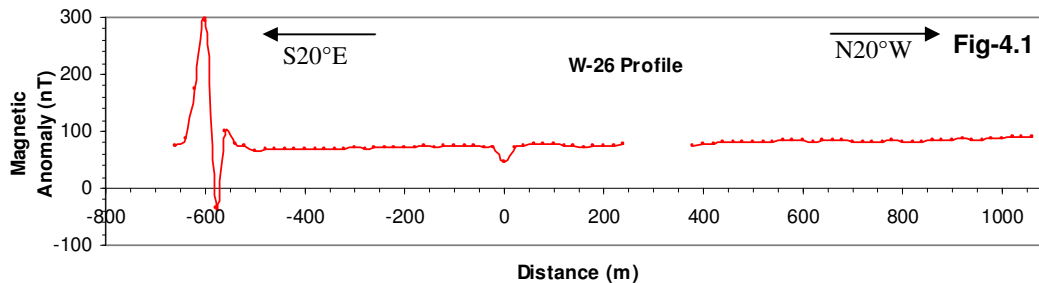
## **Interpretation**

### **4.1 General**

Interpretation of geophysical data can be pronged in to two categories namely qualitative analysis and quantitative analysis. In qualitative study, the nature and characteristics of the geophysical anomalies are studied by plotting the signatures in the form of profiles and contour maps. Anomaly trends in individual profiles are identified by correlating the anomalies with geological out crops in the study area, and are extrapolated to poorly mapped areas. Flexures and trends in the anomaly contours reflect the disposition and orientation of the sub surface geological targets. Magnitude, width and sharpness of the anomaly pattern are studied, which in turn can help in identifying the heaviness, horizontal dimension and depth of occurrence of the geological targets. Qualitative studies are usually followed up by detailed quantitative interpretations. Quantitative interpretation aims at to find out the size parameters of the geological objects/structures generating the observed anomaly. The exercise usually involves the approximation of the geological model/structure by a suitable mathematical geometry and identifies the parameters of the model, such that the theoretical response duplicates the observed anomaly. Although data interpretation can be done manually using characteristic curves, computer based algorithms are now-a days become more popular owing to their efficiency and speed in computation. In many exploration activities the number of parameters to be solved is usually large in number; therefore quantitative algorithms often utilize the principles of optimization techniques.

## 4.2 Magnetic Anomaly Map

Magnetic anomaly generated after applying various corrections is used for the interpretation. A typical magnetic anomaly observed along the profile W-26 is shown in Figure-4.1. By and large the anomaly shows smooth variation all along the profile except in the southern end.



The magnitude of the anomaly varies from -33.75nT to a maximum of 207.16nT. Maximum peak to peak anomaly of ~125nT has been observed in the southern part. Similar profiles of magnetic data were prepared for all other traverses and the same is used to prepare the magnetic anomaly map of the study area. Gridding was done using minimum curvature method with 40m cell size and blanking distance of 300m to generate the anomaly. The magnetic anomaly map (Figure 4.2) reveals the presence of high magnetic susceptible materials in the north and south in comparison to central part of the map. A conspicuous ENE-WSW trending bipolar magnetic anomaly recorded in the southern part of the area with a maximum peak to peak anomaly of 125nT seems to be representing a basic body present under the soil cover (Figure-4.2). High magnetic anomaly is also observed in the northern part of the area over the exposed granite/ granite gneiss. The magnetic data was processed using Magmap module (Geosoft software extension) and Geosoft software (Oasis Montaj - 7.1) using different available filters/tools.

### 4.2.1 Upward Continuation

It is a process of calculating the magnetic field anomaly at higher altitudes above the source of interest to suppress the magnetic effects caused by near surface sources. Upward continued anomaly is relatively stable in the sense that the field is continued into free space where there are no causative bodies to perturb the measured field. The method effectively attenuates high-wave number anomalies caused by near-surface features, thus providing a powerful method for examining deeper structures. The operator for upward continuation is given by

$$F(x', y', -h) = \frac{h}{2\pi} \iint \frac{F(x, y, 0) dx dy}{\{(x-x')^2 + (y-y')^2 + h^2\}^{1/2}} \quad (1)$$

$F(x', y', -h)$ , is total field at point  $(x', y', -h)$  above the surface on which  $F(x, y, 0)$  is known. The upward continuation images (Figure-4.3) reveal slight change in the shape and pattern of the anomaly at every stage from 20m to 150m. The 20m upward continuation has not changed much in anomaly pattern from the total intensity anomaly map, whereas 50m, 100m and 150m has gradually smoothed the data as well as curtailed high frequency near surface features as well as cultural noise. If we look carefully on 150m upward continuation map, it has very clearly retained the magnetic sources located at depth and presumably it has marked the width of shear zone from 100m north of base line to 1700m south of base line, and this is in agreement with the field observation.

### 4.2.2 Reduced to Pole (RTP)

Unlike gravity anomalies, the magnetic anomalies are strongly influenced by the strike of the target being looked for in addition to the latitude of its

occurrence. The geomagnetic vector which is horizontal at the equator varies gradually and becomes vertical at the poles. The field strength gets halved at the equator compared to its strength at the poles. A geological body with higher induced magnetization than the host rock produces a high anomaly at the poles, a low at the equator and a high-low at the middle latitudes. Interestingly, a body with lower induced magnetization than the host rock manifests with a low at the poles, a high at the equator and a high-low at the middle latitudes. At the equatorial regions, an east-west striking body produces a recognizable anomaly whereas a north-south striking one goes unrecognized, excepting at the ends.

Reduced to Pole (RTP) technique eliminates the bipolar nature of magnetic anomalies by transforming the data from the observed geomagnetic latitude as if they are measured at the pole. It converts its asymmetric shape to symmetric shape and reproduces magnetic anomaly with vertical magnetization. The RTP can be calculated in the frequency domain using the following operator (Grant and Dodds, 1972).

$$L(\theta) = \frac{1}{[\sin(I) + i \cos(I) \cos(D - \theta)]^2} \quad (2)$$

Where

$\theta$  = is the wave number direction

$I$  = is the magnetic inclination

$D$  = is the magnetic declination

From equation 2, it can be seen that as  $I$  approaches 0 (the magnetic equator),  $(D - \theta)$  approaches  $\frac{\pi}{2}$ , the operator approaches infinity (Mendonca and Silva, 1993). Effect of this operator can be distinguished on the magnetic anomalies over an east - west and north - south striking and vertically dipping dyke like

bodies. For the east - west striking dyke, the amplitude remains constant, but the shape changes. For the north - south striking dyke, the anomaly shape remains the same at all latitudes, but the amplitude is reduced as the inducing magnetic vector is rotated to be along strike at the magnetic equator and ultimately disappears. The very large amplitude correction required for north - south features at low latitudes also amplifies the north - south components of noise and magnetic effects from bodies magnetized in directions different from the inducing field. The methods either modify the amplitude correction in the magnetic north-south direction using frequency domain techniques (Hansen and Pawlowski, 1989, Mendonca and Silva, 1993), or calculate an equivalent source in the space domain (Silva, 1986). Grants and Dodds (1972) addressed this problem by introducing a second inclination ( $I'$ ) that is used to control the amplitude of the filter near the equator:

$$L(\theta) = \frac{[\sin(I) + i \cos(I) \cos(D - \theta)]^2}{[\sin^2(I') + i \cos(I') \cos^2(D - \theta)] \cdot [\sin^2(I) + i \cos(I) \cos^2(D - \theta)]} \quad (3)$$

In practice  $I' > I$  is set to an inclination greater than the true inclination of the magnetic field. By using the true inclination in the  $\cos(I)$  term, the anomaly shapes will be properly reduced to the pole (induced magnetization only), but by setting ( $I' > I$ ), unreasonably large amplitude corrections are avoided. Controlling the RTP operator then becomes a matter of choosing the smallest  $I'$  that still gives acceptable results.

Reduced to pole (RTP) filter is applied in the study area to get a clear picture of the anomaly by taking  $I$  value as  $35.34^\circ$  and  $I'$  value as  $36^\circ$ . In present case (Figure-4.4) the NNE-SSW trending structural grains of the area are picked up nicely. Also the faults/fractures trending ENE-WSW to E-W and

NNW-SSE were emplaced by magnetic bodies. Here, NNW-SSE trending fault is dissected by an ENE-WSW trending fault in en-echelon pattern, hence NNW-SSE trending fault/fracture systems are older than the ENE-WSW trending faults. Therefore it is inferred that the NNE-SSW trending faults were developed along the axial plane of second generation folds and ENE-WSW trending faults were developed during the third phase of folding. Basic dykes were emplaced along these weak structural grains, therefore they are the site along with their surrounding with elevated geotherms to mobilize the uranium bearing solution and should be looked for it.

#### **4.2.3 Horizontal and vertical Derivatives**

The magnetic anomaly measured at any point is the cumulative effect of several sources both at shallower and deeper depths. The effects of the deeper sources are characterized by anomalies of smaller amplitude and longer wavelengths while those of the near surface features are characterized by anomalies of larger amplitudes and of shorter wavelengths. Vertical derivative calculations are used to enhance the effects of near surface sources at the expense of those due to deep seated sources. These calculations also sharpen up anomalies over bodies and tend to reduce anomaly complexity, allowing a clearer imaging of the causative structures. The vertical derivative anomaly map (Figure-4.5) has brought out two significant magnetic trends parallel to each other in the southern part of the area. The NNW-SSE trending magnetic body has also been picked up nicely.

The horizontal derivative of magnetic field is a measure of the difference in magnetic value at a point relative to its neighboring point. This enhancement technique is designed to look at fault and geological contacts. It is

complementary to the filtered and first vertical derivative enhancements. The horizontal derivative map of the study area (Figure-4.6) clearly shows the presence of ENE-WSW and NNW-SSE trending magnetic features. Suspected basic body in the southern part has also been picked up along with two other less prominent bodies striking in NE-SW.

#### 4.2.4 Analytical Signal

The analytic signal or total gradient is calculated using both horizontal and vertical gradients of the magnetic anomaly (Nabighian, 1972). It is simply related to the amplitude of magnetization, which produces maxima over magnetic contacts (MacLeod et al., 1993). The analytic signal is dependent on the locations of the body (horizontal coordinate and depth) but is independent on the direction of magnetization.

Roest, et al., (1992) showed that the amplitude of analytical signal at any location (x, y) can be calculated from three orthogonal gradients of the total magnetic field as

$$|A(x, y)| = \sqrt{\left(\frac{\partial B}{\partial x}\right)^2 + \left(\frac{\partial B}{\partial y}\right)^2 + \left(\frac{\partial B}{\partial z}\right)^2} \quad (4)$$

Where B is the observed magnetic field at (x, y) and  $|A(x, y)|$  is the amplitude of the analytical signal at (x, y).

Analytical signal map (Fig-4.7) is also prepared for the area which is in agreement with the RTP image of the area. It defines the shape of the anomaly by producing maxima over the edges/contacts.

#### 4.2.5 Tilt Derivative Map

Tilt angle/derivative method was first introduced by Miller and Singh (1994) and was further refined by Verduzco (2004). Tilt derivatives are used for shallow basement structures and mineral exploration targets. The expression for tilt angle is given by

$$\theta = \tan^{-1} \left[ \frac{\frac{dM}{dz}}{\frac{dM}{dh}} \right], \text{ where} \quad (5)$$
$$\frac{dM}{dh} = \sqrt{\frac{(dM)^2}{(dx)^2}} + \sqrt{\frac{(dM)^2}{(dy)^2}}$$

where,  $dM/dx$ ,  $dM/dy$ ,  $dM/dz$  are first order derivatives of the magnetic field  $M$  in the  $x$ ,  $y$  and  $z$  directions.

The tilt angle has many interesting properties (Cooper and Cowan, 2006), for example, due to the nature of the arctan trigonometric function, all tilt values are restricted to values between  $-\pi/2$  and  $\pi/2$  regardless of the amplitude of the vertical derivative or the absolute value of the total horizontal gradient (Salem et al., 2008). Salem et al., 2007 proposed a method for depth calculation using tilt angle method. In this method the RTP map is prepared whose tilt angle derivative is calculated and the distance between -1 and 0 or 1 and 0 is referred as depth of the source. In present study (Figure-4.8) similar kind of attempt has been made to magnetic data which has sharpened the edge of the causative body. The zero contour lie on the edge of the body and distance between 0 and -1 or 1 is in the range of 34 to 45m for N-S occurring body.

#### 4.2.6 Euler Deconvolution

Euler deconvolution is quantitative method of magnetic data interpretation, based on Euler's homogeneity equation (6) that relates the magnetic field and its gradient component to identify location, depth and nature of source (Reid et al., 1990).

$$(x - x_0) \frac{\partial T}{\partial x} + (y - y_0) \frac{\partial T}{\partial y} + (z - z_0) \frac{\partial T}{\partial z} = N(B - T) \quad (6)$$

Where;  $(x_0, y_0, z_0)$ : Position of a source whose total field T is detected at any point  $(x, y, z)$

B : the background value of the total field

N : the degree of homogeneity, interpreted physically as the attenuation rate with distance and geophysically as a structural index (SI)

Specification of the structural index 'N' permits the equation to be solved for source position for a specific source geometry within a given data window. Euler's deconvolution is applied by selecting a square window from the grids of total field and its orthogonal derivatives. This window is progressively "moved" across the magnetic data grid, and solutions are generated within each. The process is repeated for various window sizes and structural indices, and the optimum parameters for the data are determined by clustering of output depth solutions and comparison with other available information. It is used for rapid interpretation of potential field data, particularly good at delineating contacts and fast depth estimation. This method has emerged as a powerful technique for estimation the depth and the geometry of the magnetic sources because it requires no prior information about the source magnetization and it assumes no

particular geological model. Further, it is insensitive to magnetic inclination, declination and remanence. Thompson (1982) developed this technique for profile data while Reid et. al (1990) extended it for gridded data.

In view of its applicability and effectiveness, this method is applied in the study area using Euler 3D module of Geosoft (Oasis Montaj) software. Structural index is chosen both 0.5 and 1.0 for faulted/fracture and dyke. Initially, taking structural index both 0.5 and 1.0, standard Euler method is performed with different window size (5X5, 8X8 & 10X10). But optimum depth solutions are obtained with structural index of 1.0 and window size of 5x 5. About 563 solutions are obtained with depth range of 20 to 200m. Maximum number of depth solutions is in the range of 20m to 50m (Figure-3.9 a,b). Good solution for dyke has been obtained, which is present in the southern part of study area. These results are further verified by 2D modeling along a profile.

#### **4.2.7 2D Profile Modeling**

Profile modeling is done using GM-SYS module of Geosoft (Oasis Montaj) software. It is an interactive forward modeling program which calculates the magnetic response from a user defined hypothetical geologic model. Any differences between the model response and the observed magnetic field are reduced by refining the model structure or properties (e.g. susceptibility of model components). 2D modeling assumes two dimensionality of every model component block, i.e. the model may change with depth (Z direction) and along the profile (X direction, perpendicular to strike), as defined by the program user, but does not change along strike (Y direction). It should be noted that magnetic models are non unique, i.e. many earth models can produce the same magnetic response, and similarly, several geological lithologies may be interpreted from a

given model block's susceptibility properties. It is therefore important to use as many independent sources of information as possible to constrain the model.

In the study area, two small profiles are selected for modelling from the southern part of the area where basic body is expected. The input parameters given for this are inclination  $35.34^\circ$ , declination  $-0.48^\circ$  and total magnetic field 45,000nT. In the modelling window, the observed magnetic field appears as seen along the profile, then assuming a dyke model, the geological parameters are given. Three blocks of basement granite, amphibolite dyke and soil cover/alluvium were constructed. Taking susceptibility of amphibolite as 0.0006, granite as 0.0001 and soil covered as 0.00001 (CGS units) the magnetic response of geological layer is calculated and tried to match with the observed curve. Magnetic susceptibility assigned to the different block was based on data collected during the survey from exposures and borehole cores. For achieving the error of  $<1.0$  in the modelling, value of susceptibility has been changed, and aforesaid value gave the best result with minimum error. From the model it is inferred that the top soil cover varies in depth from 30 to 80m. Dyke present under the soil cover is vertical in attitude and varies in thickness from 65m (AB profile) (Figure-4.10) to 40m (L1 profile) (Figure-4.11) meaning not homogeneous in thickness and following pinching and swelling character.

Another long profile from south to north of the map has been taken and the similar parameters were assigned to this model also. In present model basic dyke in the south, a migmatites patch in the centre and contact between younger granite and granite gneiss were picked up and interpreted (Figure-4.12).

#### **4.2.8 Depth Estimation by 3 D inversion**

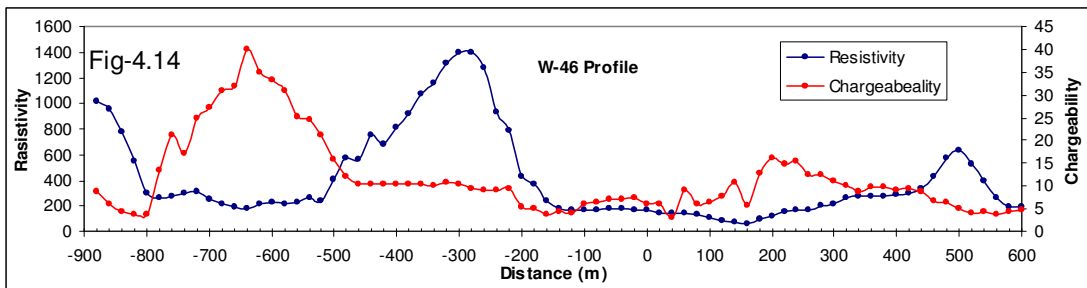
A 3D inversion technique (Chakravarthi, 2009) is used to invert the observed magnetic field anomalies for the basement structure. The novelty of the inversion is that different magnetizations can be assigned to different parts of the basement and constraints can be imposed at any grid node on the shape and size factors. Upon invoking the executable file, the code reads data from the input and prompts the user to specify five output file names, one with TXT extension and four with GRD extensions. The output file with a TXT extension provides the interpreted results in an ASCII form. On the other hand, the four output files with a GRD extension contain the information of the observed and calculated magnetic anomalies, and the depth values of the basement.

Accordingly the observed magnetic anomalies are digitized into 30x80 grids and supplied to the inversion code as input. The algorithm performed 42 iterations before it got terminated as the misfit between the observed and calculated anomalies fell below a predefined allowable error. The inferred 3D basement configuration with the theoretical magnetic response superimposed is shown in Figure-4.13. One can see from Figure-4.13 that the basement is relatively at shallower depths and deepens towards the north and south of the survey grid.

#### **4.3 Resistivity/ Induced Polarization**

Data collected from this survey were first plotted for individual profiles, which show the variation in resistivity and chargeability with respect to location. Resistivity and chargeability profiles are mostly showing antipathy relationship between them. This indicates that pervasive nature of shearing and fracturing lowering the resistivity value and allowing the hydrothermal solution to move along them. The lowest and highest resistivity value recorded in the area is 14 to

3324 ohm m, whereas lowest and highest value recorded for chargeability is 0.8 to 72mV/V respectively. It has been mostly observed in the IP/resistivity survey that, low resistivity zones are mostly occupied by high chargeability zones (Subhash Ram and Chary, M.N., 2010). To visualize this relationship one profile of W-46 traverse line is given below (Figure-4.14).



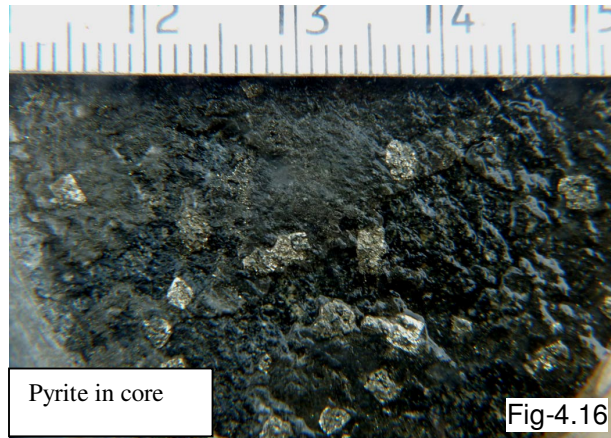
#### 4.3.1 Resistivity Map

Resistivity contour/ image map was prepared using Geosoft 7.1 version software. Data were gridded to 20x20 cell size and 300m of blanking distance, using minimum curvature method. Resistivity map (Figure-4.15) of the area reveals two prominent lows, one in upper half and another in the lower half. The upper half low resistivity zone trends ENE-WSW and follows trend of Sarguja shear, where as the lower half low resistivity zone trend NE-SW and slight oblique to the main trend. Cause of low resistivity could be inferred as pervasive shearing in these part where rocks are shattered and fractures thus increasing the porosity and permeability of the media by virtue of fluid movements. High resistivity in the northern and southern part corresponds to Granite Gneiss / Pegmatite whereas high resistivity in the western side with inverted “C” - shape corresponds to pink granite and pegmatites in the area. It has been invariably observed that high resistive part of area is either having exposures of rocks or there is very thin development of soil cover, where as low resistive zones are

mostly soil covered. Dug well sunk in low resistive part are showing shallow water table with 2 to 6 m depth.

#### 4.3.2 Chargeability Map

High chargeability zone in the area corresponds to low resistivity zones. High chargeability zone is indicative of presence of disseminated sulphide in the litho units. This is evident from presence of



pyrites, pyrotites and other sulphides in the borehole core samples (Fig-4.16). On the basis of statistical analysis of the chargeability data threshold is fixed at 18mV/V and all values above can be treated as anomalous value.

Two separate high chargeability zones (Figure- 4.17) have been picked up in the area. The zone –I, situated between 200 to 300m north of base line is trending N70°E and it is sympathetic to the Sarguja Shear zone. Here the maximum chargeability goes upto 25mV/V. The second chargeability zone, trending NE-SW (Zone-II) is located around 500m to 900m south of the base line and value goes upto 72mV/V. Therefore it become more prominent than zone-I. This finding emphasis that N70°E shear is not only important but NE-SW trending shear/ fractures are also important, and has better potential to host good uranium mineralization in the area.

To see the correlation between magnetic signatures along with IP/resistivity response together in the area, all the three parameters were plotted together. Contours of chargeability enveloping 15mV/V or more and for

resistivity, contours of 200 Ohm m or less were kept together. High chargeability contours precisely matches with low resistivity contours, in low magnetic area (Fig-4.18).

## 4.4 Miscellaneous

### 4.4.1 Radiometric Measurement

Concentration of radioelements viz, uranium, thorium and potassium in rock unit help in discriminating the rock type formation and alteration studies. The use of gamma ray spectrometry as a tool for mapping radioelement concentrations has found widespread acceptance in diverse fields. The method has evolved over several decades and the method has benefited from continuing advances in instrumentation, field procedures, and calibration and data processing procedures. Gamma ray



spectrometry is widely used for environmental mapping, geological mapping and mineral exploration.

Portable hand-held gamma ray spectrometers are widely used in field studies. In present study **DS 5067 model** (Differential spectrometer) instrument developed by Atomic Minerals Directorate, Hyderabad and fabricated by Electronic Corporation of India Ltd, Hyderabad has been used (Figure-4.20). This hand held spectrometer uses 2.0x1.75 inch NaI (TI) crystals as detectors. The energies windows used here are 1.36 to 1.56 (1.46 MeV) for potassium, 1.66 to 1.86 (1.76 MeV) for uranium and 2.42 to 2.82 (2.62 MeV) for thorium

respectively. A reference gamma ray emitting source is used for instrument calibration and gain adjustment and in present case  $^{137}\text{Cs}$  with 0.662 MeV peak energy source is used for the purpose (IAEA-TECDOC-1363, 2003). Now a days several advanced instruments are used to record the full gamma ray spectrum but this model (presently used) records sum of channels over broad energy windows (as mentioned above) for the insitu estimation of K, U and Th. At every location counts from radioelements are gathered for 100 seconds where after data in the form of total counts of uranium, thorium and potassium as well as ppm value of U, Th and % of K is displayed in screen alternatively. Gamma ray coming from 50 to 60 cm depth can be recorded by the instrument; more than this depth will be attenuated by soil or rock cover.

#### **4.4.2 Data Acquisition and Interpretation**

An area of 4.10 sqkm has been covered by carrying out the portable gamma ray spectrometer survey using **Differential spectrometer DS 5067** (Figure-4.20). The survey was carried out on the same grid pattern which was followed for magnetic survey. Here the station interval was taken 40m instead of 20m. The instrument was calibrated every day using Cs-137 source, before commencement of survey. The uranium, thorium and total radioelement (ppm) and K (%) data were taken for every location and image map for Uranium, Thorium Potassium and U/Th are prepared. Total radioelement concentration and thorium map (Figure-4.20 & 4.21) are kept together, because they are looking similar in their contour pattern, which signifies that thorium has got dominant contribution among the three radioelements present in the map. Uranium contour map showing less concentration in the central part (Figure-4.22). Presence of high concentration of thorium in the major part of the area

could be attributed to deep soil profile development due to which highly mobile element 'uranium' might have leached out and migrated downward below the water table where it can be deposited under reducing conditions and thorium being resistive to mechanical and chemical weathering accumulated insitu. Potassium contour map (Figure-4.23) show their high concentration in NE corner of the map because this part of area exposes fresh granite. Depletion of potassium in the central part could be attributed to deep weathering and removal of alkali elements viz, K and Na. U/Th map is prepared to find out the uranium enrichment zones. As we know that Clark concentration of uranium and thorium is 4 and 16 ppm respectively in granite. Ratio of U/Th ( $>0.25$ ) signifies accumulation of uranium in the system in comparison to Th. In U/Th map (Figure-4.24) slight enrichment has been noticed in the south-western side with almost ENE-WSW trend.

<b>Table-4.1 Magnetic Anomaly (nT) Data Sheet</b>											
S.No.	X(m)	Y(m)	Mag. Anomal	S.No.	X(m)	Y(m)	Mag Anomal	S.No.	X(m)	Y(m)	Mag Anomal
1	-1200	-2000	83.97	50	-1200	-1020	71.21	99	-1200	140	74.52
2	-1200	-1980	83.43	51	-1200	-1000	78.91	100	-1200	160	71.23
3	-1200	-1960	84.25	52	-1200	-980	58.81	101	-1200	180	75.31
4	-1200	-1940	82.05	53	-1200	-960	66.64	102	-1200	200	76.57
5	-1200	-1920	80.99	54	-1200	-940	72.63	103	-1200	220	77.21
6	-1200	-1900	84.31	55	-1200	-920	76.63	104	-1200	240	80.39
7	-1200	-1880	84.79	56	-1200	-900	81.88	105	-1200	260	76.35
8	-1200	-1860	87.3	57	-1200	-880		106	-1200	280	81.68
9	-1200	-1840	89.71	58	-1200	-860	57.95	107	-1200	300	82.9
10	-1200	-1820	91.18	59	-1200	-660	62.71	108	-1200	320	76.29
11	-1200	-1800	88.7	60	-1200	-640	65.13	109	-1200	440	75.88
12	-1200	-1780	84.57	61	-1200	-620	65.41	110	-1200	460	83.14
13	-1200	-1760	85.28	62	-1200	-600	59.78	111	-1200	480	83.34
14	-1200	-1740	83.79	63	-1200	-580	65.5	112	-1200	500	83.08
15	-1200	-1720	81.98	64	-1200	-560	64.01	113	-1200	520	82.14
16	-1200	-1700	83.2	65	-1200	-540	65.61	114	-1200	540	85.59
17	-1200	-1680	79.08	66	-1200	-520	65.65	115	-1200	560	88.35
18	-1200	-1660	79.21	67	-1200	-500	67.42	116	-1200	580	91.63
19	-1200	-1640	78.53	68	-1200	-480	67.29	117	-1200	600	94.53
20	-1200	-1620	79.6	69	-1200	-460	68.98	118	-1200	620	98.14
21	-1200	-1600	82.53	70	-1200	-440	68.22	119	-1200	640	108.4
22	-1200	-1580	82.84	71	-1200	-420	67.6	120	-1200	660	140.71
23	-1200	-1560	87.76	72	-1200	-400	67.62	121	-1200	680	81.51
24	-1200	-1540	99.51	73	-1200	-380	67.96	122	-1200	700	72.63
25	-1200	-1520	79.26	74	-1200	-360	69.18	123	-1200	720	69.62
26	-1200	-1500	94.85	75	-1200	-340	68.7	124	-1200	740	74.3
27	-1200	-1480	119.57	76	-1200	-320	68.47	125	-1200	760	78.5
28	-1200	-1460	67.31	77	-1200	-300	69.58	126	-1200	780	76.61
29	-1200	-1440	22.83	78	-1200	-280	68.94	127	-1200	800	76.45
30	-1200	-1420	45.42	79	-1200	-260	69.18	128	-1200	820	77.94
31	-1200	-1400	50.63	80	-1200	-240	68.01	129	-1200	840	78.34
32	-1200	-1380	55.87	81	-1200	-220	69.18	130	-1200	860	80.04
33	-1200	-1360	59.23	82	-1200	-200	70.07	131	-1200	880	80.8
34	-1200	-1340	60.9	83	-1200	-180	73.3	132	-1200	900	82.08
35	-1200	-1320	62.09	84	-1200	-160	71.84	133	-1200	920	83.67
36	-1200	-1300	43.7	85	-1200	-140	73.22	134	-1200	1100	92.13
37	-1200	-1280	65.73	86	-1200	-120	72.45	135	-1200	1120	94.27
38	-1200	-1260	65.37	87	-1200	-100	73.14	136	-1200	1140	93.51
39	-1200	-1240	68.53	88	-1200	-80	73.22	137	-1200	1160	92.43
40	-1200	-1220	67.1	89	-1200	-60	79.8	138	-1200	1180	93.55
41	-1200	-1200	66.49	90	-1200	-40	64.64	139	-1200	1200	98.01
42	-1200	-1180	65.16	91	-1200	-20	72.88	140	-1200	1220	98.25
43	-1200	-1160	64.58	92	-1200	0	71.64	141	-1200	1240	99.2
44	-1200	-1140	61.25	93	-1200	20	74.07	142	-1200	1260	102.07
45	-1200	-1120	65.05	94	-1200	40	72.26	143	-1300	1060	91.69
46	-1200	-1100	65.27	95	-1200	60	76.04	144	-1300	1040	89.46
47	-1200	-1080	66.19	96	-1200	80	74.9	145	-1300	1020	89.97
48	-1200	-1060	68.52	97	-1200	100	77.75	146	-1300	1000	87.78
49	-1200	-1040	70.53	98	-1200	120	77.01	147	-1300	980	86.56

148	-1300	960	85.16	199	-1300	-180	72.58	250	-1300	-1280	69.89
149	-1300	940	85.6	200	-1300	-200	73.26	251	-1300	-1300	68.4
150	-1300	920	86.58	201	-1300	-220	71.55	252	-1300	-1320	65.89
151	-1300	900	84.51	202	-1300	-240	71.5	253	-1300	-1340	63.39
152	-1300	880	85.25	203	-1300	-260	70.7	254	-1300	-1360	60.79
153	-1300	860	83.44	204	-1300	-280	69.73	255	-1300	-1380	58.68
154	-1300	840	82.33	205	-1300	-300	70.86	256	-1300	-1400	58.74
155	-1300	820	80.96	206	-1300	-320	68.71	257	-1300	-1420	55.41
156	-1300	800	81.37	207	-1300	-340	68.57	258	-1300	-1440	52.34
157	-1300	780	82.86	208	-1300	-360	67.3	259	-1300	-1460	39.71
158	-1300	760	80.8	209	-1300	-380	68.42	260	-1300	-1480	33.67
159	-1300	740	82.21	210	-1300	-400	69.79	261	-1300	-1500	117.38
160	-1300	720	81.82	211	-1300	-420	69	262	-1300	-1520	125.85
161	-1300	700	82.07	212	-1300	-440	68.47	263	-1300	-1540	104.92
162	-1300	680	83.48	213	-1300	-460	69.02	264	-1300	-1560	97.17
163	-1300	660	83.57	214	-1300	-480	67.37	265	-1300	-1580	87.24
164	-1300	640	84.43	215	-1300	-500	66.45	266	-1300	-1600	87.8
165	-1300	620	82.54	216	-1300	-520	73.44	267	-1300	-1620	83.95
166	-1300	600	83.86	217	-1300	-540	77.27	268	-1300	-1640	81.68
167	-1300	580	85.88	218	-1300	-560	100.24	269	-1300	-1660	80.58
168	-1300	560	83.77	219	-1300	-580	-33.75	270	-1300	-1680	80.35
169	-1300	540	82.33	220	-1300	-600	145	271	-1300	-1700	77.12
170	-1300	520	81.75	221	-1300	-620	175.51	272	-1300	-1720	80.92
171	-1300	500	80.98	222	-1300	-640	88.43	273	-1300	-1740	84.89
172	-1300	480	82.32	223	-1300	-660	75.93	274	-1300	-1760	87.88
173	-1300	460	81.87	224	-1300	-680	69.3	275	-1300	-1780	93.85
174	-1300	440	82.67	225	-1300	-700	65.39	276	-1300	-1800	93.53
175	-1300	420	79.39	226	-1300	-720	62.26	277	-1300	-1820	86.4
176	-1300	400	78.42	227	-1300	-740	45.3	278	-1300	-1840	88.17
177	-1300	380	76	228	-1300	-760	15.4	279	-1300	-1860	86.94
178	-1300	240	77.55	229	-1300	-860	84.34	280	-1300	-1880	86.26
179	-1300	220	73.7	230	-1300	-880	61.57	281	-1300	-1900	84.37
180	-1300	200	74.97	231	-1300	-900	70.55	282	-1300	-1920	82.64
181	-1300	180	75.53	232	-1300	-920	72.63	283	-1300	-1940	82.84
182	-1300	160	72.76	233	-1300	-940	70.01	284	-1300	-1960	84.22
183	-1300	140	75.46	234	-1300	-960	67.4	285	-1300	-1980	83.07
184	-1300	120	76.49	235	-1300	-980	69.76	286	-1300	-2000	80.35
185	-1300	100	76.83	236	-1300	-1000	58.79	287	-1400	-1820	84
186	-1300	80	77.77	237	-1300	-1020	71.15	288	-1400	-1800	83
187	-1300	60	76.69	238	-1300	-1040	69.98	289	-1400	-1780	83
188	-1300	40	75.91	239	-1300	-1060	64.26	290	-1400	-1760	78
189	-1300	20	72.43	240	-1300	-1080	71.33	291	-1400	-1740	79
190	-1300	0	47.05	241	-1300	-1100	74.58	292	-1400	-1720	78
191	-1300	-20	72.32	242	-1300	-1120	70	293	-1400	-1700	86
192	-1300	-40	73.1	243	-1300	-1140	68.13	294	-1400	-1680	91
193	-1300	-60	74	244	-1300	-1160	70.94	295	-1400	-1660	104
194	-1300	-80	74.16	245	-1300	-1180	69.01	296	-1400	-1640	105
195	-1300	-100	75.52	246	-1300	-1200	66.86	297	-1400	-1620	96
196	-1300	-120	74.92	247	-1300	-1220	70.13	298	-1400	-1600	72
197	-1300	-140	72.7	248	-1300	-1240	70.95	299	-1400	-1580	88
198	-1300	-160	73.8	249	-1300	-1260	72.93	300	-1400	-1560	98

<b>301</b>	-1400	-1540	109	<b>352</b>	-1400	-520	64.23	<b>403</b>	-1400	540	79
<b>302</b>	-1400	-1520	113	<b>353</b>	-1400	-500	65.66	<b>404</b>	-1400	560	77.34
<b>303</b>	-1400	-1500	38	<b>354</b>	-1400	-480	68.55	<b>405</b>	-1400	580	79.6
<b>304</b>	-1400	-1480	43	<b>355</b>	-1400	-460	66.84	<b>406</b>	-1400	600	80.76
<b>305</b>	-1400	-1460	55	<b>356</b>	-1400	-440	69.33	<b>407</b>	-1400	620	80
<b>306</b>	-1400	-1440	59	<b>357</b>	-1400	-420	66.72	<b>408</b>	-1400	640	80.56
<b>307</b>	-1400	-1420	58	<b>358</b>	-1400	-400	68.06	<b>409</b>	-1400	660	82.11
<b>308</b>	-1400	-1400	61	<b>359</b>	-1400	-380	67.93	<b>410</b>	-1400	680	80.72
<b>309</b>	-1400	-1380	64	<b>360</b>	-1400	-360	67.83	<b>411</b>	-1400	700	80.1
<b>310</b>	-1400	-1360	64	<b>361</b>	-1400	-340	68.09	<b>412</b>	-1400	720	81.4
<b>311</b>	-1400	-1340	66	<b>362</b>	-1400	-320	68.8	<b>413</b>	-1400	740	84.94
<b>312</b>	-1400	-1320	67	<b>363</b>	-1400	-300	70.41	<b>414</b>	-1400	760	80.51
<b>313</b>	-1400	-1300	69	<b>364</b>	-1400	-280	70.47	<b>415</b>	-1400	780	78.79
<b>314</b>	-1400	-1280	69	<b>365</b>	-1400	-260	70.62	<b>416</b>	-1400	800	83.47
<b>315</b>	-1400	-1260	72	<b>366</b>	-1400	-240	70.95	<b>417</b>	-1400	820	78.82
<b>316</b>	-1400	-1240	69	<b>367</b>	-1400	-220	71.31	<b>418</b>	-1400	840	81.86
<b>317</b>	-1400	-1220	70	<b>368</b>	-1400	-200	72.7	<b>419</b>	-1400	860	83.07
<b>318</b>	-1400	-1200	72	<b>369</b>	-1400	-180	69.45	<b>420</b>	-1400	880	80.94
<b>319</b>	-1400	-1180	73	<b>370</b>	-1400	-160	71.36	<b>421</b>	-1400	900	79.6
<b>320</b>	-1400	-1160	74	<b>371</b>	-1400	-140	71.52	<b>422</b>	-1400	920	84.84
<b>321</b>	-1400	-1140	77	<b>372</b>	-1400	-120	73.52	<b>423</b>	-1400	940	85.57
<b>322</b>	-1400	-1120	77	<b>373</b>	-1400	-100	72.9	<b>424</b>	-1400	960	88.26
<b>323</b>	-1400	-1100	83	<b>374</b>	-1400	-80	72.1	<b>425</b>	-1400	980	87.83
<b>324</b>	-1400	-1080	72	<b>375</b>	-1400	-60	73.35	<b>426</b>	-1400	1000	88.33
<b>325</b>	-1400	-1060	67	<b>376</b>	-1400	-40	72.7	<b>427</b>	-1400	1020	97.37
<b>326</b>	-1400	-1040	83	<b>377</b>	-1400	-20	73.28	<b>428</b>	-1400	1040	86.83
<b>327</b>	-1400	-1020	66	<b>378</b>	-1400	0	71.2	<b>429</b>	-1400	1060	88.61
<b>328</b>	-1400	-1000	71	<b>379</b>	-1400	20	73.34	<b>430</b>	-1400	1080	89.86
<b>329</b>	-1400	-980	67	<b>380</b>	-1400	40	74.3	<b>431</b>	-1400	1100	90.77
<b>330</b>	-1400	-960	64	<b>381</b>	-1400	60	75.35	<b>432</b>	-1400	1120	94.35
<b>331</b>	-1400	-940	69	<b>382</b>	-1400	80	76.64	<b>433</b>	-1400	1140	91.4
<b>332</b>	-1400	-920	77	<b>383</b>	-1400	100	74.7	<b>434</b>	-1400	1160	92.89
<b>333</b>	-1400	-900	29	<b>384</b>	-1400	120	74.39	<b>435</b>	-1400	1180	92.5
<b>334</b>	-1400	-880	54	<b>385</b>	-1400	140	74.64	<b>436</b>	-1400	1200	95.22
<b>335</b>	-1400	-860	66	<b>386</b>	-1400	160	72.75	<b>437</b>	-1500	-1840	90.43
<b>336</b>	-1400	-840	65	<b>387</b>	-1400	180	72.9	<b>438</b>	-1500	-1820	85.58
<b>337</b>	-1400	-820	66	<b>388</b>	-1400	200	76.1	<b>439</b>	-1500	-1800	71.42
<b>338</b>	-1400	-800	67	<b>389</b>	-1400	260	75.33	<b>440</b>	-1500	-1780	82.13
<b>339</b>	-1400	-780	61	<b>390</b>	-1400	280	91.97	<b>441</b>	-1500	-1760	78.37
<b>340</b>	-1400	-760	63.9	<b>391</b>	-1400	300	91.43	<b>442</b>	-1500	-1740	76.94
<b>341</b>	-1400	-740	66.8	<b>392</b>	-1400	320	86.8	<b>443</b>	-1500	-1720	78.37
<b>342</b>	-1400	-720	62.89	<b>393</b>	-1400	340	81.49	<b>444</b>	-1500	-1700	83.25
<b>343</b>	-1400	-700	62.4	<b>394</b>	-1400	360	76.68	<b>445</b>	-1500	-1680	87.69
<b>344</b>	-1400	-680	63.85	<b>395</b>	-1400	380	70.71	<b>446</b>	-1500	-1660	99.95
<b>345</b>	-1400	-660	66.12	<b>396</b>	-1400	400	73.93	<b>447</b>	-1500	-1640	101.16
<b>346</b>	-1400	-640	64.52	<b>397</b>	-1400	420	78.01	<b>448</b>	-1500	-1620	94.14
<b>347</b>	-1400	-620	64.05	<b>398</b>	-1400	440	78.76	<b>449</b>	-1500	-1600	89.34
<b>348</b>	-1400	-600	67.92	<b>399</b>	-1400	460	83.91	<b>450</b>	-1500	-1580	98.97
<b>349</b>	-1400	-580	64.14	<b>400</b>	-1400	480	87.16	<b>451</b>	-1500	-1560	110.09
<b>350</b>	-1400	-560	64.35	<b>401</b>	-1400	500	77.63	<b>452</b>	-1500	-1540	131.7
<b>351</b>	-1400	-540	65.81	<b>402</b>	-1400	520	77.87	<b>453</b>	-1500	-1520	154.62

454	-1500	-1500	-12.46	505	-1500	-300	71.92	556	-1500	800	69.34
455	-1500	-1480	34.49	506	-1500	-280	78.22	557	-1500	820	75.36
456	-1500	-1460	51.27	507	-1500	-260	79.72	558	-1500	840	77.27
457	-1500	-1440	54.68	508	-1500	-240	82.22	559	-1500	860	81
458	-1500	-1420	60.13	509	-1500	-220	83.12	560	-1500	880	82.78
459	-1500	-1400	62.42	510	-1500	-200	76.12	561	-1500	900	83.58
460	-1500	-1380	62.81	511	-1500	-180	75.42	562	-1500	920	84.89
461	-1500	-1360	66.21	512	-1500	-160	77.92	563	-1500	940	82.12
462	-1500	-1340	65.87	513	-1500	-140	77.42	564	-1500	960	86.09
463	-1500	-1320	66.08	514	-1500	-120	79.42	565	-1500	980	87.6
464	-1500	-1300	68.74	515	-1500	-100	78.92	566	-1500	1000	85.18
465	-1500	-1280	71.05	516	-1500	-80	77.42	567	-1500	1020	88.93
466	-1500	-1260	71.53	517	-1500	-60	76.42	568	-1500	1040	88.89
467	-1500	-1240	70.23	518	-1500	-40	81.22	569	-1500	1060	89.66
468	-1500	-1220	69.37	519	-1500	-20	81.92	570	-1500	1080	90.88
469	-1500	-1200	64.83	520	-1500	0	95.22	571	-1500	1100	90.21
470	-1500	-1180	69.56	521	-1500	20	76.82	572	-1600	1060	91.77
471	-1500	-1160	73.79	522	-1500	40	78.32	573	-1600	1040	89.33
472	-1500	-1140	76.44	523	-1500	60	78.42	574	-1600	1020	87.5
473	-1500	-1120	71.78	524	-1500	80	79.52	575	-1600	1000	86.66
474	-1500	-1100	80.66	525	-1500	100	82.62	576	-1600	980	83.03
475	-1500	-1080	73.06	526	-1500	120	80.82	577	-1600	960	84.84
476	-1500	-1060	66.24	527	-1500	220	88.62	578	-1600	940	86.53
477	-1500	-880	67.12	528	-1500	240	83.62	579	-1600	920	84.85
478	-1500	-860	68.7	529	-1500	260	93.32	580	-1600	900	83.17
479	-1500	-840	65.99	530	-1500	280	84.72	581	-1600	880	79.01
480	-1500	-820	70.02	531	-1500	300	88.92	582	-1600	860	89.31
481	-1500	-800	74.32	532	-1500	320	100.92	583	-1600	840	74.46
482	-1500	-780	73.22	533	-1500	340	99.22	584	-1600	820	67.78
483	-1500	-760	71.82	534	-1500	360	78.62	585	-1600	800	73.57
484	-1500	-740	72.52	535	-1500	380	77.22	586	-1600	780	99.46
485	-1500	-720	71.52	536	-1500	400	81.72	587	-1600	760	84.92
486	-1500	-700	72.12	537	-1500	420	82.42	588	-1600	740	83.66
487	-1500	-680	73.12	538	-1500	440	86.82	589	-1600	720	79.41
488	-1500	-640	72.12	539	-1500	460	84.02	590	-1600	700	76.73
489	-1500	-620	72.12	540	-1500	480	73.32	591	-1600	680	97.75
490	-1500	-600	72.72	541	-1500	500	77.42	592	-1600	660	86.54
491	-1500	-580	73.52	542	-1500	520	81.02	593	-1600	640	83.26
492	-1500	-560	78.22	543	-1500	540	79.42	594	-1600	620	81.99
493	-1500	-540	72.42	544	-1500	560	79.13	595	-1600	600	80.71
494	-1500	-520	75.02	545	-1500	580	78.46	596	-1600	580	80.86
495	-1500	-500	72.42	546	-1500	600	79.86	597	-1600	560	76.74
496	-1500	-480	73.62	547	-1500	620	82.59	598	-1600	540	77
497	-1500	-460	73.32	548	-1500	640	85.72	599	-1600	520	73.13
498	-1500	-440	70.82	549	-1500	660	101.85	600	-1600	500	76.41
499	-1500	-420	73.92	550	-1500	680	156.42	601	-1600	480	81.67
500	-1500	-400	75.62	551	-1500	700	207.16	602	-1600	460	81.43
501	-1500	-380	76.12	552	-1500	720	-9.13	603	-1600	440	80.26
502	-1500	-360	72.72	553	-1500	740	42.38	604	-1600	420	77.91
503	-1500	-340	76.62	554	-1500	760	71.4	605	-1600	400	79.1
504	-1500	-320	74.42	555	-1500	780	79.79	606	-1600	380	75.75

<b>607</b>	-1600	360	79.26	<b>658</b>	-1600	-780	70	<b>709</b>	-1600	-1800	55
<b>608</b>	-1600	340	82.49	<b>659</b>	-1600	-800	69	<b>710</b>	-1700	-2020	81
<b>609</b>	-1600	300	79.32	<b>660</b>	-1600	-820	68	<b>711</b>	-1700	-2000	89
<b>610</b>	-1600	280	76.98	<b>661</b>	-1600	-840	62	<b>712</b>	-1700	-1980	97
<b>611</b>	-1600	260	78.47	<b>662</b>	-1600	-860	70	<b>713</b>	-1700	-1960	100
<b>612</b>	-1600	240	71.45	<b>663</b>	-1600	-880	70	<b>714</b>	-1700	-1940	125
<b>613</b>	-1600	220	72.42	<b>664</b>	-1600	-900	64	<b>715</b>	-1700	-1920	131
<b>614</b>	-1600	200	74.49	<b>665</b>	-1600	-920	47	<b>716</b>	-1700	-1900	73
<b>615</b>	-1600	180	75.2	<b>666</b>	-1600	-940	67	<b>717</b>	-1700	-1880	93
<b>616</b>	-1600	160	77.98	<b>667</b>	-1600	-960	60	<b>718</b>	-1700	-1860	90
<b>617</b>	-1600	60	75.4	<b>668</b>	-1600	-980	63	<b>719</b>	-1700	-1840	81
<b>618</b>	-1600	40	74.58	<b>669</b>	-1600	-1000	62	<b>720</b>	-1700	-1820	59
<b>619</b>	-1600	20	72.76	<b>670</b>	-1600	-1020	69	<b>721</b>	-1700	-1800	102
<b>620</b>	-1600	0	77.85	<b>671</b>	-1600	-1040	71	<b>722</b>	-1700	-1780	63
<b>621</b>	-1600	-20	78.16	<b>672</b>	-1600	-1060	65	<b>723</b>	-1700	-1760	77
<b>622</b>	-1600	-40	75.05	<b>673</b>	-1600	-1080	64	<b>724</b>	-1700	-1740	82
<b>623</b>	-1600	-60	75.42	<b>674</b>	-1600	-1100	73	<b>725</b>	-1700	-1720	83
<b>624</b>	-1600	-80	74.44	<b>675</b>	-1600	-1120	66	<b>726</b>	-1700	-1700	94
<b>625</b>	-1600	-100	72.41	<b>676</b>	-1600	-1140	56	<b>727</b>	-1700	-1680	99
<b>626</b>	-1600	-120	73.36	<b>677</b>	-1600	-1160	73	<b>728</b>	-1700	-1660	87
<b>627</b>	-1600	-140	73.87	<b>678</b>	-1600	-1180	77	<b>729</b>	-1700	-1640	91
<b>628</b>	-1600	-160	74.48	<b>679</b>	-1600	-1200	87	<b>730</b>	-1700	-1620	105
<b>629</b>	-1600	-180	76.96	<b>680</b>	-1600	-1220	83	<b>731</b>	-1700	-1600	117
<b>630</b>	-1600	-220	70.5	<b>681</b>	-1600	-1240	84	<b>732</b>	-1700	-1580	126
<b>631</b>	-1600	-240	72.07	<b>682</b>	-1600	-1260	78	<b>733</b>	-1700	-1560	111
<b>632</b>	-1600	-260	71.98	<b>683</b>	-1600	-1280	71	<b>734</b>	-1700	-1540	67
<b>633</b>	-1600	-280	71.99	<b>684</b>	-1600	-1300	74	<b>735</b>	-1700	-1520	48
<b>634</b>	-1600	-300	70.43	<b>685</b>	-1600	-1320	68	<b>736</b>	-1700	-1500	58
<b>635</b>	-1600	-320	70.24	<b>686</b>	-1600	-1340	68	<b>737</b>	-1700	-1480	65
<b>636</b>	-1600	-340	71.77	<b>687</b>	-1600	-1360	64	<b>738</b>	-1700	-1460	65
<b>637</b>	-1600	-360	71.94	<b>688</b>	-1600	-1380	61	<b>739</b>	-1700	-1440	65.1
<b>638</b>	-1600	-380	72.84	<b>689</b>	-1600	-1400	59	<b>740</b>	-1700	-1420	67.33
<b>639</b>	-1600	-400	71.35	<b>690</b>	-1600	-1420	59	<b>741</b>	-1700	-1400	66.34
<b>640</b>	-1600	-420	71.95	<b>691</b>	-1600	-1440	55	<b>742</b>	-1700	-1380	64.87
<b>641</b>	-1600	-440	69.09	<b>692</b>	-1600	-1460	53	<b>743</b>	-1700	-1360	67.46
<b>642</b>	-1600	-460	70.18	<b>693</b>	-1600	-1480	50	<b>744</b>	-1700	-1340	69.74
<b>643</b>	-1600	-480	71.22	<b>694</b>	-1600	-1500	33	<b>745</b>	-1700	-1320	73.86
<b>644</b>	-1600	-500	70.87	<b>695</b>	-1600	-1520	31	<b>746</b>	-1700	-1300	74.93
<b>645</b>	-1600	-520	67.42	<b>696</b>	-1600	-1540	138	<b>747</b>	-1700	-1280	75.93
<b>646</b>	-1600	-540	68.27	<b>697</b>	-1600	-1560	135	<b>748</b>	-1700	-1260	74.75
<b>647</b>	-1600	-560	67.83	<b>698</b>	-1600	-1580	130	<b>749</b>	-1700	-1240	78.81
<b>648</b>	-1600	-580	68.35	<b>699</b>	-1600	-1600	111	<b>750</b>	-1700	-1220	80.78
<b>649</b>	-1600	-600	69.43	<b>700</b>	-1600	-1620	99	<b>751</b>	-1700	-1200	71.45
<b>650</b>	-1600	-620	70.21	<b>701</b>	-1600	-1640	97	<b>752</b>	-1700	-1180	67.87
<b>651</b>	-1600	-640	71.04	<b>702</b>	-1600	-1660	96	<b>753</b>	-1700	-1160	70.88
<b>652</b>	-1600	-660	69.71	<b>703</b>	-1600	-1680	88	<b>754</b>	-1700	-1140	67.65
<b>653</b>	-1600	-680	69	<b>704</b>	-1600	-1700	86	<b>755</b>	-1700	-1120	65.28
<b>654</b>	-1600	-700	68	<b>705</b>	-1600	-1720	80	<b>756</b>	-1700	-1100	71.1
<b>655</b>	-1600	-720	69	<b>706</b>	-1600	-1740	81	<b>757</b>	-1700	-1080	65.49
<b>656</b>	-1600	-740	67	<b>707</b>	-1600	-1760	79	<b>758</b>	-1700	-1060	50.37
<b>657</b>	-1600	-760	68	<b>708</b>	-1600	-1780	69	<b>759</b>	-1700	-1040	67.45

<b>760</b>	-1700	-1020	70.89	<b>811</b>	-1700	100	76.37	<b>862</b>	-1700	1160	79.35
<b>761</b>	-1700	-1000	67.28	<b>812</b>	-1700	120	76.56	<b>863</b>	-1700	1180	95.79
<b>762</b>	-1700	-980	76.88	<b>813</b>	-1700	140	75.17	<b>864</b>	-1700	1200	91.02
<b>763</b>	-1700	-960	61.93	<b>814</b>	-1700	160	75.63	<b>865</b>	-1700	1220	89.81
<b>764</b>	-1700	-940	53	<b>815</b>	-1700	180	75.09	<b>866</b>	-1700	1240	81.04
<b>765</b>	-1700	-920	73.18	<b>816</b>	-1700	200	74.54	<b>867</b>	-1700	1260	90.04
<b>766</b>	-1700	-900	65.45	<b>817</b>	-1700	220	75.5	<b>868</b>	-1700	1280	89.96
<b>767</b>	-1700	-880	64.02	<b>818</b>	-1700	240	76.43	<b>869</b>	-1700	1300	88.93
<b>768</b>	-1700	-860	56.17	<b>819</b>	-1700	260	76.74	<b>870</b>	-1800	1260	96.33
<b>769</b>	-1700	-840	49.91	<b>820</b>	-1700	280	76.99	<b>871</b>	-1800	1240	90.43
<b>770</b>	-1700	-820	65.59	<b>821</b>	-1700	300	76.95	<b>872</b>	-1800	1220	94.76
<b>771</b>	-1700	-800	66.62	<b>822</b>	-1700	320	78.42	<b>873</b>	-1800	1200	97.47
<b>772</b>	-1700	-780	65.77	<b>823</b>	-1700	340	79.26	<b>874</b>	-1800	1180	95.04
<b>773</b>	-1700	-760	67.09	<b>824</b>	-1700	360	77.71	<b>875</b>	-1800	1160	90.18
<b>774</b>	-1700	-740	67.62	<b>825</b>	-1700	380	79.81	<b>876</b>	-1800	1140	91.66
<b>775</b>	-1700	-720	66.12	<b>826</b>	-1700	400	80.48	<b>877</b>	-1800	1120	81.08
<b>776</b>	-1700	-700	66.34	<b>827</b>	-1700	420	74.84	<b>878</b>	-1800	1100	84.7
<b>777</b>	-1700	-680	67.81	<b>828</b>	-1700	440	81.8	<b>879</b>	-1800	1080	93.31
<b>778</b>	-1700	-660	68.07	<b>829</b>	-1700	460	78.31	<b>880</b>	-1800	1060	90.24
<b>779</b>	-1700	-640	67.01	<b>830</b>	-1700	480	79.23	<b>881</b>	-1800	1040	88.68
<b>780</b>	-1700	-620	67.57	<b>831</b>	-1700	500	78.7	<b>882</b>	-1800	1020	88.49
<b>781</b>	-1700	-600	66.47	<b>832</b>	-1700	520	78.1	<b>883</b>	-1800	1000	86.46
<b>782</b>	-1700	-580	74.49	<b>833</b>	-1700	540	79.74	<b>884</b>	-1800	980	87.67
<b>783</b>	-1700	-560	67.84	<b>834</b>	-1700	600	70.99	<b>885</b>	-1800	960	83.92
<b>784</b>	-1700	-540	68.02	<b>835</b>	-1700	620	73.59	<b>886</b>	-1800	940	85.22
<b>785</b>	-1700	-520	66.66	<b>836</b>	-1700	640	76.38	<b>887</b>	-1800	920	83.7
<b>786</b>	-1700	-500	62.83	<b>837</b>	-1700	660	75.86	<b>888</b>	-1800	900	83.31
<b>787</b>	-1700	-480	69.32	<b>838</b>	-1700	680	80.25	<b>889</b>	-1800	880	81.86
<b>788</b>	-1700	-460	66.94	<b>839</b>	-1700	700	80.93	<b>890</b>	-1800	860	84.82
<b>789</b>	-1700	-440	68.24	<b>840</b>	-1700	720	81.79	<b>891</b>	-1800	840	84.56
<b>790</b>	-1700	-420	67.74	<b>841</b>	-1700	740	81.34	<b>892</b>	-1800	820	81.08
<b>791</b>	-1700	-400	68.16	<b>842</b>	-1700	760	78.47	<b>893</b>	-1800	800	82.14
<b>792</b>	-1700	-380	68.86	<b>843</b>	-1700	780	77.22	<b>894</b>	-1800	780	81.53
<b>793</b>	-1700	-360	63.61	<b>844</b>	-1700	800	78.65	<b>895</b>	-1800	760	84.46
<b>794</b>	-1700	-340	70.73	<b>845</b>	-1700	820	83.49	<b>896</b>	-1800	740	81.28
<b>795</b>	-1700	-320	69.92	<b>846</b>	-1700	840	84.74	<b>897</b>	-1800	720	82.43
<b>796</b>	-1700	-300	68.53	<b>847</b>	-1700	860	76.5	<b>898</b>	-1800	700	83.9
<b>797</b>	-1700	-280	69.51	<b>848</b>	-1700	880	80.21	<b>899</b>	-1800	680	81.49
<b>798</b>	-1700	-260	68.42	<b>849</b>	-1700	900	79.67	<b>900</b>	-1800	660	84.2
<b>799</b>	-1700	-240	69.67	<b>850</b>	-1700	920	80.04	<b>901</b>	-1800	600	84.09
<b>800</b>	-1700	-220	69.39	<b>851</b>	-1700	940	80.67	<b>902</b>	-1800	580	79.17
<b>801</b>	-1700	-200	69.31	<b>852</b>	-1700	960	78.44	<b>903</b>	-1800	560	79.07
<b>802</b>	-1700	-180	64.79	<b>853</b>	-1700	980	83.4	<b>904</b>	-1800	540	81.19
<b>803</b>	-1700	-160	63.25	<b>854</b>	-1700	1000	85.12	<b>905</b>	-1800	520	79.94
<b>804</b>	-1700	-140	70.89	<b>855</b>	-1700	1020	80.09	<b>906</b>	-1800	500	79.71
<b>805</b>	-1700	-120	72.31	<b>856</b>	-1700	1040	83.77	<b>907</b>	-1800	480	80.6
<b>806</b>	-1700	-100	70.25	<b>857</b>	-1700	1060	84.15	<b>908</b>	-1800	460	78.23
<b>807</b>	-1700	-80	70.67	<b>858</b>	-1700	1080	91.01	<b>909</b>	-1800	450	79.02
<b>808</b>	-1700	-60	71.61	<b>859</b>	-1700	1100	84.17	<b>910</b>	-1800	440	77.91
<b>809</b>	-1700	-40	71.26	<b>860</b>	-1700	1120	76.6	<b>911</b>	-1800	420	78.82
<b>810</b>	-1700	-20	74.7	<b>861</b>	-1700	1140	79.92	<b>912</b>	-1800	400	78.13

913	-1800	380	77.55	964	-1800	-800	66	1015	-1800	-1820	82
914	-1800	360	77.82	965	-1800	-820	66.36	1016	-1800	-1840	108
915	-1800	340	77.98	966	-1800	-840	64.9	1017	-1800	-1860	67
916	-1800	320	75.92	967	-1800	-860	66.85	1018	-1800	-1880	65
917	-1800	300	72.71	968	-1800	-880	65.87	1019	-1800	-1900	121
918	-1800	280	80.58	969	-1800	-900	65.48	1020	-1800	-1920	124
919	-1800	260	71.14	970	-1800	-920	66.7	1021	-1800	-1940	130
920	-1800	240	76.18	971	-1800	-940	65.79	1022	-1800	-1960	102
921	-1800	220	75.07	972	-1800	-960	66.67	1023	-1800	-1980	95
922	-1800	200	74.88	973	-1800	-980	63.43	1024	-1800	-2000	97
923	-1800	180	75.51	974	-1800	-1000	63.91	1025	-1800	-2020	84
924	-1800	160	75.06	975	-1800	-1020	66.95	1026	-1900	780	80.99
925	-1800	140	76.43	976	-1800	-1040	67.31	1027	-1900	760	81.53
926	-1800	120	75.24	977	-1800	-1060	64.6	1028	-1900	740	82.77
927	-1800	100	75.37	978	-1800	-1080	65.08	1029	-1900	720	83.17
928	-1800	80	75.48	979	-1800	-1100	68.81	1030	-1900	700	84.11
929	-1800	60	74.87	980	-1800	-1120	67	1031	-1900	680	83.21
930	-1800	40	76.82	981	-1800	-1140	76	1032	-1900	660	84.14
931	-1800	20	80.21	982	-1800	-1160	72	1033	-1900	640	82.3
932	-1800	0	89.53	983	-1800	-1180	72	1034	-1900	620	81.59
933	-1800	-100	69.36	984	-1800	-1200	73	1035	-1900	600	80.98
934	-1800	-120	68.84	985	-1800	-1220	75	1036	-1900	580	79.99
935	-1800	-140	69.21	986	-1800	-1240	73	1037	-1900	560	78.18
936	-1800	-160	77.54	987	-1800	-1260	73	1038	-1900	540	82.23
937	-1800	-180	66.02	988	-1800	-1280	70	1039	-1900	520	79.61
938	-1800	-200	69.34	989	-1800	-1300	79	1040	-1900	500	80.43
939	-1800	-220	70.7	990	-1800	-1320	81	1041	-1900	480	83.63
940	-1800	-240	67.3	991	-1800	-1340	77	1042	-1900	460	78.63
941	-1800	-260	70.61	992	-1800	-1360	72	1043	-1900	440	78.28
942	-1800	-280	68.4	993	-1800	-1380	70	1044	-1900	420	77.5
943	-1800	-300	71.58	994	-1800	-1400	69	1045	-1900	400	82.82
944	-1800	-320	64.1	995	-1800	-1420	70	1046	-1900	380	77.58
945	-1800	-340	65.34	996	-1800	-1440	67	1047	-1900	360	76.89
946	-1800	-360	68.26	997	-1800	-1460	63	1048	-1900	340	75.55
947	-1800	-380	70.91	998	-1800	-1480	63	1049	-1900	320	77.36
948	-1800	-400	74.5	999	-1800	-1500	58	1050	-1900	300	77.35
949	-1800	-440	68.24	1000	-1800	-1520	48	1051	-1900	280	75.98
950	-1800	-460	69.43	1001	-1800	-1540	31	1052	-1900	260	76.11
951	-1800	-480	70.11	1002	-1800	-1560	52	1053	-1900	240	78.2
952	-1800	-500	67.11	1003	-1800	-1580	107	1054	-1900	220	76.62
953	-1800	-520	67.62	1004	-1800	-1600	125	1055	-1900	200	75.97
954	-1800	-540	67.41	1005	-1800	-1620	112	1056	-1900	180	74.83
955	-1800	-560	64.97	1006	-1800	-1640	101	1057	-1900	160	74.54
956	-1800	-580	66.59	1007	-1800	-1660	91	1058	-1900	140	73.9
957	-1800	-600	57.07	1008	-1800	-1680	95	1059	-1900	120	73.98
958	-1800	-640	66.81	1009	-1800	-1700	96	1060	-1900	100	73.64
959	-1800	-680	70.08	1010	-1800	-1720	82	1061	-1900	80	73.4
960	-1800	-700	69.76	1011	-1800	-1740	85	1062	-1900	60	73.67
961	-1800	-720	66.76	1012	-1800	-1760	89	1063	-1900	40	74.49
962	-1800	-740	66.75	1013	-1800	-1780	114	1064	-1900	20	72.77
963	-1800	-760	67.15	1014	-1800	-1800	87	1065	-1900	0	72.98

1066	-1900	-20	73.38	1117	-1900	-1120	67.77	1168	-2000	-1900	76.56
1067	-1900	-40	72.87	1118	-1900	-1140	70.17	1169	-2000	-1880	80.2
1068	-1900	-60	75.36	1119	-1900	-1160	69.21	1170	-2000	-1860	84.11
1069	-1900	-160	70.02	1120	-1900	-1180	67.52	1171	-2000	-1840	86.74
1070	-1900	-180	71.23	1121	-1900	-1200	69.62	1172	-2000	-1820	92.49
1071	-1900	-200	65.14	1122	-1900	-1220	76.34	1173	-2000	-1800	95.96
1072	-1900	-220	68.8	1123	-1900	-1240	77.52	1174	-2000	-1780	96.86
1073	-1900	-240	72.05	1124	-1900	-1260	71.96	1175	-2000	-1760	96.61
1074	-1900	-260	69.51	1125	-1900	-1280	69.41	1176	-2000	-1740	83.24
1075	-1900	-280	69.09	1126	-1900	-1300	63.96	1177	-2000	-1720	93.84
1076	-1900	-300	67.8	1127	-1900	-1320	63.94	1178	-2000	-1700	98.81
1077	-1900	-320	67.1	1128	-1900	-1340	86.55	1179	-2000	-1680	103.63
1078	-1900	-340	62.96	1129	-1900	-1360	92.79	1180	-2000	-1660	112.67
1079	-1900	-360	70.08	1130	-1900	-1380	76.09	1181	-2000	-1640	133.64
1080	-1900	-380	71.87	1131	-1900	-1400	70.01	1182	-2000	-1620	102.57
1081	-1900	-400	67.7	1132	-1900	-1420	65.26	1183	-2000	-1600	80.52
1082	-1900	-420	61.65	1133	-1900	-1440	63.91	1184	-2000	-1580	18.91
1083	-1900	-440	63.69	1134	-1900	-1460	71.55	1185	-2000	-1560	41.85
1084	-1900	-460	65.81	1135	-1900	-1480	59.6	1186	-2000	-1540	56.33
1085	-1900	-480	75.66	1136	-1900	-1500	55.31	1187	-2000	-1520	57.4
1086	-1900	-500	70.69	1137	-1900	-1520	64.77	1188	-2000	-1500	62.84
1087	-1900	-520	70.37	1138	-1900	-1540	37.26	1189	-2000	-1480	62.91
1088	-1900	-540	69.19	1139	-1900	-1560	11.02	1190	-2000	-1460	62.01
1089	-1900	-560	69.74	1140	-1900	-1580	69.98	1191	-2000	-1440	64.97
1090	-1900	-580	68.21	1141	-1900	-1600	91.26	1192	-2000	-1420	72.11
1091	-1900	-600	68.68	1142	-1900	-1620	106.02	1193	-2000	-1400	85.45
1092	-1900	-620	68.39	1143	-1900	-1640	97.47	1194	-2000	-1380	82.03
1093	-1900	-640	67.35	1144	-1900	-1660	91.1	1195	-2000	-1360	65.84
1094	-1900	-660	71.07	1145	-1900	-1680	99.62	1196	-2000	-1340	65.26
1095	-1900	-680	67.12	1146	-1900	-1700	92.53	1197	-2000	-1320	67.52
1096	-1900	-700	66.69	1147	-1900	-1720	86.63	1198	-2000	-1300	69.04
1097	-1900	-720	72.27	1148	-1900	-1740	88.98	1199	-2000	-1280	72.87
1098	-1900	-740	67.29	1149	-1900	-1760	91.99	1200	-2000	-1260	72.43
1099	-1900	-760	65.13	1150	-1900	-1780	90.71	1201	-2000	-1240	60.39
1100	-1900	-780	66.45	1151	-1900	-1800	91.32	1202	-2000	-1220	62.88
1101	-1900	-800	67.71	1152	-1900	-1820	88.82	1203	-2000	-1200	72.91
1102	-1900	-820	66.39	1153	-1900	-1840	88.74	1204	-2000	-1180	75.71
1103	-1900	-840	67.69	1154	-1900	-1860	85.4	1205	-2000	-1080	69.21
1104	-1900	-860	66	1155	-1900	-1880	88.06	1206	-2000	-1060	66.56
1105	-1900	-880	63.46	1156	-1900	-1900	87.13	1207	-2000	-1040	70.24
1106	-1900	-900	66.21	1157	-1900	-1920	89.6	1208	-2000	-1020	68.89
1107	-1900	-920	67.51	1158	-1900	-1940	87.51	1209	-2000	-1000	70.2
1108	-1900	-940	65.33	1159	-1900	-1960	85.02	1210	-2000	-980	66.94
1109	-1900	-960	66.7	1160	-1900	-1980	80.7	1211	-2000	-960	63.91
1110	-1900	-980	64.38	1161	-1900	-2000	75.25	1212	-2000	-940	68.1
1111	-1900	-1000	62.51	1162	-2000	-2020	83.03	1213	-2000	-920	67.16
1112	-1900	-1020	61.69	1163	-2000	-2000	81.13	1214	-2000	-900	65.55
1113	-1900	-1040	65.3	1164	-2000	-1980	84.9	1215	-2000	-880	66.98
1114	-1900	-1060	55.55	1165	-2000	-1960	89.9	1216	-2000	-860	67.5
1115	-1900	-1080	70.95	1166	-2000	-1940	96.92	1217	-2000	-840	67.42
1116	-1900	-1100	69.54	1167	-2000	-1920	79.52	1218	-2000	-820	65.09

<b>1219</b>	-2000	-800	70.21	<b>1270</b>	-2000	380	77.27	<b>1321</b>	-2100	1080	88.05
<b>1220</b>	-2000	-780	62.76	<b>1271</b>	-2000	420	77.03	<b>1322</b>	-2100	1060	91.3
<b>1221</b>	-2000	-760	67.5	<b>1272</b>	-2000	440	76.03	<b>1323</b>	-2100	1040	87.3
<b>1222</b>	-2000	-740	66.78	<b>1273</b>	-2000	460	76.01	<b>1324</b>	-2100	1020	88.18
<b>1223</b>	-2000	-700	68.36	<b>1274</b>	-2000	480	77.21	<b>1325</b>	-2100	1000	89.32
<b>1224</b>	-2000	-680	65.42	<b>1275</b>	-2000	500	79.32	<b>1326</b>	-2100	980	92.34
<b>1225</b>	-2000	-660	66.77	<b>1276</b>	-2000	520	80.03	<b>1327</b>	-2100	860	79.21
<b>1226</b>	-2000	-640	66.97	<b>1277</b>	-2000	540	81.92	<b>1328</b>	-2100	840	82.2
<b>1227</b>	-2000	-620	68.17	<b>1278</b>	-2000	560	81.61	<b>1329</b>	-2100	820	81.82
<b>1228</b>	-2000	-600	68.31	<b>1279</b>	-2000	580	81.59	<b>1330</b>	-2100	800	81.66
<b>1229</b>	-2000	-580	68.12	<b>1280</b>	-2000	600	81.09	<b>1331</b>	-2100	780	82.01
<b>1230</b>	-2000	-560	71.16	<b>1281</b>	-2000	620	83.66	<b>1332</b>	-2100	760	81.24
<b>1231</b>	-2000	-540	69.42	<b>1282</b>	-2000	640	82.75	<b>1333</b>	-2100	740	86.91
<b>1232</b>	-2000	-520	66.85	<b>1283</b>	-2000	660	82.42	<b>1334</b>	-2100	720	83.27
<b>1233</b>	-2000	-500	69.6	<b>1284</b>	-2000	680	81.76	<b>1335</b>	-2100	700	83.17
<b>1234</b>	-2000	-480	67.01	<b>1285</b>	-2000	700	82.71	<b>1336</b>	-2100	680	83.17
<b>1235</b>	-2000	-460	67.1	<b>1286</b>	-2000	720	82.98	<b>1337</b>	-2100	660	81.43
<b>1236</b>	-2000	-440	68.15	<b>1287</b>	-2000	740	83.48	<b>1338</b>	-2100	640	83.1
<b>1237</b>	-2000	-420	68.23	<b>1288</b>	-2000	760	82	<b>1339</b>	-2100	620	81.28
<b>1238</b>	-2000	-400	67.1	<b>1289</b>	-2000	780	82.92	<b>1340</b>	-2100	600	80.98
<b>1239</b>	-2000	-380	63.96	<b>1290</b>	-2000	800	83.54	<b>1341</b>	-2100	580	79.54
<b>1240</b>	-2000	-360	69.72	<b>1291</b>	-2000	820	85.62	<b>1342</b>	-2100	560	81.81
<b>1241</b>	-2000	-340	69.16	<b>1292</b>	-2000	840	75.08	<b>1343</b>	-2100	540	80.06
<b>1242</b>	-2000	-320	70	<b>1293</b>	-2000	980	98.13	<b>1344</b>	-2100	520	79.56
<b>1243</b>	-2000	-300	67.36	<b>1294</b>	-2000	1000	89.21	<b>1345</b>	-2100	500	78.55
<b>1244</b>	-2000	-280	64.7	<b>1295</b>	-2000	1020	88.76	<b>1346</b>	-2100	480	76.34
<b>1245</b>	-2000	-260	66.18	<b>1296</b>	-2000	1040	87.2	<b>1347</b>	-2100	460	78.2
<b>1246</b>	-2000	-240	58.14	<b>1297</b>	-2000	1060	91.35	<b>1348</b>	-2100	440	75.78
<b>1247</b>	-2000	-120	76.04	<b>1298</b>	-2000	1080	89.72	<b>1349</b>	-2100	420	77.3
<b>1248</b>	-2000	-100	73.69	<b>1299</b>	-2000	1100	89.64	<b>1350</b>	-2100	400	80.42
<b>1249</b>	-2000	-80	73.17	<b>1300</b>	-2000	1120	92.61	<b>1351</b>	-2100	380	83.22
<b>1250</b>	-2000	-60	73.66	<b>1301</b>	-2000	1140	93.39	<b>1352</b>	-2100	360	82.5
<b>1251</b>	-2000	-40	73.38	<b>1302</b>	-2000	1160	91.47	<b>1353</b>	-2100	340	79.34
<b>1252</b>	-2000	-20	71.76	<b>1303</b>	-2000	1180	93.15	<b>1354</b>	-2100	320	79.84
<b>1253</b>	-2000	0	72.15	<b>1304</b>	-2000	1200	93.06	<b>1355</b>	-2100	300	77.17
<b>1254</b>	-2000	20	74	<b>1305</b>	-2000	1220	95.26	<b>1356</b>	-2100	280	77.57
<b>1255</b>	-2000	60	75.55	<b>1306</b>	-2000	1240	99.72	<b>1357</b>	-2100	260	76.72
<b>1256</b>	-2000	80	75.16	<b>1307</b>	-2000	1260	99.35	<b>1358</b>	-2100	240	76.74
<b>1257</b>	-2000	100	74.29	<b>1308</b>	-2000	1280	98.31	<b>1359</b>	-2100	220	81.62
<b>1258</b>	-2000	120	74.52	<b>1309</b>	-2000	1300	98.83	<b>1360</b>	-2100	200	77.67
<b>1259</b>	-2000	140	75.26	<b>1310</b>	-2100	1300	99.27	<b>1361</b>	-2100	180	75.72
<b>1260</b>	-2000	160	73.43	<b>1311</b>	-2100	1280	97.56	<b>1362</b>	-2100	160	76.74
<b>1261</b>	-2000	180	79.55	<b>1312</b>	-2100	1260	95.3	<b>1363</b>	-2100	140	76.52
<b>1262</b>	-2000	200	74.7	<b>1313</b>	-2100	1240	95.25	<b>1364</b>	-2100	120	75.82
<b>1263</b>	-2000	220	74.79	<b>1314</b>	-2100	1220	95.23	<b>1365</b>	-2100	100	76.68
<b>1264</b>	-2000	240	74.22	<b>1315</b>	-2100	1200	94.89	<b>1366</b>	-2100	80	75.79
<b>1265</b>	-2000	260	77.24	<b>1316</b>	-2100	1180	95.75	<b>1367</b>	-2100	60	75.49
<b>1266</b>	-2000	280	76.68	<b>1317</b>	-2100	1160	93.08	<b>1368</b>	-2100	40	74.84
<b>1267</b>	-2000	320	77.65	<b>1318</b>	-2100	1140	93.9	<b>1369</b>	-2100	20	72.02
<b>1268</b>	-2000	340	75.52	<b>1319</b>	-2100	1120	90.67	<b>1370</b>	-2100	0	74.19
<b>1269</b>	-2000	360	77.1	<b>1320</b>	-2100	1100	89.5	<b>1371</b>	-2100	-20	73.9

1372	-2100	-40	72.14	1423	-2100	-1240	92.04	1474	-2200	-1860	78.9
1373	-2100	-60	72.65	1424	-2100	-1260	79.35	1475	-2200	-1840	82.08
1374	-2100	-80	71.89	1425	-2100	-1280	72.56	1476	-2200	-1820	79.03
1375	-2100	-100	72.35	1426	-2100	-1300	72.44	1477	-2200	-1800	87.44
1376	-2100	-120	71.96	1427	-2100	-1320	68.08	1478	-2200	-1780	86
1377	-2100	-140	71.51	1428	-2100	-1340	66.46	1479	-2200	-1760	86.48
1378	-2100	-160	70.39	1429	-2100	-1360	66.27	1480	-2200	-1740	96.04
1379	-2100	-180	73.81	1430	-2100	-1380	64.54	1481	-2200	-1720	97.96
1380	-2100	-320	77.43	1431	-2100	-1400	68.04	1482	-2200	-1700	107.39
1381	-2100	-340	71.44	1432	-2100	-1420	64.76	1483	-2200	-1680	124.22
1382	-2100	-360	69.76	1433	-2100	-1440	65.51	1484	-2200	-1660	140.54
1383	-2100	-380	70.46	1434	-2100	-1460	66.79	1485	-2200	-1640	100.7
1384	-2100	-400	69.58	1435	-2100	-1480	65.88	1486	-2200	-1620	27
1385	-2100	-420	67.34	1436	-2100	-1500	68.27	1487	-2200	-1600	28.71
1386	-2100	-440	63.63	1437	-2100	-1520	65.88	1488	-2200	-1580	46.7
1387	-2100	-460	73.39	1438	-2100	-1540	63.18	1489	-2200	-1560	55.12
1388	-2100	-480	73.18	1439	-2100	-1560	59.96	1490	-2200	-1540	57.96
1389	-2100	-500	69.77	1440	-2100	-1580	53.03	1491	-2200	-1520	61.26
1390	-2100	-520	72.18	1441	-2100	-1600	45.98	1492	-2200	-1500	61.91
1391	-2100	-540	72.55	1442	-2100	-1620	81.87	1493	-2200	-1480	63.66
1392	-2100	-560	68.18	1443	-2100	-1640	114.17	1494	-2200	-1460	64.77
1393	-2100	-580	68.69	1444	-2100	-1660	125.93	1495	-2200	-1440	70
1394	-2100	-600	69.17	1445	-2100	-1680	118.16	1496	-2200	-1420	73
1395	-2100	-620	68.7	1446	-2100	-1700	106.76	1497	-2200	-1400	67.44
1396	-2100	-640	68.48	1447	-2100	-1720	93.42	1498	-2200	-1380	68.17
1397	-2100	-660	65.05	1448	-2100	-1740	96.18	1499	-2200	-1360	68.55
1398	-2100	-680	65.8	1449	-2100	-1760	91.92	1500	-2200	-1340	71.95
1399	-2100	-700	66.65	1450	-2100	-1780	88.77	1501	-2200	-1320	75.64
1400	-2100	-720	64.34	1451	-2100	-1800	92.54	1502	-2200	-1300	75.86
1401	-2100	-740	64.44	1452	-2100	-1820	91.65	1503	-2200	-1280	71.28
1402	-2100	-760	65.8	1453	-2100	-1840	90.85	1504	-2200	-1260	69.37
1403	-2100	-780	66.66	1454	-2100	-1860	88.72	1505	-2200	-1240	71.54
1404	-2100	-800	69.14	1455	-2100	-1880	85.21	1506	-2200	-1220	71.49
1405	-2100	-820	69.17	1456	-2100	-1900	82.59	1507	-2200	-1200	69.85
1406	-2100	-840	68.15	1457	-2100	-1920	78.67	1508	-2200	-1180	66.32
1407	-2100	-860	68.78	1458	-2100	-1940	81.69	1509	-2200	-1160	62.67
1408	-2100	-880	67.75	1459	-2100	-1960	79.58	1510	-2200	-1140	63.06
1409	-2100	-900	66.24	1460	-2100	-1980	92.21	1511	-2200	-1120	63.43
1410	-2100	-920	68.04	1461	-2100	-2000	86.92	1512	-2200	-1100	66.62
1411	-2100	-940	63.94	1462	-2200	-2100	70.62	1513	-2200	-1080	63.58
1412	-2100	-960	63.26	1463	-2200	-2080	70.4	1514	-2200	-1060	64.17
1413	-2100	-980	64.94	1464	-2200	-2060	74.36	1515	-2200	-1040	66.25
1414	-2100	-1000	67.45	1465	-2200	-2040	77.94	1516	-2200	-1020	60.79
1415	-2100	-1020	69.32	1466	-2200	-2020	80.39	1517	-2200	-1000	68.6
1416	-2100	-1040	67.92	1467	-2200	-2000	79	1518	-2200	-980	65.46
1417	-2100	-1060	66.88	1468	-2200	-1980	88.94	1519	-2200	-960	64.51
1418	-2100	-1080	68.03	1469	-2200	-1960	105.3	1520	-2200	-940	72.38
1419	-2100	-1100	69.23	1470	-2200	-1940	99.47	1521	-2200	-920	65.25
1420	-2100	-1120	74.58	1471	-2200	-1920	73.9	1522	-2200	-900	70.42
1421	-2100	-1140	82.18	1472	-2200	-1900	73.96	1523	-2200	-880	62.57
1422	-2100	-1160	85.79	1473	-2200	-1880	76.51	1524	-2200	-860	70.44

1525	-2200	-840	67.13	1576	-2200	260	72.9	1627	-2300	-2000	96.81
1526	-2200	-820	69.4	1577	-2200	280	73.25	1628	-2300	-1980	83.02
1527	-2200	-800	71.71	1578	-2200	300	74.82	1629	-2300	-1960	79.45
1528	-2200	-780	69.23	1579	-2200	320	73.32	1630	-2300	-1940	84.12
1529	-2200	-760	66.92	1580	-2200	340	75.12	1631	-2300	-1920	81.58
1530	-2200	-740	67.65	1581	-2200	360	74.6	1632	-2300	-1900	83.41
1531	-2200	-720	71.92	1582	-2200	380	73.51	1633	-2300	-1880	85.77
1532	-2200	-700	72.16	1583	-2200	400	75.64	1634	-2300	-1860	85.53
1533	-2200	-680	65.88	1584	-2200	420	75.49	1635	-2300	-1840	87.33
1534	-2200	-660	69.67	1585	-2200	440	75.86	1636	-2300	-1820	89.21
1535	-2200	-640	59.12	1586	-2200	460	75.91	1637	-2300	-1800	92.68
1536	-2200	-620	62.63	1587	-2200	480	74.99	1638	-2300	-1780	99.19
1537	-2200	-600	57.94	1588	-2200	500	75.59	1639	-2300	-1760	105.63
1538	-2200	-580	67.76	1589	-2200	520	76.9	1640	-2300	-1740	118.15
1539	-2200	-560	67.21	1590	-2200	540	77.4	1641	-2300	-1720	136.25
1540	-2200	-540	66.08	1591	-2200	560	77.95	1642	-2300	-1700	155.01
1541	-2200	-520	66.59	1592	-2200	580	78.95	1643	-2300	-1680	120.53
1542	-2200	-500	66.31	1593	-2200	600	79.04	1644	-2300	-1660	13.78
1543	-2200	-480	67.2	1594	-2200	620	77.79	1645	-2300	-1640	37.3
1544	-2200	-460	69.58	1595	-2200	640	82.69	1646	-2300	-1620	53.71
1545	-2200	-440	67.77	1596	-2200	660	80.99	1647	-2300	-1600	58.89
1546	-2200	-420	67.7	1597	-2200	680	82.62	1648	-2300	-1580	61.06
1547	-2200	-400	67.78	1598	-2200	700	80.88	1649	-2300	-1560	66.12
1548	-2200	-380	69.67	1599	-2200	720	81.28	1650	-2300	-1540	69.88
1549	-2200	-360	77.99	1600	-2200	740	81.84	1651	-2300	-1520	63.64
1550	-2200	-260	63.02	1601	-2200	760	81.88	1652	-2300	-1500	66.23
1551	-2200	-240	68.2	1602	-2200	780	80.46	1653	-2300	-1480	69.17
1552	-2200	-220	58.95	1603	-2200	800	82.16	1654	-2300	-1460	71.61
1553	-2200	-200	74.88	1604	-2200	820	83.04	1655	-2300	-1440	71.57
1554	-2200	-180	71.91	1605	-2200	840	80.63	1656	-2300	-1420	73.15
1555	-2200	-160	67.7	1606	-2200	860	82.89	1657	-2300	-1400	68.12
1556	-2200	-140	71.03	1607	-2200	880	83.41	1658	-2300	-1380	77.87
1557	-2200	-120	69.34	1608	-2200	900	85.2	1659	-2300	-1360	75.11
1558	-2200	-100	68.81	1609	-2200	920	83.41	1660	-2300	-1340	79.56
1559	-2200	-80	68.95	1610	-2200	940	84.63	1661	-2300	-1320	79.04
1560	-2200	-60	70.83	1611	-2200	960	86.21	1662	-2300	-1300	64.87
1561	-2200	-40	70.85	1612	-2200	980	86.89	1663	-2300	-1280	58.54
1562	-2200	-20	71.23	1613	-2200	1000	84.39	1664	-2300	-1260	68.59
1563	-2200	0	71.39	1614	-2200	1020	85.16	1665	-2300	-1240	73.12
1564	-2200	20	71.52	1615	-2200	1040	88.19	1666	-2300	-1220	68.83
1565	-2200	40	71.71	1616	-2200	1060	86.92	1667	-2300	-1200	65.07
1566	-2200	60	72.43	1617	-2200	1080	88.98	1668	-2300	-1180	62.55
1567	-2200	80	72.27	1618	-2200	1100	89.53	1669	-2300	-1160	62.18
1568	-2200	100	72.48	1619	-2200	1120	90.75	1670	-2300	-1140	71.09
1569	-2200	120	72.82	1620	-2200	1140	89.51	1671	-2300	-1120	70.59
1570	-2200	140	74.25	1621	-2200	1160	92.55	1672	-2300	-1100	69.32
1571	-2200	160	73.43	1622	-2200	1180	92.14	1673	-2300	-1080	68.14
1572	-2200	180	72.65	1623	-2200	1200	91.54	1674	-2300	-1060	68.68
1573	-2200	200	73.48	1624	-2200	1220	93.37	1675	-2300	-1040	68.72
1574	-2200	220	77.68	1625	-2200	1240	93.26	1676	-2300	-1020	69.57
1575	-2200	240	72.53	1626	-2200	1260	93.96	1677	-2300	-1000	72.27

<b>1678</b>	-2300	-980	71.12	<b>1729</b>	-2300	160	75.46	<b>1780</b>	-2300	1200	93.13
<b>1679</b>	-2300	-960	69.05	<b>1730</b>	-2300	180	75.29	<b>1781</b>	-2400	1400	104.98
<b>1680</b>	-2300	-940	70.94	<b>1731</b>	-2300	200	74.88	<b>1782</b>	-2400	1380	104.57
<b>1681</b>	-2300	-920	69.18	<b>1732</b>	-2300	220	73.29	<b>1783</b>	-2400	1360	105.62
<b>1682</b>	-2300	-900	70.68	<b>1733</b>	-2300	240	74.02	<b>1784</b>	-2400	1340	100.63
<b>1683</b>	-2300	-880	69.91	<b>1734</b>	-2300	260	75.15	<b>1785</b>	-2400	1320	99.15
<b>1684</b>	-2300	-860	70.31	<b>1735</b>	-2300	280	75.28	<b>1786</b>	-2400	1300	99.15
<b>1685</b>	-2300	-840	75.55	<b>1736</b>	-2300	300	73.23	<b>1787</b>	-2400	1280	98.82
<b>1686</b>	-2300	-820	69.42	<b>1737</b>	-2300	320	73.45	<b>1788</b>	-2400	1260	98.07
<b>1687</b>	-2300	-800	71.48	<b>1738</b>	-2300	340	78.3	<b>1789</b>	-2400	1240	97.5
<b>1688</b>	-2300	-780	71.26	<b>1739</b>	-2300	380	78.47	<b>1790</b>	-2400	1220	96.15
<b>1689</b>	-2300	-760	72.1	<b>1740</b>	-2300	400	76.96	<b>1791</b>	-2400	1200	96.54
<b>1690</b>	-2300	-740	71.92	<b>1741</b>	-2300	420	74.66	<b>1792</b>	-2400	1180	94.81
<b>1691</b>	-2300	-720	69.53	<b>1742</b>	-2300	440	76.98	<b>1793</b>	-2400	1160	94.43
<b>1692</b>	-2300	-700	71.48	<b>1743</b>	-2300	460	78.5	<b>1794</b>	-2400	1140	94.5
<b>1693</b>	-2300	-680	72.64	<b>1744</b>	-2300	480	79.52	<b>1795</b>	-2400	1120	94.15
<b>1694</b>	-2300	-660	66.81	<b>1745</b>	-2300	500	78.48	<b>1796</b>	-2400	1100	93.19
<b>1695</b>	-2300	-640	63.61	<b>1746</b>	-2300	520	77.17	<b>1797</b>	-2400	1080	92.35
<b>1696</b>	-2300	-620	61.4	<b>1747</b>	-2300	540	80.23	<b>1798</b>	-2400	1060	91.74
<b>1697</b>	-2300	-600	68.48	<b>1748</b>	-2300	560	78.37	<b>1799</b>	-2400	1040	90.23
<b>1698</b>	-2300	-580	69.26	<b>1749</b>	-2300	580	79.09	<b>1800</b>	-2400	1020	90.53
<b>1699</b>	-2300	-560	69.33	<b>1750</b>	-2300	600	80.44	<b>1801</b>	-2400	1000	88.76
<b>1700</b>	-2300	-540	67.97	<b>1751</b>	-2300	620	80.31	<b>1802</b>	-2400	980	89.11
<b>1701</b>	-2300	-520	69.14	<b>1752</b>	-2300	640	80.31	<b>1803</b>	-2400	960	87.08
<b>1702</b>	-2300	-500	67.22	<b>1753</b>	-2300	660	81.58	<b>1804</b>	-2400	940	88.33
<b>1703</b>	-2300	-480	69.96	<b>1754</b>	-2300	680	82.88	<b>1805</b>	-2400	920	87.17
<b>1704</b>	-2300	-340	74.83	<b>1755</b>	-2300	700	79.71	<b>1806</b>	-2400	900	87.44
<b>1705</b>	-2300	-320	66.98	<b>1756</b>	-2300	720	82.97	<b>1807</b>	-2400	880	91.17
<b>1706</b>	-2300	-300	68.23	<b>1757</b>	-2300	740	80.58	<b>1808</b>	-2400	860	89.28
<b>1707</b>	-2300	-280	69.01	<b>1758</b>	-2300	760	82.56	<b>1809</b>	-2400	840	87.27
<b>1708</b>	-2300	-260	70.77	<b>1759</b>	-2300	780	83.01	<b>1810</b>	-2400	820	87.05
<b>1709</b>	-2300	-240	71.32	<b>1760</b>	-2300	800	82.3	<b>1811</b>	-2400	800	85.02
<b>1710</b>	-2300	-220	70.84	<b>1761</b>	-2300	820	80.16	<b>1812</b>	-2400	780	84.86
<b>1711</b>	-2300	-200	70.25	<b>1762</b>	-2300	840	84.6	<b>1813</b>	-2400	760	86.3
<b>1712</b>	-2300	-180	71.32	<b>1763</b>	-2300	860	83.72	<b>1814</b>	-2400	740	85.56
<b>1713</b>	-2300	-160	71.75	<b>1764</b>	-2300	880	81.86	<b>1815</b>	-2400	720	85.26
<b>1714</b>	-2300	-140	72.8	<b>1765</b>	-2300	900	84.51	<b>1816</b>	-2400	700	86.14
<b>1715</b>	-2300	-120	72.14	<b>1766</b>	-2300	920	83.17	<b>1817</b>	-2400	680	84.8
<b>1716</b>	-2300	-100	72.57	<b>1767</b>	-2300	940	84.83	<b>1818</b>	-2400	660	84.76
<b>1717</b>	-2300	-80	68.98	<b>1768</b>	-2300	960	86.03	<b>1819</b>	-2400	640	83.74
<b>1718</b>	-2300	-60	71.25	<b>1769</b>	-2300	980	87.8	<b>1820</b>	-2400	620	83.21
<b>1719</b>	-2300	-40	72.7	<b>1770</b>	-2300	1000	85.18	<b>1821</b>	-2400	600	82.51
<b>1720</b>	-2300	-20	73.41	<b>1771</b>	-2300	1020	85.61	<b>1822</b>	-2400	580	82.33
<b>1721</b>	-2300	0	71.77	<b>1772</b>	-2300	1040	90.68	<b>1823</b>	-2400	560	79.34
<b>1722</b>	-2300	20	73.65	<b>1773</b>	-2300	1060	92.33	<b>1824</b>	-2400	540	83.68
<b>1723</b>	-2300	40	72.84	<b>1774</b>	-2300	1080	90.84	<b>1825</b>	-2400	520	83.24
<b>1724</b>	-2300	60	73.4	<b>1775</b>	-2300	1100	88.09	<b>1826</b>	-2400	500	81.69
<b>1725</b>	-2300	80	75.3	<b>1776</b>	-2300	1120	93.92	<b>1827</b>	-2400	480	80.97
<b>1726</b>	-2300	100	71.57	<b>1777</b>	-2300	1140	92.71	<b>1828</b>	-2400	460	80.14
<b>1727</b>	-2300	120	76.2	<b>1778</b>	-2300	1160	88.41	<b>1829</b>	-2400	440	77.77
<b>1728</b>	-2300	140	76.32	<b>1779</b>	-2300	1180	91.57	<b>1830</b>	-2400	420	77.61

<b>1831</b>	-2400	400	71.41	<b>1882</b>	-2400	-760	74.76	<b>1933</b>	-2400	-1760	103.57
<b>1832</b>	-2400	380	77.19	<b>1883</b>	-2400	-780	72.57	<b>1934</b>	-2400	-1780	97.54
<b>1833</b>	-2400	340	77.97	<b>1884</b>	-2400	-800	72.43	<b>1935</b>	-2400	-1800	92.67
<b>1834</b>	-2400	320	79.43	<b>1885</b>	-2400	-820	70.07	<b>1936</b>	-2400	-1820	90.33
<b>1835</b>	-2400	300	76.49	<b>1886</b>	-2400	-840	70	<b>1937</b>	-2400	-1840	91.72
<b>1836</b>	-2400	280	78	<b>1887</b>	-2400	-860	69.9	<b>1938</b>	-2400	-1860	92.01
<b>1837</b>	-2400	260	80.67	<b>1888</b>	-2400	-880	71.36	<b>1939</b>	-2400	-1880	87.63
<b>1838</b>	-2400	240	79.22	<b>1889</b>	-2400	-900	69.41	<b>1940</b>	-2400	-1900	84.76
<b>1839</b>	-2400	220	78.98	<b>1890</b>	-2400	-920	70.18	<b>1941</b>	-2400	-1920	85.35
<b>1840</b>	-2400	200	78.77	<b>1891</b>	-2400	-940	68.85	<b>1942</b>	-2400	-1940	84.88
<b>1841</b>	-2400	180	78.97	<b>1892</b>	-2400	-960	70.04	<b>1943</b>	-2500	1300	91.88
<b>1842</b>	-2400	160	76.99	<b>1893</b>	-2400	-980	70.44	<b>1944</b>	-2500	1280	107.3
<b>1843</b>	-2400	140	77.1	<b>1894</b>	-2400	-1000	69.05	<b>1945</b>	-2500	1260	97.35
<b>1844</b>	-2400	120	77.68	<b>1895</b>	-2400	-1020	69.62	<b>1946</b>	-2500	1240	103.66
<b>1845</b>	-2400	100	77.37	<b>1896</b>	-2400	-1040	68.44	<b>1947</b>	-2500	1220	102.69
<b>1846</b>	-2400	80	76.85	<b>1897</b>	-2400	-1060	68.98	<b>1948</b>	-2500	1200	100.11
<b>1847</b>	-2400	60	76.13	<b>1898</b>	-2400	-1080	68.1	<b>1949</b>	-2500	1180	94.15
<b>1848</b>	-2400	40	75.67	<b>1899</b>	-2400	-1100	70.9	<b>1950</b>	-2500	1160	95.87
<b>1849</b>	-2400	20	75.67	<b>1900</b>	-2400	-1120	68.84	<b>1951</b>	-2500	1140	93.76
<b>1850</b>	-2400	0	74.88	<b>1901</b>	-2400	-1140	68	<b>1952</b>	-2500	1120	93.46
<b>1851</b>	-2400	-20	74.06	<b>1902</b>	-2400	-1160	65.69	<b>1953</b>	-2500	1100	92.21
<b>1852</b>	-2400	-40	73.96	<b>1903</b>	-2400	-1180	82.09	<b>1954</b>	-2500	1080	90.79
<b>1853</b>	-2400	-60	73.85	<b>1904</b>	-2400	-1200	72.57	<b>1955</b>	-2500	1060	91.75
<b>1854</b>	-2400	-80	74.28	<b>1905</b>	-2400	-1220	72.73	<b>1956</b>	-2500	1040	90.05
<b>1855</b>	-2400	-100	74.02	<b>1906</b>	-2400	-1240	67.13	<b>1957</b>	-2500	1020	89.12
<b>1856</b>	-2400	-120	71.22	<b>1907</b>	-2400	-1260	66.53	<b>1958</b>	-2500	1000	88.88
<b>1857</b>	-2400	-140	72.73	<b>1908</b>	-2400	-1280	71.9	<b>1959</b>	-2500	980	89.11
<b>1858</b>	-2400	-160	72.78	<b>1909</b>	-2400	-1300	66.63	<b>1960</b>	-2500	960	87.97
<b>1859</b>	-2400	-180	72.2	<b>1910</b>	-2400	-1300	67.77	<b>1961</b>	-2500	940	89.92
<b>1860</b>	-2400	-200	71.84	<b>1911</b>	-2400	-1320	73.17	<b>1962</b>	-2500	920	87.32
<b>1861</b>	-2400	-220	71.74	<b>1912</b>	-2400	-1340	71.76	<b>1963</b>	-2500	900	88.49
<b>1862</b>	-2400	-240	72.01	<b>1913</b>	-2400	-1360	59.85	<b>1964</b>	-2500	880	89.16
<b>1863</b>	-2400	-260	71.53	<b>1914</b>	-2400	-1380	57.31	<b>1965</b>	-2500	860	87.34
<b>1864</b>	-2400	-280	71.36	<b>1915</b>	-2400	-1400	61.35	<b>1966</b>	-2500	840	87.61
<b>1865</b>	-2400	-300	72.71	<b>1916</b>	-2400	-1420	66.6	<b>1967</b>	-2500	820	86.12
<b>1866</b>	-2400	-320	74.26	<b>1917</b>	-2400	-1440	69.77	<b>1968</b>	-2500	800	82.99
<b>1867</b>	-2400	-340	69.06	<b>1918</b>	-2400	-1460	66.12	<b>1969</b>	-2500	780	83.86
<b>1868</b>	-2400	-360	64.45	<b>1919</b>	-2400	-1480	78.65	<b>1970</b>	-2500	760	86.88
<b>1869</b>	-2400	-380	68.48	<b>1920</b>	-2400	-1500	74.72	<b>1971</b>	-2500	740	87.38
<b>1870</b>	-2400	-520	65	<b>1921</b>	-2400	-1520	68.62	<b>1972</b>	-2500	720	83.2
<b>1871</b>	-2400	-540	70.41	<b>1922</b>	-2400	-1540	63.79	<b>1973</b>	-2500	700	87.29
<b>1872</b>	-2400	-560	68	<b>1923</b>	-2400	-1560	71.12	<b>1974</b>	-2500	680	84.07
<b>1873</b>	-2400	-580	67.91	<b>1924</b>	-2400	-1580	72.85	<b>1975</b>	-2500	660	84.97
<b>1874</b>	-2400	-600	69.88	<b>1925</b>	-2400	-1600	73.41	<b>1976</b>	-2500	640	85.8
<b>1875</b>	-2400	-620	73.77	<b>1926</b>	-2400	-1620	64.7	<b>1977</b>	-2500	620	85.35
<b>1876</b>	-2400	-640	70.5	<b>1927</b>	-2400	-1640	59.46	<b>1978</b>	-2500	600	83.93
<b>1877</b>	-2400	-660	70.87	<b>1928</b>	-2400	-1660	54.26	<b>1979</b>	-2500	580	83.5
<b>1878</b>	-2400	-680	70.34	<b>1929</b>	-2400	-1680	40.28	<b>1980</b>	-2500	560	84.94
<b>1879</b>	-2400	-700	69.41	<b>1930</b>	-2400	-1700	85.15	<b>1981</b>	-2500	540	84.02
<b>1880</b>	-2400	-720	72.06	<b>1931</b>	-2400	-1720	102.96	<b>1982</b>	-2500	520	82.02
<b>1881</b>	-2400	-740	66.11	<b>1932</b>	-2400	-1740	108.43	<b>1983</b>	-2500	500	83.83

<b>1984</b>	-2500	480	83.05	<b>2035</b>	-2500	-640	71.91	<b>2086</b>	-2500	-1660	54.94
<b>1985</b>	-2500	460	81.91	<b>2036</b>	-2500	-660	60.83	<b>2087</b>	-2500	-1680	44.7
<b>1986</b>	-2500	440	80.75	<b>2037</b>	-2500	-680	69.9	<b>2088</b>	-2500	-1700	65.57
<b>1987</b>	-2500	420	79.1	<b>2038</b>	-2500	-700	70.69	<b>2089</b>	-2500	-1720	100.55
<b>1988</b>	-2500	400	79.55	<b>2039</b>	-2500	-720	70.1	<b>2090</b>	-2500	-1740	115.4
<b>1989</b>	-2500	380	68.84	<b>2040</b>	-2500	-740	70.79	<b>2091</b>	-2500	-1760	112.02
<b>1990</b>	-2500	360	72.4	<b>2041</b>	-2500	-760	69.37	<b>2092</b>	-2500	-1780	102.52
<b>1991</b>	-2500	340	78.87	<b>2042</b>	-2500	-780	70.77	<b>2093</b>	-2500	-1800	93.39
<b>1992</b>	-2500	320	85.58	<b>2043</b>	-2500	-800	71.76	<b>2094</b>	-2500	-1820	88.9
<b>1993</b>	-2500	300	80.86	<b>2044</b>	-2500	-820	72.53	<b>2095</b>	-2500	-1840	86.75
<b>1994</b>	-2500	280	79.44	<b>2045</b>	-2500	-840	71.66	<b>2096</b>	-2500	-1860	95.24
<b>1995</b>	-2500	260	77.89	<b>2046</b>	-2500	-860	72.75	<b>2097</b>	-2500	-1880	89.55
<b>1996</b>	-2500	240	76.86	<b>2047</b>	-2500	-880	72.45	<b>2098</b>	-2500	-1900	86.37
<b>1997</b>	-2500	220	77.65	<b>2048</b>	-2500	-900	71.9	<b>2099</b>	-2500	-1920	84.22
<b>1998</b>	-2500	200	76.7	<b>2049</b>	-2500	-920	71.53	<b>2100</b>	-2500	-1940	83.33
<b>1999</b>	-2500	180	79.13	<b>2050</b>	-2500	-940	71.21	<b>2101</b>	-2500	-1960	83.23
<b>2000</b>	-2500	160	77.62	<b>2051</b>	-2500	-960	70.78	<b>2102</b>	-2500	-1980	80.45
<b>2001</b>	-2500	140	78.59	<b>2052</b>	-2500	-980	69.58	<b>2103</b>	-2500	-2000	90.98
<b>2002</b>	-2500	120	77.95	<b>2053</b>	-2500	-1000	70.25	<b>2104</b>	-2700	1300	95.18
<b>2003</b>	-2500	100	77.88	<b>2054</b>	-2500	-1020	69.46	<b>2105</b>	-2700	1280	97.56
<b>2004</b>	-2500	80	77.39	<b>2055</b>	-2500	-1040	68.18	<b>2106</b>	-2700	1260	97.69
<b>2005</b>	-2500	60	77.32	<b>2056</b>	-2500	-1060	60.41	<b>2107</b>	-2700	1240	97.2
<b>2006</b>	-2500	40	76.5	<b>2057</b>	-2500	-1080	68.74	<b>2108</b>	-2700	1220	93.92
<b>2007</b>	-2500	20	75.71	<b>2058</b>	-2500	-1100	68.36	<b>2109</b>	-2700	1200	94.59
<b>2008</b>	-2500	0	71.1	<b>2059</b>	-2500	-1120	59.71	<b>2110</b>	-2700	1180	91.98
<b>2009</b>	-2500	-20	73.11	<b>2060</b>	-2500	-1140	61.54	<b>2111</b>	-2700	1160	85.94
<b>2010</b>	-2500	-40	73.34	<b>2061</b>	-2500	-1160	66.9	<b>2112</b>	-2700	1140	92.99
<b>2011</b>	-2500	-60	75.12	<b>2062</b>	-2500	-1180	73.11	<b>2113</b>	-2700	1120	96.85
<b>2012</b>	-2500	-80	74.84	<b>2063</b>	-2500	-1200	73.64	<b>2114</b>	-2700	1100	93.83
<b>2013</b>	-2500	-100	73.08	<b>2064</b>	-2500	-1220	70.92	<b>2115</b>	-2700	1080	92.32
<b>2014</b>	-2500	-120	72.19	<b>2065</b>	-2500	-1240	73.6	<b>2116</b>	-2700	1060	90.49
<b>2015</b>	-2500	-140	73.95	<b>2066</b>	-2500	-1260	68.22	<b>2117</b>	-2700	1040	91.24
<b>2016</b>	-2500	-160	76.89	<b>2067</b>	-2500	-1280	66.36	<b>2118</b>	-2700	1020	90.26
<b>2017</b>	-2500	-180	74.83	<b>2068</b>	-2500	-1300	68.84	<b>2119</b>	-2700	1000	87.26
<b>2018</b>	-2500	-200	76.27	<b>2069</b>	-2500	-1320	65.52	<b>2120</b>	-2700	980	88.39
<b>2019</b>	-2500	-220	77.59	<b>2070</b>	-2500	-1340	71.69	<b>2121</b>	-2700	960	92.53
<b>2020</b>	-2500	-240	75.35	<b>2071</b>	-2500	-1360	68.94	<b>2122</b>	-2700	940	90.33
<b>2021</b>	-2500	-260	74.14	<b>2072</b>	-2500	-1380	73.93	<b>2123</b>	-2700	920	88.06
<b>2022</b>	-2500	-280	75.53	<b>2073</b>	-2500	-1400	56.16	<b>2124</b>	-2700	900	88.35
<b>2023</b>	-2500	-300	72.16	<b>2074</b>	-2500	-1420	67.71	<b>2125</b>	-2700	880	90.91
<b>2024</b>	-2500	-320	72.59	<b>2075</b>	-2500	-1440	76.72	<b>2126</b>	-2700	860	90.12
<b>2025</b>	-2500	-340	76.2	<b>2076</b>	-2500	-1460	74.06	<b>2127</b>	-2700	840	89.51
<b>2026</b>	-2500	-360	68.24	<b>2077</b>	-2500	-1480	55.52	<b>2128</b>	-2700	820	87.37
<b>2027</b>	-2500	-380	68.98	<b>2078</b>	-2500	-1500	76.97	<b>2129</b>	-2700	800	87.96
<b>2028</b>	-2500	-400	84.39	<b>2079</b>	-2500	-1520	69.9	<b>2130</b>	-2700	780	88.26
<b>2029</b>	-2500	-420	70.17	<b>2080</b>	-2500	-1540	68.53	<b>2131</b>	-2700	760	88.38
<b>2030</b>	-2500	-440	76.33	<b>2081</b>	-2500	-1560	68.78	<b>2132</b>	-2700	740	86.66
<b>2031</b>	-2500	-460	74.82	<b>2082</b>	-2500	-1580	74.95	<b>2133</b>	-2700	720	85.34
<b>2032</b>	-2500	-480	70.51	<b>2083</b>	-2500	-1600	75.08	<b>2134</b>	-2700	700	89.63
<b>2033</b>	-2500	-600	79.77	<b>2084</b>	-2500	-1620	62.47	<b>2135</b>	-2700	680	85.45
<b>2034</b>	-2500	-620	71.48	<b>2085</b>	-2500	-1640	60.26	<b>2136</b>	-2700	660	85.62

<b>2137</b>	-2700	640	85.05	<b>2188</b>	-2700	-380	72.69	<b>2239</b>	-2700	-1540	72.16
<b>2138</b>	-2700	620	84.43	<b>2189</b>	-2700	-400	78.87	<b>2240</b>	-2700	-1560	66.62
<b>2139</b>	-2700	600	84.44	<b>2190</b>	-2700	-420	74.66	<b>2241</b>	-2700	-1580	66.54
<b>2140</b>	-2700	580	83.45	<b>2191</b>	-2700	-440	71.79	<b>2242</b>	-2700	-1600	61.76
<b>2141</b>	-2700	560	83.03	<b>2192</b>	-2700	-460	64.57	<b>2243</b>	-2700	-1620	68.91
<b>2142</b>	-2700	540	85.38	<b>2193</b>	-2700	-480	60.24	<b>2244</b>	-2700	-1640	66.28
<b>2143</b>	-2700	520	81.63	<b>2194</b>	-2700	-500	74.48	<b>2245</b>	-2700	-1660	61.67
<b>2144</b>	-2700	500	71.27	<b>2195</b>	-2700	-520	66.98	<b>2246</b>	-2700	-1680	49.72
<b>2145</b>	-2700	480	85.72	<b>2196</b>	-2700	-540	64.16	<b>2247</b>	-2700	-1700	36.21
<b>2146</b>	-2700	460	82.2	<b>2197</b>	-2700	-560	84.39	<b>2248</b>	-2700	-1720	81.3
<b>2147</b>	-2700	440	82.14	<b>2198</b>	-2700	-580	74.1	<b>2249</b>	-2700	-1740	112.25
<b>2148</b>	-2700	420	76.77	<b>2199</b>	-2700	-600	58.4	<b>2250</b>	-2700	-1760	115.38
<b>2149</b>	-2700	400	74.89	<b>2200</b>	-2700	-760	72.62	<b>2251</b>	-2700	-1780	99.14
<b>2150</b>	-2700	380	84.09	<b>2201</b>	-2700	-780	71.07	<b>2252</b>	-2700	-1800	88.86
<b>2151</b>	-2700	360	86.42	<b>2202</b>	-2700	-800	71.05	<b>2253</b>	-2700	-1820	79
<b>2152</b>	-2700	340	80.3	<b>2203</b>	-2700	-820	71.78	<b>2254</b>	-2700	-1840	93.69
<b>2153</b>	-2700	320	75.66	<b>2204</b>	-2700	-840	72.05	<b>2255</b>	-2700	-1860	77.1
<b>2154</b>	-2700	300	78	<b>2205</b>	-2700	-860	73.6	<b>2256</b>	-2700	-1880	94.68
<b>2155</b>	-2700	280	81.57	<b>2206</b>	-2700	-880	71.93	<b>2257</b>	-2700	-1900	88.21
<b>2156</b>	-2700	260	76.48	<b>2207</b>	-2700	-900	71.61	<b>2258</b>	-2700	-1920	91.76
<b>2157</b>	-2700	240	81.19	<b>2208</b>	-2700	-920	70.66	<b>2259</b>	-2700	-1940	88.35
<b>2158</b>	-2700	220	80.79	<b>2209</b>	-2700	-940	69.96	<b>2260</b>	-2700	-1960	86.61
<b>2159</b>	-2700	200	81.67	<b>2210</b>	-2700	-960	73.49	<b>2261</b>	-2700	-1980	83.26
<b>2160</b>	-2700	180	80.07	<b>2211</b>	-2700	-980	71.75	<b>2262</b>	-2700	-2000	85.99
<b>2161</b>	-2700	160	83.01	<b>2212</b>	-2700	-1000	70.29				
<b>2162</b>	-2700	140	82.71	<b>2213</b>	-2700	-1020	71.68			END	
<b>2163</b>	-2700	120	80.58	<b>2214</b>	-2700	-1040	71.92				
<b>2164</b>	-2700	100	78.69	<b>2215</b>	-2700	-1060	71.01				
<b>2165</b>	-2700	80	77.53	<b>2216</b>	-2700	-1080	70.41				
<b>2166</b>	-2700	60	78.1	<b>2217</b>	-2700	-1100	72.78				
<b>2167</b>	-2700	40	77.43	<b>2218</b>	-2700	-1120	67.3				
<b>2168</b>	-2700	20	77.69	<b>2219</b>	-2700	-1140	72.22				
<b>2169</b>	-2700	0	75.34	<b>2220</b>	-2700	-1160	73.39				
<b>2170</b>	-2700	-20	78.15	<b>2221</b>	-2700	-1180	72.75				
<b>2171</b>	-2700	-40	76.12	<b>2222</b>	-2700	-1200	73.71				
<b>2172</b>	-2700	-60	74.88	<b>2223</b>	-2700	-1220	71.23				
<b>2173</b>	-2700	-80	75.15	<b>2224</b>	-2700	-1240	70.36				
<b>2174</b>	-2700	-100	76.82	<b>2225</b>	-2700	-1260	70.66				
<b>2175</b>	-2700	-120	74.77	<b>2226</b>	-2700	-1280	70.91				
<b>2176</b>	-2700	-140	77.68	<b>2227</b>	-2700	-1300	58.28				
<b>2177</b>	-2700	-160	77.33	<b>2228</b>	-2700	-1320	71.63				
<b>2178</b>	-2700	-180	75.5	<b>2229</b>	-2700	-1340	73.85				
<b>2179</b>	-2700	-200	75.98	<b>2230</b>	-2700	-1360	65.48				
<b>2180</b>	-2700	-220	74.34	<b>2231</b>	-2700	-1380	83.27				
<b>2181</b>	-2700	-240	76.2	<b>2232</b>	-2700	-1400	59.06				
<b>2182</b>	-2700	-260	73.45	<b>2233</b>	-2700	-1420	72.28				
<b>2183</b>	-2700	-280	82.5	<b>2234</b>	-2700	-1440	69.9				
<b>2184</b>	-2700	-300	77.34	<b>2235</b>	-2700	-1460	74.81				
<b>2185</b>	-2700	-320	75.24	<b>2236</b>	-2700	-1480	63.22				
<b>2186</b>	-2700	-340	76.96	<b>2237</b>	-2700	-1500	52.58				
<b>2187</b>	-2700	-360	65.99	<b>2238</b>	-2700	-1520	90.86				

Table 4.2 Resistivity (Ohm m) and Chargeability (mV/V) Data Sheet									
S.No.	X(m)	Y(m)	Resistivity	Chargeability	S.No.	X(m)	Y(m)	Resistivity	Chargeability
1	-1200	600	1633.8	6.3	50	-1200	-380	173.35	28.8
2	-1200	580	1715.8	6.8	51	-1200	-400	200.30	30.2
3	-1200	560	1461.1	7.2	52	-1200	-420	266.91	25.3
4	-1200	540	1277.9	7.9	53	-1200	-440	444.56	15.4
5	-1200	520	1202.6	8.5	54	-1200	-460	646.12	8.7
6	-1200	500	920.67	9.2	55	-1400	600	1855.82	5.5
7	-1200	480	858.57	7.3	56	-1400	580	2411.82	5.2
8	-1200	460	709.20	6.8	57	-1400	560	2862.76	4.4
9	-1200	440	598.35	7.9	58	-1400	540	2339.02	6.7
10	-1200	420	598.65	10.3	59	-1400	520	1640.42	6.8
11	-1200	400	499.98	11.8	60	-1400	500	914.82	9.2
12	-1200	380	515.98	11.7	61	-1400	480	414.34	15.1
13	-1200	360	414.15	17.1	62	-1400	460	439.16	9.4
14	-1200	340	263.35	16.8	63	-1400	440	479.03	8.3
15	-1200	320	314.17	15	64	-1400	420	407.73	7.7
16	-1200	300	352.86	11.5	65	-1400	400	326.99	9.1
17	-1200	280	454.72	13.4	66	-1400	380	301.72	10.4
18	-1200	260	652.56	16.5	67	-1400	360	329.33	9.1
19	-1200	240	592.19	20.7	68	-1400	340	488.41	8.7
20	-1200	220	479.60	21.5	69	-1400	320	494.59	8.8
21	-1200	200	421.91	20.9	70	-1400	300	431.03	10
22	-1200	180	304.90	21.5	71	-1400	280	322.51	14.7
23	-1200	160	403.29	21.1	72	-1400	260	265.74	17.6
24	-1200	140	379.26	21.4	73	-1400	240	248.78	23.5
25	-1200	120	387.39	20.1	74	-1400	220	221.22	25.5
26	-1200	100	496.53	23.6	75	-1400	200	215.07	25.1
27	-1200	80	421.83	21	76	-1400	180	220.66	24.8
28	-1200	60	605.78	16.5	77	-1400	160	203.61	22.3
29	-1200	40	601.99	14.9	78	-1400	140	198.92	21.5
30	-1200	20	402.30	13.4	79	-1400	120	205.14	22.5
31	-1200	0	287.12	11.3	80	-1400	100	190.58	23.1
32	-1200	-20	347.19	9.7	81	-1400	80	185.27	22.9
33	-1200	-40	364.34	8.5	82	-1400	60	161.34	20
34	-1200	-60	360.56	8.7	83	-1400	40	125.26	15.2
35	-1200	-80	164.07	8.4	84	-1400	20	154.09	14.2
36	-1200	-100	152.36	3.4	85	-1400	0	165.78	14.2
37	-1200	-120	130.52	13	86	-1400	-20	220.92	12.4
38	-1200	-140	113.44	16.4	87	-1400	-40	274.89	7.3
39	-1200	-160	100.18	9.4	88	-1400	-60	351.76	5.6
40	-1200	-180	111.17	14.3	89	-1400	-80	402.29	4.3
41	-1200	-200	108.52	11.3	90	-1400	-100	359.74	4.6
42	-1200	-220	119.56	10.7	91	-1400	-120	326.08	5.3
43	-1200	-240	98.29	19.3	92	-1400	-140	236.09	5.9
44	-1200	-260	111.79	14.7	93	-1400	-160	176.64	5.4
45	-1200	-280	124.97	15.7	94	-1400	-180	141.41	6
46	-1200	-300	101.47	16.9	95	-1400	-200	103.12	5.5
47	-1200	-320	150.86	19.1	96	-1400	-220	94.05	5.1
48	-1200	-340	165.78	22.2	97	-1400	-240	131.87	5.3
49	-1200	-360	163.15	25	98	-1400	-260	166.95	5.8

<b>99</b>	-1400	-280	214.06	7.4	<b>150</b>	-1500	-160	177.61	8.3
<b>100</b>	-1400	-300	294.36	8.4	<b>151</b>	-1500	-180	119.02	5.2
<b>101</b>	-1400	-320	333.84	9	<b>152</b>	-1500	-200	111.63	3.9
<b>102</b>	-1400	-340	388.42	10.1	<b>153</b>	-1500	-220	137.60	4.9
<b>103</b>	-1400	-360	386.80	11.2	<b>154</b>	-1400	-320	333.84	9
<b>104</b>	-1400	-380	372.03	10.6	<b>155</b>	-1400	-340	388.42	10.1
<b>105</b>	-1400	-400	375.43	10.8	<b>156</b>	-1400	-360	386.80	11.2
<b>106</b>	-1400	-420	365.16	8.6	<b>157</b>	-1400	-380	372.03	10.6
<b>107</b>	-1400	-440	397.95	8.4	<b>158</b>	-1400	-400	375.43	10.8
<b>108</b>	-1400	-460	329.29	7.3	<b>159</b>	-1400	-420	365.16	8.6
<b>109</b>	-1400	-480	270.32	6.1	<b>160</b>	-1400	-440	397.95	8.4
<b>110</b>	-1400	-500	217.54	4.4	<b>161</b>	-1400	-460	329.29	7.3
<b>111</b>	-1400	-520	174.60	3.9	<b>162</b>	-1400	-480	270.32	6.1
<b>112</b>	-1500	600	2283.00	5.8	<b>163</b>	-1400	-500	217.54	4.4
<b>113</b>	-1500	580	2284.15	6	<b>164</b>	-1400	-520	174.60	3.9
<b>114</b>	-1500	560	1891.56	5	<b>165</b>	-1500	600	2283.00	5.8
<b>115</b>	-1500	540	1350.07	6.3	<b>166</b>	-1500	580	2284.15	6
<b>116</b>	-1500	520	809.80	5	<b>167</b>	-1500	560	1891.56	5
<b>117</b>	-1500	500	660.14	9	<b>168</b>	-1500	540	1350.07	6.3
<b>118</b>	-1500	480	694.67	9	<b>169</b>	-1500	520	809.80	5
<b>119</b>	-1500	460	610.51	7.9	<b>170</b>	-1500	500	660.14	9
<b>120</b>	-1500	440	427.23	6.9	<b>171</b>	-1500	480	694.67	9
<b>121</b>	-1500	420	381.18	8.1	<b>172</b>	-1500	460	610.51	7.9
<b>122</b>	-1500	400	415.19	7.1	<b>173</b>	-1500	440	427.23	6.9
<b>123</b>	-1500	380	408.98	5.9	<b>174</b>	-1500	420	381.18	8.1
<b>124</b>	-1500	360	464.45	8.7	<b>175</b>	-1500	400	415.19	7.1
<b>125</b>	-1500	340	452.18	9.6	<b>176</b>	-1500	380	408.98	5.9
<b>126</b>	-1500	320	295.80	11	<b>177</b>	-1500	360	464.45	8.7
<b>127</b>	-1500	300	209.77	13	<b>178</b>	-1500	340	452.18	9.6
<b>128</b>	-1500	280	250.25	16	<b>179</b>	-1500	320	295.80	11
<b>129</b>	-1500	260	269.33	20.5	<b>180</b>	-1500	300	209.77	13
<b>130</b>	-1500	240	241.84	20.5	<b>181</b>	-1500	280	250.25	16
<b>131</b>	-1500	220	189.12	22.9	<b>182</b>	-1500	260	269.33	20.5
<b>132</b>	-1500	200	171.31	19.9	<b>183</b>	-1500	240	241.84	20.5
<b>133</b>	-1500	180	174.54	19.1	<b>184</b>	-1500	220	189.12	22.9
<b>134</b>	-1500	160	125.46	17.7	<b>185</b>	-1500	200	171.31	19.9
<b>135</b>	-1500	140	105.73	18.5	<b>186</b>	-1500	180	174.54	19.1
<b>136</b>	-1500	120	71.70	20	<b>187</b>	-1500	160	125.46	17.7
<b>137</b>	-1500	100	63.91	20.2	<b>188</b>	-1500	140	105.73	18.5
<b>138</b>	-1500	80	77.91	20.4	<b>189</b>	-1500	120	71.70	20
<b>139</b>	-1500	60	75.28	13.3	<b>190</b>	-1500	100	63.91	20.2
<b>140</b>	-1500	40	99.48	9.6	<b>191</b>	-1500	80	77.91	20.4
<b>141</b>	-1500	20	107.03	8.6	<b>192</b>	-1500	60	75.28	13.3
<b>142</b>	-1500	0	112.38	10.9	<b>193</b>	-1500	40	99.48	9.6
<b>143</b>	-1500	-20	123.99	8.6	<b>194</b>	-1500	20	107.03	8.6
<b>144</b>	-1500	-40	171.73	6.6	<b>195</b>	-1500	0	112.38	10.9
<b>145</b>	-1500	-60	228.78	8.1	<b>196</b>	-1500	-20	123.99	8.6
<b>146</b>	-1500	-80	335.24	6.9	<b>197</b>	-1500	-40	171.73	6.6
<b>147</b>	-1500	-100	393.37	5.5	<b>198</b>	-1500	-60	228.78	8.1
<b>148</b>	-1500	-120	333.57	5.3	<b>199</b>	-1500	-80	335.24	6.9
<b>149</b>	-1500	-140	268.55	4.1	<b>200</b>	-1500	-100	393.37	5.5

<b>201</b>	-1500	-120	333.57	5.3	<b>252</b>	-1600	200	213.82	18.3
<b>202</b>	-1500	-140	268.55	4.1	<b>253</b>	-1600	180	144.89	13.4
<b>203</b>	-1500	-160	177.61	8.3	<b>254</b>	-1600	160	117.17	12.4
<b>204</b>	-1500	-180	119.02	5.2	<b>255</b>	-1600	140	91.12	12.9
<b>205</b>	-1500	-200	111.63	3.9	<b>256</b>	-1600	120	68.33	12.5
<b>206</b>	-1500	-220	137.60	4.9	<b>257</b>	-1600	100	68.49	11.1
<b>207</b>	-1500	-240	135.42	4.1	<b>258</b>	-1600	80	69.63	8.5
<b>208</b>	-1500	-260	171.96	4	<b>259</b>	-1600	60	73.49	12.2
<b>209</b>	-1500	-280	194.71	7	<b>260</b>	-1600	40	73.21	8.8
<b>210</b>	-1500	-300	186.14	5.6	<b>261</b>	-1600	20	81.55	21.4
<b>211</b>	-1500	-320	217.39	7.9	<b>262</b>	-1600	0	104.63	13.4
<b>212</b>	-1500	-340	229.32	11.2	<b>263</b>	-1600	-20	140.18	10
<b>213</b>	-1500	-360	255.87	10.4	<b>264</b>	-1600	-40	205.52	9.2
<b>214</b>	-1500	-380	323.50	10.4	<b>265</b>	-1600	-60	253.21	7.8
<b>215</b>	-1500	-400	404.25	11.8	<b>266</b>	-1600	-80	250.65	4
<b>216</b>	-1500	-420	454.51	10.2	<b>267</b>	-1600	-100	251.22	4.4
<b>217</b>	-1500	-440	438.17	7.9	<b>268</b>	-1600	-120	219.07	4.4
<b>218</b>	-1500	-460	330.01	7.5	<b>269</b>	-1600	-140	182.37	4.3
<b>219</b>	-1500	-480	233.83	7.5	<b>270</b>	-1600	-160	144.60	5
<b>220</b>	-1500	-500	165.63	5.5	<b>271</b>	-1600	-180	116.65	4.7
<b>221</b>	-1500	-520	142.43	4	<b>272</b>	-1600	-200	130.68	3
<b>222</b>	-1500	-540	165.52	6.8	<b>273</b>	-1600	-220	129.63	5.1
<b>223</b>	-1500	-560	193.09	6.8	<b>274</b>	-1600	-240	126.45	4.6
<b>224</b>	-1500	-580	269.13	7.4	<b>275</b>	-1600	-260	125.59	2.4
<b>225</b>	-1500	-600	330.51	10.2	<b>276</b>	-1600	-280	109.94	2.8
<b>226</b>	-1500	-620	426.02	9.7	<b>277</b>	-1600	-300	145.73	6.9
<b>227</b>	-1500	-640	536.57	4.4	<b>278</b>	-1600	-320	206.01	7.8
<b>228</b>	-1500	-660	579.13	15.6	<b>279</b>	-1600	-340	300.31	10.8
<b>229</b>	-1500	-680	430.27	23.4	<b>280</b>	-1600	-360	354.29	13.3
<b>230</b>	-1500	-700	643.37	20	<b>281</b>	-1600	-380	371.79	11.1
<b>231</b>	-1500	-720	686.11	18.1	<b>282</b>	-1600	-400	362.22	8.9
<b>232</b>	-1600	600	1133.56	2.3	<b>283</b>	-1600	-420	332.23	9.5
<b>233</b>	-1600	580	1700.69	5.5	<b>284</b>	-1600	-440	322.68	5.6
<b>234</b>	-1600	560	1473.92	5.4	<b>285</b>	-1600	-460	285.02	7.2
<b>235</b>	-1600	540	1400.09	5.3	<b>286</b>	-1600	-480	251.43	7.4
<b>236</b>	-1600	520	901.21	4.5	<b>287</b>	-1600	-500	217.51	6.7
<b>237</b>	-1600	500	780.56	8.2	<b>288</b>	-1600	-520	199.87	3.4
<b>238</b>	-1600	480	495.01	4.4	<b>289</b>	-1600	-540	197.11	7.1
<b>239</b>	-1600	460	431.03	8	<b>290</b>	-1600	-560	189.66	4.6
<b>240</b>	-1600	440	355.02	5.6	<b>291</b>	-1600	-580	186.51	2.4
<b>241</b>	-1600	420	346.30	6.7	<b>292</b>	-1600	-600	299.96	7.9
<b>242</b>	-1600	400	309.73	2.5	<b>293</b>	-1700	600	715.79	3.8
<b>243</b>	-1600	380	276.01	8.4	<b>294</b>	-1700	580	751.46	3.4
<b>244</b>	-1600	360	297.59	8.5	<b>295</b>	-1700	560	943.65	5.8
<b>245</b>	-1600	340	307.39	7.7	<b>296</b>	-1700	540	771.98	7.4
<b>246</b>	-1600	320	334.24	4.5	<b>297</b>	-1700	520	764.70	4.4
<b>247</b>	-1600	300	346.93	7.3	<b>298</b>	-1700	500	681.57	6.4
<b>248</b>	-1600	280	387.93	11.3	<b>299</b>	-1700	480	460.45	3.5
<b>249</b>	-1600	260	397.96	12.6	<b>300</b>	-1700	460	296.94	9.7
<b>250</b>	-1600	240	316.62	19.2	<b>301</b>	-1700	440	271.91	6.3
<b>251</b>	-1600	220	282.46	19.1	<b>302</b>	-1700	420	253.78	5

<b>303</b>	-1700	400	249.23	6	<b>354</b>	-1700	-620	224.73	6.9
<b>304</b>	-1700	380	253.10	6.7	<b>355</b>	-1700	-640	278.30	3.3
<b>305</b>	-1700	360	211.05	4.4	<b>356</b>	-1700	-660	378.57	4.1
<b>306</b>	-1700	340	171.54	3.7	<b>357</b>	-1700	-680	547.67	4.1
<b>307</b>	-1700	320	168.45	5.4	<b>358</b>	-1700	-700	642.83	7.1
<b>308</b>	-1700	300	182.72	8.9	<b>359</b>	-1700	-720	773.41	8.9
<b>309</b>	-1700	280	224.08	12.7	<b>360</b>	-1700	-740	778.72	9.6
<b>310</b>	-1700	260	286.44	13.8	<b>361</b>	-1700	-760	756.79	17.1
<b>311</b>	-1700	240	271.10	16.5	<b>362</b>	-1700	-780	780.17	12.4
<b>312</b>	-1700	220	246.91	14.6	<b>363</b>	-1700	-800	564.67	13.8
<b>313</b>	-1700	200	180.13	11.5	<b>364</b>	-1700	-820	403.11	11.5
<b>314</b>	-1700	180	154.56	14.9	<b>365</b>	-1800	600	946.18	3
<b>315</b>	-1700	160	122.88	13.5	<b>366</b>	-1800	580	594.94	2.3
<b>316</b>	-1700	140	91.48	10.4	<b>367</b>	-1800	560	478.03	2.8
<b>317</b>	-1700	120	83.36	11.8	<b>368</b>	-1800	540	346.81	3.6
<b>318</b>	-1700	100	61.50	16.9	<b>369</b>	-1800	520	371.60	4.8
<b>319</b>	-1700	80	51.40	7.2	<b>370</b>	-1800	500	394.19	4.3
<b>320</b>	-1700	60	54.52	11.3	<b>371</b>	-1800	480	366.81	7.8
<b>321</b>	-1700	40	55.92	9.5	<b>372</b>	-1800	460	412.24	8.4
<b>322</b>	-1700	20	67.75	7.1	<b>373</b>	-1800	440	256.35	7.6
<b>323</b>	-1700	0	107.38	14.8	<b>374</b>	-1800	420	290.65	5.3
<b>324</b>	-1700	-20	140.99	11.2	<b>375</b>	-1800	400	267.81	5.8
<b>325</b>	-1700	-40	193.37	12.8	<b>376</b>	-1800	380	190.03	9.1
<b>326</b>	-1700	-60	191.61	10.2	<b>377</b>	-1800	360	194.85	7.2
<b>327</b>	-1700	-80	180.79	6.3	<b>378</b>	-1800	340	186.41	7.1
<b>328</b>	-1700	-100	182.07	2.2	<b>379</b>	-1800	320	194.74	6.8
<b>329</b>	-1700	-120	152.78	4.4	<b>380</b>	-1800	300	249.95	9.1
<b>330</b>	-1700	-140	146.67	4.6	<b>381</b>	-1800	280	251.65	9.4
<b>331</b>	-1700	-160	151.50	7.2	<b>382</b>	-1800	260	218.54	11.3
<b>332</b>	-1700	-180	146.02	8.4	<b>383</b>	-1800	240	195.87	13.4
<b>333</b>	-1700	-200	154.73	6.7	<b>384</b>	-1800	220	146.87	14.7
<b>334</b>	-1700	-220	158.32	7.3	<b>385</b>	-1800	200	137.25	7
<b>335</b>	-1700	-240	163.20	3.7	<b>386</b>	-1800	180	138.15	6.5
<b>336</b>	-1700	-260	155.81	4.9	<b>387</b>	-1800	160	152.02	6.3
<b>337</b>	-1700	-280	186.70	7.1	<b>388</b>	-1800	140	137.46	8.5
<b>338</b>	-1700	-300	198.55	7.2	<b>389</b>	-1800	120	66.29	6.1
<b>339</b>	-1700	-320	226.07	10	<b>390</b>	-1800	100	39.03	40.8
<b>340</b>	-1700	-340	239.68	12.6	<b>391</b>	-1800	80	24.91	89
<b>341</b>	-1700	-360	251.14	14.8	<b>392</b>	-1800	60	44.14	22.6
<b>342</b>	-1700	-380	293.30	12.4	<b>393</b>	-1800	40	50.46	10.6
<b>343</b>	-1700	-400	303.05	5.9	<b>394</b>	-1800	20	63.50	11.7
<b>344</b>	-1700	-420	357.75	19.4	<b>395</b>	-1800	0	89.02	11
<b>345</b>	-1700	-440	282.58	8.5	<b>396</b>	-1800	-20	142.80	11.4
<b>346</b>	-1700	-460	299.88	10.9	<b>397</b>	-1800	-40	182.18	7.3
<b>347</b>	-1700	-480	273.34	12.7	<b>398</b>	-1800	-60	183.20	7.3
<b>348</b>	-1700	-500	278.46	12.8	<b>399</b>	-1800	-80	155.09	4.6
<b>349</b>	-1700	-520	288.95	11.6	<b>400</b>	-1800	-100	144.83	6.6
<b>350</b>	-1700	-540	289.60	10.6	<b>401</b>	-1800	-120	165.07	4.6
<b>351</b>	-1700	-560	256.37	6.5	<b>402</b>	-1800	-140	92.00	25.4
<b>352</b>	-1700	-580	214.02	7.6	<b>403</b>	-1800	-160	108.82	33.7
<b>353</b>	-1700	-600	190.49	3.7	<b>404</b>	-1800	-180	146.96	12.6

405	-1800	-200	173.21	6	456	-1900	200	122.29	14.9
406	-1800	-220	211.78	2.9	457	-1900	180	119.28	12.3
407	-1800	-240	228.58	2.3	458	-1900	160	107.83	11.4
408	-1800	-260	200.20	2	459	-1900	140	88.47	11.3
409	-1800	-280	175.46	5.9	460	-1900	120	77.21	9.2
410	-1800	-300	193.33	7.5	461	-1900	100	71.46	10.8
411	-1800	-320	206.98	6	462	-1900	80	73.24	8.9
412	-1800	-340	206.89	12	463	-1900	60	75.88	8.2
413	-1800	-360	214.22	8	464	-1900	40	79.25	5.5
414	-1800	-380	279.96	12.5	465	-1900	20	111.38	12.4
415	-1800	-400	313.90	13.3	466	-1900	0	132.53	12.5
416	-1800	-420	326.81	15.8	467	-1900	-20	174.53	9.7
417	-1800	-440	350.91	13.3	468	-1900	-40	183.81	8
418	-1800	-460	321.24	12.8	469	-1900	-60	160.92	9.9
419	-1800	-480	283.57	17.4	470	-1900	-80	148.54	19.2
420	-1800	-500	340.61	15.2	471	-1900	-100	157.66	13
421	-1800	-520	429.33	12.9	472	-1900	-120	196.87	6
422	-1800	-540	398.05	11.3	473	-1900	-140	159.97	12.1
423	-1800	-560	360.26	12.4	474	-1900	-160	136.52	11.7
424	-1800	-580	269.53	4.7	475	-1900	-180	139.05	5.4
425	-1800	-600	167.09	4.2	476	-1900	-200	176.68	6.5
426	-1800	-620	152.66	3.5	477	-1900	-220	189.44	7.3
427	-1800	-640	223.91	5.2	478	-1900	-240	221.39	7.2
428	-1800	-660	140.77	5.7	479	-1900	-260	210.29	5.6
429	-1800	-680	376.26	5.8	480	-1900	-280	198.27	9.1
430	-1800	-700	558.60	5.7	481	-1900	-300	263.51	11.1
431	-1800	-720	666.99	5.7	482	-1900	-320	236.25	16.6
432	-1800	-740	694.78	4.4	483	-1900	-340	253.52	9.8
433	-1800	-760	633.73	6	484	-1900	-360	211.10	12
434	-1800	-780	608.06	5.8	485	-1900	-380	238.55	14.7
435	-1800	-800	530.50	9.2	486	-1900	-400	306.31	28.9
436	-1900	600	785.14	4.5	487	-1900	-420	345.41	12.4
437	-1900	580	568.96	6.8	488	-1900	-440	438.47	15.5
438	-1900	560	464.89	5	489	-1900	-460	449.42	14.3
439	-1900	540	379.11	5	490	-1900	-480	652.02	13.3
440	-1900	520	334.15	5.8	491	-1900	-500	759.61	10.7
441	-1900	500	290.17	6.5	492	-1900	-520	392.35	14.8
442	-1900	480	260.10	6.4	493	-1900	-540	309.42	12
443	-1900	460	255.91	8.2	494	-1900	-560	241.38	14.5
444	-1900	440	226.09	8.2	495	-1900	-580	95.61	31.7
445	-1900	420	229.94	9	496	-1900	-600	126.76	21
446	-1900	400	279.37	8.3	497	-1900	-620	156.80	9.5
447	-1900	380	307.18	9.2	498	-1900	-640	130.05	4.8
448	-1900	360	405.82	8.4	499	-1900	-660	197.48	6
449	-1900	340	436.62	7.9	500	-1900	-680	334.45	5.2
450	-1900	320	362.64	8.4	501	-1900	-700	504.53	5.1
451	-1900	300	317.92	10.3	502	-2000	-700	288.42	4.4
452	-1900	280	258.34	10.2	503	-2000	-680	296.31	13.5
453	-1900	260	207.80	11.3	504	-2000	-660	271.29	8.9
454	-1900	240	171.88	12.8	505	-2000	-640	288.02	20.3
455	-1900	220	138.26	13.8	506	-2000	-620	290.89	16.4

507	-2000	-600	316.07	21.5	558	-2000	620	906.19	4.8
508	-2000	-580	317.58	20.3	559	-2000	640	844.37	4.6
509	-2000	-560	308.40	24.4	560	-2000	660	932.43	4.6
510	-2000	-540	319.11	34.3	561	-2000	680	545.28	4.6
511	-2000	-520	375.06	21.1	562	-2000	700	439.96	6.9
512	-2000	-500	338.82	18.9	563	-2000	720	383.40	7
513	-2000	-460	422.54	16.5	564	-2100	700	590.13	4.8
514	-2000	-440	370.45	11.5	565	-2100	680	727.50	4.6
515	-2000	-420	323.91	20	566	-2100	660	866.36	5.7
516	-2000	-400	273.60	14.2	567	-2100	640	1097.54	4.3
517	-2000	-380	270.35	6.7	568	-2100	620	1086.74	5.2
518	-2000	-360	305.76	15.5	569	-2100	600	1045.15	5.1
519	-2000	-340	267.57	14.9	570	-2100	580	881.55	8
520	-2000	-320	292.64	11	571	-2100	560	573.92	6.6
521	-2000	-300	285.01	11.6	572	-2100	540	387.08	4.4
522	-2000	-280	110.24	10.8	573	-2100	520	284.76	3.6
523	-2000	-260	343.88	5.3	574	-2100	500	225.57	4.8
524	-2000	-240	334.58	5.2	575	-2100	480	201.04	8
525	-2000	-220	323.48	6	576	-2100	460	183.40	8.9
526	-2000	-200	351.64	7.7	577	-2100	440	148.63	5.3
527	-2000	-180	314.58	6	578	-2100	420	153.08	10.5
528	-2000	-160	319.67	4.6	579	-2100	400	175.89	8.7
529	-2000	-140	284.29	2.8	580	-2100	380	218.73	10.6
530	-2000	-120	255.25	3.1	581	-2100	360	236.60	9.4
531	-2000	-100	291.11	4.7	582	-2100	340	248.45	12.2
532	-2000	-80	280.50	3.3	583	-2100	320	240.37	11.2
533	-2000	-60	220.69	4.9	584	-2100	300	248.50	11.3
534	-2000	-40	184.85	6.6	585	-2100	280	223.03	13.8
535	-2000	-20	138.71	8.5	586	-2100	260	190.43	13.7
536	-2000	0	117.00	3.6	587	-2100	240	160.99	15.4
537	-2000	20	95.60	2.8	588	-2100	220	152.56	16.6
538	-2000	40	90.61	5.9	589	-2100	200	162.25	17.3
539	-2000	60	76.70	5.5	590	-2100	180	151.67	17.2
540	-2000	80	71.91	8.3	591	-2100	160	149.91	14.2
541	-2000	100	102.18	8.6	592	-2100	140	151.47	13.7
542	-2000	120	90.22	12.7	593	-2100	120	136.62	12.3
543	-2000	140	126.97	15.1	594	-2100	100	150.62	10.9
544	-2000	160	152.12	16.3	595	-2100	80	174.16	15.9
545	-2000	180	145.94	16.9	596	-2100	60	178.21	9.6
546	-2000	200	154.25	20.2	597	-2100	40	139.47	6.6
547	-2000	220	192.72	18	598	-2100	20	153.94	3.5
548	-2000	240	235.11	13.4	599	-2100	0	155.43	7.3
549	-2000	260	216.53	16.3	600	-2100	-20	176.51	6.9
550	-2000	280	192.10	12.3	601	-2100	-40	225.25	4.9
551	-2000	300	179.60	10	602	-2100	-60	299.92	3.4
552	-2000	320	176.19	8.1	603	-2100	-80	212.32	1.8
553	-2000	340	190.99	7	604	-2100	-100	178.78	2.3
554	-2000	360	189.79	6.6	605	-2100	-120	90.71	3
555	-2000	560	1082.91	6.5	606	-2100	-140	13.93	4
556	-2000	580	921.92	5.4	607	-2100	-160	98.46	1.3
557	-2000	600	1155.94	7.7	608	-2100	-180	141.62	2.3

609	-2100	-200	195.89	6.7	660	-2200	380	255.65	8.9
610	-2100	-220	258.82	6.5	661	-2200	360	152.06	6.7
611	-2100	-240	285.84	6.1	662	-2200	340	194.90	8.6
612	-2100	-260	362.26	7.4	663	-2200	320	147.32	8.2
613	-2100	-280	445.36	9.9	664	-2200	300	118.19	7.7
614	-2100	-300	297.95	9	665	-2200	280	189.00	12.1
615	-2100	-320	260.85	10.4	666	-2200	260	163.90	13.3
616	-2100	-340	134.52	11	667	-2200	240	145.53	16.2
617	-2100	-360	13.80	12.5	668	-2200	220	172.51	17.2
618	-2100	-380	32.16	15.8	669	-2200	200	152.11	15.6
619	-2100	-400	149.94	10.2	670	-2200	180	122.88	14.8
620	-2100	-420	304.44	27.8	671	-2200	160	113.00	12.2
621	-2100	-440	468.61	24.6	672	-2200	140	112.68	10.6
622	-2100	-460	543.20	23.2	673	-2200	120	115.90	8.8
623	-2100	-480	474.73	13.5	674	-2200	100	127.70	7.9
624	-2100	-500	371.80	19.5	675	-2200	80	148.53	7.6
625	-2100	-520	270.18	20.6	676	-2200	60	178.69	9.2
626	-2100	-540	216.85	19.3	677	-2200	40	198.71	9.6
627	-2100	-560	204.44	26.1	678	-2200	20	207.43	8.1
628	-2100	-580	173.49	20	679	-2200	0	180.77	6.7
629	-2100	-600	221.85	19	680	-2200	-20	152.35	3.8
630	-2100	-620	263.26	34.1	681	-2200	-40	144.30	3.1
631	-2100	-640	245.24	32	682	-2200	-60	148.93	4.1
632	-2100	-660	229.59	30	683	-2200	-80	163.51	4.3
633	-2100	-680	197.79	16.7	684	-2200	-100	166.11	3.3
634	-2100	-700	135.97	15.2	685	-2200	-120	177.82	5.7
635	-2100	-720	322.18	4	686	-2200	-140	214.07	8.4
636	-2100	-740	212.59	3.3	687	-2200	-160	189.03	10.7
637	-2100	-760	1060.04	11.1	688	-2200	-180	272.47	10
638	-2100	-780	540.20	8.6	689	-2200	-200	295.47	6.8
639	-2100	-800	620.82	8.2	690	-2200	-220	328.32	9.9
640	-2100	-820	950.80	8.1	691	-2200	-240	382.81	9.2
641	-2100	-840	800.86	7.5	692	-2200	-260	475.56	8.2
642	-2100	-860	1015.40	9	693	-2200	-280	536.78	10.8
643	-2100	-880	1390.07	15.3	694	-2200	-300	620.88	8.6
644	-2100	-900	570.18	26.1	695	-2200	-320	631.46	12.4
645	-2100	-920	384.41	28.7	696	-2200	-340	669.31	13.6
646	-2100	-940	114.43	43.8	697	-2200	-360	603.44	14.1
647	-2100	-960	556.58	14.6	698	-2200	-380	639.55	16.6
648	-2100	-980	156.51	5.9	699	-2200	-400	513.62	20.9
649	-2200	600	430.75	5.1	700	-2200	-420	476.90	19.5
650	-2200	580	317.80	4.1	701	-2200	-440	410.86	23.8
651	-2200	560	281.34	2.2	702	-2200	-460	314.86	22.6
652	-2200	540	293.04	5.4	703	-2200	-480	285.35	25.4
653	-2200	520	356.83	4.8	704	-2200	-500	232.09	20.8
654	-2200	500	380.15	3.9	705	-2200	-520	204.33	25.6
655	-2200	480	346.57	5.4	706	-2200	-540	180.70	25.9
656	-2200	460	267.65	3.5	707	-2200	-560	181.70	23.1
657	-2200	440	226.61	6.7	708	-2200	-580	157.24	25.8
658	-2200	420	209.78	9.5	709	-2200	-600	158.71	32.4
659	-2200	400	148.12	4.3	710	-2200	-620	228.88	33.8

<b>711</b>	-2200	-640	242.96	28.9	<b>762</b>	-2200	-760	284.38	7.4
<b>712</b>	-2200	-660	263.11	33.2	<b>763</b>	-2200	-780	492.97	4.1
<b>713</b>	-2200	-680	217.24	38	<b>764</b>	-2300	600	191.53	4.6
<b>714</b>	-2200	-700	192.93	27.8	<b>765</b>	-2300	580	187.03	4.4
<b>715</b>	-2200	-720	213.03	22.8	<b>766</b>	-2300	560	257.67	3.6
<b>716</b>	-2200	-740	236.51	12.4	<b>767</b>	-2300	540	393.91	4.2
<b>717</b>	-2200	-760	284.38	7.4	<b>768</b>	-2300	520	530.05	4.1
<b>718</b>	-2200	-780	492.97	4.1	<b>769</b>	-2300	500	628.05	5
<b>719</b>	-2300	600	191.53	4.6	<b>770</b>	-2300	480	570.42	6.5
<b>720</b>	-2300	580	187.03	4.4	<b>771</b>	-2300	460	427.38	6.6
<b>721</b>	-2300	560	257.67	3.6	<b>772</b>	-2300	440	332.17	8.7
<b>722</b>	-2300	540	393.91	4.2	<b>773</b>	-2300	420	294.40	9.4
<b>723</b>	-2300	520	530.05	4.1	<b>774</b>	-2300	400	283.69	9
<b>724</b>	-2300	500	628.05	5	<b>775</b>	-2300	380	276.20	9.8
<b>725</b>	-2300	480	570.42	6.5	<b>776</b>	-2300	360	275.96	9.8
<b>726</b>	-2300	460	427.38	6.6	<b>777</b>	-2300	340	280.17	8.8
<b>727</b>	-2300	440	332.17	8.7	<b>778</b>	-2300	320	266.22	10.2
<b>728</b>	-2300	420	294.40	9.4	<b>779</b>	-2300	300	217.34	11
<b>729</b>	-2300	400	283.69	9	<b>780</b>	-2300	280	197.45	12.4
<b>730</b>	-2300	380	276.20	9.8	<b>781</b>	-2300	260	170.90	12.5
<b>731</b>	-2300	360	275.96	9.8	<b>782</b>	-2300	240	161.83	15.5
<b>732</b>	-2300	340	280.17	8.8	<b>783</b>	-2300	220	154.39	14.7
<b>733</b>	-2300	320	266.22	10.2	<b>784</b>	-2300	200	120.65	16
<b>734</b>	-2300	300	217.34	11	<b>785</b>	-2300	180	92.51	12.8
<b>735</b>	-2300	280	197.45	12.4	<b>786</b>	-2300	160	61.99	5.8
<b>736</b>	-2300	260	170.90	12.5	<b>787</b>	-2300	140	73.10	10.9
<b>737</b>	-2300	240	161.83	15.5	<b>788</b>	-2300	120	87.31	7.8
<b>738</b>	-2300	220	154.39	14.7	<b>789</b>	-2300	100	106.49	6.3
<b>739</b>	-2300	200	120.65	16	<b>790</b>	-2300	80	131.53	6.2
<b>740</b>	-2300	180	92.51	12.8	<b>791</b>	-2300	60	137.65	9
<b>741</b>	-2300	160	61.99	5.8	<b>792</b>	-2300	40	140.85	2.9
<b>742</b>	-2300	140	73.10	10.9	<b>793</b>	-2300	20	147.50	5.9
<b>743</b>	-2300	120	87.31	7.8	<b>794</b>	-2300	0	164.77	6
<b>744</b>	-2300	100	106.49	6.3	<b>795</b>	-2300	-20	166.25	7.3
<b>745</b>	-2300	80	131.53	6.2	<b>796</b>	-2300	-40	178.16	7
<b>746</b>	-2300	60	137.65	9	<b>797</b>	-2300	-60	180.58	7.1
<b>747</b>	-2300	40	140.85	2.9	<b>798</b>	-2300	-80	168.24	6.5
<b>748</b>	-2300	20	147.50	5.9	<b>799</b>	-2300	-100	163.57	6
<b>749</b>	-2300	0	164.77	6	<b>800</b>	-2300	-120	164.69	4.1
<b>750</b>	-2300	-20	166.25	7.3	<b>801</b>	-2300	-140	174.30	4.2
<b>751</b>	-2300	-40	178.16	7	<b>802</b>	-2300	-160	238.10	3.8
<b>752</b>	-2300	-60	180.58	7.1	<b>803</b>	-2300	-180	371.37	5
<b>753</b>	-2300	-80	168.24	6.5	<b>804</b>	-2300	-200	433.32	5.3
<b>754</b>	-2300	-100	163.57	6	<b>805</b>	-2300	-220	785.27	9.3
<b>755</b>	-2300	-120	164.69	4.1	<b>806</b>	-2300	-240	931.47	8.9
<b>756</b>	-2300	-140	174.30	4.2	<b>807</b>	-2300	-260	1273.57	8.9
<b>757</b>	-2200	-660	263.11	33.2	<b>808</b>	-2300	-280	1579.44	9.5
<b>758</b>	-2200	-680	217.24	38	<b>809</b>	-2300	-300	1396.61	10.4
<b>759</b>	-2200	-700	192.93	27.8	<b>810</b>	-2300	-320	1313.52	10.8
<b>760</b>	-2200	-720	213.03	22.8	<b>811</b>	-2300	-340	1156.06	10.1
<b>761</b>	-2200	-740	236.51	12.4	<b>812</b>	-2300	-360	1070.12	10.5

<b>813</b>	-2300	-380	924.90	10.3	<b>864</b>	-2400	100	100.27	3.1
<b>814</b>	-2300	-400	814.04	10.4	<b>865</b>	-2400	80	132.65	9.8
<b>815</b>	-2300	-420	681.45	10.3	<b>866</b>	-2400	60	166.15	8.6
<b>816</b>	-2300	-440	749.03	10.5	<b>867</b>	-2400	40	171.49	8.6
<b>817</b>	-2300	-460	566.93	10.3	<b>868</b>	-2400	20	163.43	11.5
<b>818</b>	-2300	-480	567.49	12.2	<b>869</b>	-2400	0	165.90	10.7
<b>819</b>	-2300	-500	409.69	15.8	<b>870</b>	-2400	-20	179.22	8.8
<b>820</b>	-2300	-520	236.39	<b>21.3</b>	<b>871</b>	-2400	-40	191.57	8.4
<b>821</b>	-2300	-540	264.44	<b>24.6</b>	<b>872</b>	-2400	-60	216.86	6.1
<b>822</b>	-2300	-560	221.34	<b>25.1</b>	<b>873</b>	-2400	-80	239.00	7.2
<b>823</b>	-2300	-580	220.25	<b>30.9</b>	<b>874</b>	-2400	-100	249.50	6.7
<b>824</b>	-2300	-600	228.79	<b>33.2</b>	<b>875</b>	-2400	-120	259.87	6.9
<b>825</b>	-2300	-620	209.22	<b>34.9</b>	<b>876</b>	-2400	-140	398.25	6.8
<b>826</b>	-2300	-640	184.89	<b>40</b>	<b>877</b>	-2400	-160	354.31	5.6
<b>827</b>	-2300	-660	195.96	<b>32</b>	<b>878</b>	-2400	-180	428.51	5.6
<b>828</b>	-2300	-680	210.88	<b>31</b>	<b>879</b>	-2400	-200	577.67	5.3
<b>829</b>	-2300	-700	250.26	<b>27.2</b>	<b>880</b>	-2400	-220	595.87	5.8
<b>830</b>	-2300	-720	310.89	<b>24.7</b>	<b>881</b>	-2400	-240	867.54	7.6
<b>831</b>	-2300	-740	298.36	<b>17</b>	<b>882</b>	-2400	-260	1717.48	10.9
<b>832</b>	-2300	-760	275.68	<b>21</b>	<b>883</b>	-2400	-280	2119.07	11.5
<b>833</b>	-2300	-780	265.58	13.6	<b>884</b>	-2400	-300	2213.06	12
<b>834</b>	-2300	-800	302.68	3.7	<b>885</b>	-2400	-320	1887.59	11.4
<b>835</b>	-2300	-820	544.23	3.7	<b>886</b>	-2400	-340	1184.05	10.5
<b>836</b>	-2300	-840	778.28	4.3	<b>887</b>	-2400	-360	426.61	8
<b>837</b>	-2300	-860	957.70	6	<b>888</b>	-2400	-380	359.69	10.1
<b>838</b>	-2300	-880	1016.80	8.8	<b>889</b>	-2400	-400	751.71	10.5
<b>839</b>	-2400	600	394.03	4.9	<b>890</b>	-2400	-420	1304.91	10.2
<b>840</b>	-2400	580	335.88	4.4	<b>891</b>	-2400	-440	1463.19	11.3
<b>841</b>	-2400	560	409.19	4.6	<b>892</b>	-2400	-460	1603.97	10.8
<b>842</b>	-2400	540	432.48	5.1	<b>893</b>	-2400	-480	1163.49	11.5
<b>843</b>	-2400	520	467.83	5.8	<b>894</b>	-2400	-500	761.44	12.2
<b>844</b>	-2400	500	391.37	6.6	<b>895</b>	-2400	-520	513.16	11.5
<b>845</b>	-2400	480	405.40	3.4	<b>896</b>	-2400	-540	277.96	18.2
<b>846</b>	-2400	460	338.20	7.5	<b>897</b>	-2400	-560	240.26	26.1
<b>847</b>	-2400	440	284.20	7.2	<b>898</b>	-2400	-580	248.13	30.8
<b>848</b>	-2400	420	290.63	9.4	<b>899</b>	-2400	-600	249.46	29.1
<b>849</b>	-2400	400	266.10	7.4	<b>900</b>	-2400	-620	827.57	18.8
<b>850</b>	-2400	380	304.59	10.4	<b>901</b>	-2400	-640	252.73	16.9
<b>851</b>	-2400	360	296.39	10.8	<b>902</b>	-2400	-660	150.33	20.4
<b>852</b>	-2400	340	205.81	10.2	<b>903</b>	-2400	-680	125.21	32.8
<b>853</b>	-2400	320	181.82	8.7	<b>904</b>	-2400	-700	170.04	26.6
<b>854</b>	-2400	300	166.91	11.2	<b>905</b>	-2400	-720	187.84	32.4
<b>855</b>	-2400	280	139.69	10.3	<b>906</b>	-2400	-740	216.70	28.4
<b>856</b>	-2400	260	151.23	14.3	<b>907</b>	-2400	-760	199.51	37.7
<b>857</b>	-2400	240	140.39	15.3	<b>908</b>	-2400	-780	170.28	34.2
<b>858</b>	-2400	220	126.27	16.9	<b>909</b>	-2400	-800	195.33	24.2
<b>859</b>	-2400	200	110.67	10	<b>910</b>	-2400	-820	206.60	18.3
<b>860</b>	-2400	180	88.48	13.3	<b>911</b>	-2400	-840	278.65	12.9
<b>861</b>	-2400	160	75.51	9.7	<b>912</b>	-2400	-860	324.54	5.4
<b>862</b>	-2400	140	60.72	10.1	<b>913</b>	-2500	600	824.85	4.2
<b>863</b>	-2400	120	80.06	2.1	<b>914</b>	-2500	580	708.51	5.2

<b>915</b>	-2500	560	652.26	5.7	<b>966</b>	-2500	-460	1095.95	15.4
<b>916</b>	-2500	540	562.37	6.1	<b>967</b>	-2500	-480	1566.87	14.2
<b>917</b>	-2500	520	519.63	6.2	<b>968</b>	-2500	-500	1339.23	15
<b>918</b>	-2500	500	490.98	6.1	<b>969</b>	-2500	-520	1022.36	11.7
<b>919</b>	-2500	480	282.34	5.6	<b>970</b>	-2500	-540	689.04	17.4
<b>920</b>	-2500	460	266.57	6.4	<b>971</b>	-2500	-560	726.13	17.2
<b>921</b>	-2500	440	205.72	7.6	<b>972</b>	-2500	-580	264.66	34.1
<b>922</b>	-2500	420	153.67	14.5	<b>973</b>	-2500	-600	100.31	31.1
<b>923</b>	-2500	400	224.29	10.5	<b>974</b>	-2500	-620	67.86	32.9
<b>924</b>	-2500	380	259.36	13	<b>975</b>	-2500	-640	47.81	35
<b>925</b>	-2500	360	264.72	13.4	<b>976</b>	-2500	-660	22.51	45.4
<b>926</b>	-2500	340	254.39	16.4	<b>977</b>	-2500	-680	37.48	19.2
<b>927</b>	-2500	320	233.53	15.2	<b>978</b>	-2500	-700	79.06	22.3
<b>928</b>	-2500	300	175.97	15.5	<b>979</b>	-2500	-720	132.65	22.7
<b>929</b>	-2500	280	171.33	16.8	<b>980</b>	-2500	-740	191.43	31.3
<b>930</b>	-2500	260	142.65	17.1	<b>981</b>	-2500	-760	180.48	29.7
<b>931</b>	-2500	240	137.61	14.6	<b>982</b>	-2500	-780	168.29	30
<b>932</b>	-2500	220	107.02	11.3	<b>983</b>	-2500	-800	171.98	35.4
<b>933</b>	-2500	200	88.98	10.9	<b>984</b>	-2500	-820	171.88	36.8
<b>934</b>	-2500	180	77.87	11.6	<b>985</b>	-2500	-840	187.76	28.1
<b>935</b>	-2500	160	73.21	10.2	<b>986</b>	-2500	-860	189.65	29.1
<b>936</b>	-2500	140	94.58	8.5	<b>987</b>	-2500	-880	260.10	17.7
<b>937</b>	-2500	120	124.90	8	<b>988</b>	-2500	-900	439.21	10
<b>938</b>	-2500	100	165.55	8.4	<b>989</b>	-2500	-920	639.47	9
<b>939</b>	-2500	80	183.64	7.2	<b>990</b>	-2700	600	802.92	5.4
<b>940</b>	-2500	60	190.46	2.8	<b>991</b>	-2700	580	701.03	4.2
<b>941</b>	-2500	40	207.67	10.3	<b>992</b>	-2700	560	657.11	4.4
<b>942</b>	-2500	20	195.37	8.6	<b>993</b>	-2700	540	662.17	5.3
<b>943</b>	-2500	0	196.27	9.5	<b>994</b>	-2700	520	692.72	7.7
<b>944</b>	-2500	-20	216.17	8.5	<b>995</b>	-2700	500	734.85	9.3
<b>945</b>	-2500	-40	230.08	8.6	<b>996</b>	-2700	480	590.60	7.3
<b>946</b>	-2500	-60	240.31	8.3	<b>997</b>	-2700	460	355.99	8.5
<b>947</b>	-2500	-80	246.20	6.6	<b>998</b>	-2700	440	254.60	9.5
<b>948</b>	-2500	-100	267.61	9.3	<b>999</b>	-2700	420	88.02	18.1
<b>949</b>	-2500	-120	284.67	10.6	<b>1000</b>	-2700	400	82.14	22.9
<b>950</b>	-2500	-140	437.64	15.9	<b>1001</b>	-2700	380	93.52	21.9
<b>951</b>	-2500	-160	787.62	17	<b>1002</b>	-2700	360	121.83	24.7
<b>952</b>	-2500	-180	1045.67	14.4	<b>1003</b>	-2700	340	130.56	23.9
<b>953</b>	-2500	-200	1155.40	11.1	<b>1004</b>	-2700	320	112.00	26.7
<b>954</b>	-2500	-220	1423.54	10.8	<b>1005</b>	-2700	300	80.49	25.8
<b>955</b>	-2500	-240	1540.97	9.8	<b>1006</b>	-2700	280	69.92	22.7
<b>956</b>	-2500	-260	2212.32	10.7	<b>1007</b>	-2700	260	71.01	19.7
<b>957</b>	-2500	-280	2519.90	10.9	<b>1008</b>	-2700	240	72.20	23.8
<b>958</b>	-2500	-300	2353.42	10.5	<b>1009</b>	-2700	220	116.98	15.3
<b>959</b>	-2500	-320	2201.95	8.5	<b>1010</b>	-2700	200	140.33	17.4
<b>960</b>	-2500	-340	1139.29	7.9	<b>1011</b>	-2700	180	214.20	13.8
<b>961</b>	-2500	-360	485.94	10.2	<b>1012</b>	-2700	160	238.29	10.8
<b>962</b>	-2500	-380	326.16	15.6	<b>1013</b>	-2700	140	228.53	5.6
<b>963</b>	-2500	-400	89.80	17.8	<b>1014</b>	-2700	120	227.15	4.7
<b>964</b>	-2500	-420	52.61	20.1	<b>1015</b>	-2700	100	181.11	4.7
<b>965</b>	-2500	-440	545.21	19.8	<b>1016</b>	-2700	80	163.18	8.3

<b>1017</b>	-2700	60	147.02	14.2	<b>1068</b>	-2700	-960	437.87	<b>18.6</b>
<b>1018</b>	-2700	40	134.22	14.8	<b>1069</b>	-2700	-980	763.41	12.2
<b>1019</b>	-2700	20	134.36	14.8	<b>1070</b>	-2700	-1000	761.16	12
<b>1020</b>	-2700	0	189.52	12.9					
<b>1021</b>	-2700	-20	216.00	14.9			END		
<b>1022</b>	-2700	-40	293.17	16.1					
<b>1023</b>	-2700	-60	373.87	17.1					
<b>1024</b>	-2700	-80	546.42	19.1					
<b>1025</b>	-2700	-100	957.84	20.3					
<b>1026</b>	-2700	-120	1665.01	20.3					
<b>1027</b>	-2700	-140	2851.23	22.9					
<b>1028</b>	-2700	-160	3324.03	23.2					
<b>1029</b>	-2700	-180	3017.20	22.8					
<b>1030</b>	-2700	-200	2168.61	18.5					
<b>1031</b>	-2700	-220	942.88	14.5					
<b>1032</b>	-2700	-240	609.95	9.9					
<b>1033</b>	-2700	-260	473.19	8.3					
<b>1034</b>	-2700	-280	506.18	7.6					
<b>1035</b>	-2700	-300	678.05	6.1					
<b>1036</b>	-2700	-320	939.14	4.7					
<b>1037</b>	-2700	-340	1127.11	4.7					
<b>1038</b>	-2700	-360	1343.87	4.5					
<b>1039</b>	-2700	-380	1376.18	4.5					
<b>1040</b>	-2700	-400	1280.26	5					
<b>1041</b>	-2700	-420	1354.95	5					
<b>1042</b>	-2700	-440	1918.34	4.6					
<b>1043</b>	-2700	-460	2313.93	10.9					
<b>1044</b>	-2700	-480	2714.37	6.4					
<b>1045</b>	-2700	-500	2564.02	7					
<b>1046</b>	-2700	-520	2077.06	5.6					
<b>1047</b>	-2700	-540	1511.54	4.5					
<b>1048</b>	-2700	-560	1309.00	5.2					
<b>1049</b>	-2700	-580	1108.00	6.9					
<b>1050</b>	-2700	-600	974.58	9.3					
<b>1051</b>	-2700	-620	752.96	13.9					
<b>1052</b>	-2700	-640	230.80	17.6					
<b>1053</b>	-2700	-660	197.90	31.4					
<b>1054</b>	-2700	-680	40.51	50.4					
<b>1055</b>	-2700	-700	49.11	60.3					
<b>1056</b>	-2700	-720	45.79	57					
<b>1057</b>	-2700	-740	42.93	59					
<b>1058</b>	-2700	-760	41.00	66					
<b>1059</b>	-2700	-780	38.83	52					
<b>1060</b>	-2700	-800	43.21	72					
<b>1061</b>	-2700	-820	57.70	62					
<b>1062</b>	-2700	-840	87.02	51					
<b>1063</b>	-2700	-860	110.39	60					
<b>1064</b>	-2700	-880	127.38	50					
<b>1065</b>	-2700	-900	136.33	63					
<b>1066</b>	-2700	-920	135.77	61					
<b>1067</b>	-2700	-940	761.16	12					

# ***Chapter 5***

## **Conclusion**

Magnetic, IP/Resistivity, Magnetic susceptibility measurement and Gamma ray spectrometry survey (PGRS) carried out in Devri area of Surguja district of Chhattisgarh state to delineate the uranium bearing shear zone have given number of vital clues about its presence and characters.

Magnetic survey infers that the Central Surguja Shear zone is continuing under the soil cover in this part with the established trend of ENE-WSW. Low magnetic in the central part could be attributed to this shear. A very conspicuous ENE-WSW trending magnetic body has been picked up in southern part of the area. Similar kind of basic body has given very good uranium mineralized bands in Dumhat area. It seems that this basic body is emplaced along the axial plane of 3rd phase of folding. This indicates reactivation of the area in time and again which falls under the structural grain of Satpura Orogeny. Quantitative interpretation and depth estimation by various methods indicates presence of magnetic source at various depths.

Induced Polarization/Resistivity survey revealed presence of two low resistivity and high chargeability zone in the north and south of the area. Northern zone follow the trend of shear zone (ENE-WSW) whereas the southern zone seems to be fault splay of main shear/fracture zone trending NE-SW, 20° oblique to main shear zone with more concentration of disseminated sulphides

indicated by very high chargeability (upto 72mV/V). Therefore a new target location for subsurface exploration has been established by this study. Presently on going subsurface exploration in northern zone has intercepted correlatable uranium mineralized bands, and southern chargeability zone is going to be future target of exploration.

Magnetic susceptibility and gamma ray correlation logs of four boreholes suggest positive association of radioactivity and sulphides and/or ferromagnesian minerals. The ferromagnesian minerals seem to be developed during the retrograde metamorphism and sulphides were developed due to hydrothermal action in the area, they have played a great role in fixation of uranium minerals along with them.

Radioelemental mapping of the area using PGRS equipment signifies that uranium minerals present in the rocks of shear zone have been leached out and must have migrated with meteoric water below the water table where it can precipitate under reducing conditions. High potassium content in fresh rock exposure indicates evolved nature of granite which is a good indication for uranium mineralisation point of view.

## REFERENCES

1. Ansari, A.H. and Alamdar, K., 2009: Reduction to the Pole of Magnetic Anomalies Using Analytic Signal. *World Applied Science Journal* 7(4), pp 405-409.
2. Bhimashankaram, V.L.S. and Gaur, V. K., 1977: Lectures on exploration geophysics for geologists and engineers, Osmania University, Hyderabad,. p 449.
3. Chaki, A., 1976: Annual Report for the field season 1975-76, Unpublished Report, Atomic Minerals Directorate for Exploration and Research, Hyderabad.
4. Chakravarthi, V., 2009: Automatic gravity inversion for simultaneous estimation of model parameters and regional gravity background: an application to 2D pull-apart basins. *Current Science*, V. 96, No. 10.
5. Cooper, G. R. J., and D. R. Cowan, 2006: Enhancing potential field data using filters based on the local phase: *Computers and Geosciences*, 32, pp 1585–1591.
6. Field Manual for *TSQ-3 Time and Frequency Domain IP Transmitter*, Scintrex Ltd.
7. Frantisek Hrouda, Marta Chlupacova and Martin Chadima, 2009: The Use of Magnetic Susceptibility of Rocks in Geological Exploration, *Terraplius*, p 27.
8. Grant, F. S. and Dodds, J., 1972: MAGMAP FFT processing system development notes. Paterson Grant and Watson Limited.

9. Geosoft, 2008: Geosoft mapping and processing system (Oasis Montaj 7.0), Quick Start Tutorial, Geosoft Inc., Toronto, Ontario, Canada. p 325.
10. Geosoft, 2007: Montaj magmap filtering, 2D processing of potential field data, tutorial, (Oasis Montaj 6.4). Geosoft Inc., Toronto, Ontario, Canada. p 82.
11. Hansen, R.O. and Pawlowski, R. S., 1989: Reduction to pole at low latitudes by Weiner filtering. *Geophysics*, v. 54, pp 1607-1613.
12. IAEA-TECDOC-1363, 2003: Guidelines for radioelement mapping using gamma ray spectrometry data, International Atomic Energy Agency, p 179.
13. Joshi, V.N., 1976: Annual Report for the field season 1975-76, Unpublished Report, Atomic Minerals Directorate for Exploration and Research, Hyderabad.
14. Kak, S.N., Perumal, N.V.A.S., Satyanarayana Rao, S.R., Krishnamurthy, B., Phadke, A.V., 1983: Three case studies illustrating the use of Remote Sensing Techniques in uranium exploration. *Proc. NNRMS Seminar, Hyderabad, Vol III*, p 50-52.
15. Kearey, P., Brooks, M., 2002: *An Introduction to Geophysical Exploration*, Blackwell, p 262.
16. MacLeod, I. N., Jones, K. and Dai, T. F., 1993: 3-D Analytic signal in the interpretation of total magnetic field data at low magnetic latitudes. *Exploration Geophysics*, v. 24, pp 679-688.

17. Mendonca, C.A., Silva, J.B.C., 1993: A stable truncated series approximation of the reduction-to-pole operator. *Geophysics*, V.58, pp. 1084-1090.
18. Miller, H. G., and V. Singh, 1994: Potential field tilt —A new concept for location of potential field sources: *Journal of Applied Geophysics*, 32, pp 213–217.
19. Nair, K.K.K., Jain, S.C. and Yedekar, D.B. 1988: Geology, structure and tectonics of the Son-narmada-Tapti Lineament zone, *Rec. Geol. Surv. India*, v.117 pt 3-8. pp136-147.
20. Nabighian, M. N., 1972: The analytical signal of two –dimensional magnetic bodies with polygonal cross section: Its properties and use for automated anomaly interpretation. *Geophysics*, v. 37, pp 507-517.
21. Ramakrishnan, M., Vaidyanadhan, R., 2010: *Geology of India*, Geological Society of India, Bangalore, v 1, p 556.
22. Ramachandra Rao, M. B., 1975: *Outlines of geophysical prospecting – a manual for geologists*, EBD Educational Private Limited, 15, Rajpur Road, Dehradun-248001, India, 425p.
23. Reid, A. B., Allsop, J. M., Granser, H., Millet, A. J. and Somerton, I. W., 1990: Magnetic interpretation in 3-D using Euler deconvolution. *Geophysics*, v. 55, pp 80-91.
24. Roest, W. R., Verhoef, J. and Pilkington, M., 1992: Magnetic interpretation using 3-D analytic signal. *Geophysics*, v. 57, pp 116-125.

25. Salem, A and Simon William, 2007: Tilt-depth method: A simple depth estimation method using first-order magnetic derivatives: The Leading Edge, pp 1502-1505.
26. Salem, A., Williams, S., Fairhead, D., Smith, R., and Dhananjay Ravat, 2008: Interpretation of magnetic data using tilt-angle derivatives: GEOPHYSICS, 73, pp L1-L10.
27. Saxena, V.P., 1975: Annual Report for the field season 1974-75, on ground checking of radioactive anomalies in parts of Surguja district and detailed investigation involving drilling, test pitting and trenching in Dumhat radioactive mineralized zone in Surguja district, Madhya Pradesh, Unpublished Report, Atomic Minerals Directorate for Exploration and Research, Hyderabad.
28. Saxena, V.P., Bahukandi, N.K., Bhatt, A.K. and Singh S.N., 1990: Uranium metallogeny in the Central Surguja Shear Zone, Surguja district, Madhya Pradesh, Geological Survey of India, Sp. Publ. n. 28, p. 818-638.
29. Saxena, V.P., Krishnamurthy, P. Murugan, C., and Sabot, H.K., 1992: Geochemistry of the granitoids from central Surguja shear zone, India: geological evolution and implication on uranium mineralization and exploration. Exploration and research for Atomic Minerals v.5, p.27-40.
30. Saxena, V.P., Bahukandi, N.K., Reddy, S.V.S., Sabot, H.K. and Verma, S.C., 1998: Uranium mineralization in Surguja Crystalline Complex, Madhya Pradesh, India - A review for evolving new exploration strategy. Exploration and research for Atomic Minerals v.11, p.61-75.

31. Seshadri, K.V., 1970: Annual Report for the field season 1969-70. Unpublished Report, Atomic Minerals Directorate for Exploration and Research, Hyderabad.
32. Seth, D.K., 1989: Structure and uranium mineralization in the Proterozoic rocks of Dumhat area, Surguja district, Madhya Pradesh, Exploration and research for Atomic Minerals v.2, p.77-91.
33. Silva, J. B. C. 1986: Reduction to the pole as an inverse problem and its application to low latitude anomalies. *Geophysics*, v. 51, pp 369-382.
34. Subhash Ram and Chary, M.N., 2010: Annual Report for the field season 2009-10. Unpublished Report (EGPG), Atomic Minerals Directorate for Exploration and Research, Hyderabad.
35. Telford, W. M., Geldart, L. P., and Sheriff, R. E., 1990: *Applied Geophysics (Second Edition)*: Cambridge University Press, London, p 770.
36. Thompson, D. T., 1982: EULDPH - A new technique for making computer-assisted depth estimates from magnetic data. *Geophysics*, v. 47, pp 31-37.
37. Verduzco, B., J.D. Fairhead, C. M. Green, and C. MacKenzie, 2004, New insights into magnetic derivatives for structural mapping: *The Leading Edge*, 23, pp 116–119.
38. Vernon, R.H., Clarke, G.L., 2008: *Principles of Metamorphic Petrology*, Cambridge University Press. p 556.

# CHAPTER -1

“Rocks are records of events that took place at the time they formed. They are books. They have a different vocabulary, a different alphabet, but you learn how to read them.”

-John McPhee

# CHAPTER -2

A geologist is a fault-finder.

Anonymous

# CHAPTER -3

Unfolding the mystery of nature by science is not always true.

RR

# CHAPTER -4

The only certainty in this data-poor, imagination-rich, endlessly fascinating field is that there are plenty of surprises left to come".

Michael Lemonick

# CHAPTER -5

Satisfaction kills desire, be curious.

RR